The Design of an Efficient Routing Protocol and Energy Supply for Wireless Sensor Networks

Xiaobo Liu

Submitted in total fulfilment of the requirements of the degree of

Master of Philosophy

Department of Electrical and Electronic Engineering
THE UNIVERSITY OF MELBOURNE

July 2012

Abstract

In recent years, there has been a rapid development of wireless sensor network (WSN) technology due to an increasing need for automatic monitoring and control in many areas. The key benefits of using WSN technology for monitoring and control include low cost, low power consumption and self-organizing operation of the sensor network. However, there are still several challenges remaining in practical deployments. Major concerns are improving WSN efficiency in terms of data routing and energy consumption. In this thesis, we address three problems, namely efficient converge-cast routing in tree-based WSNs, battery lifetime extension for outdoor WSN applications and the measurement of soil moisture over large areas using a WSN.

Converge-cast data collection is a typical pattern in WSN communications. Given a large number of sensor nodes formed in a tree topology, the objective is to achieve low latency for source-destination data packet delivery, while keeping the network overhead at low levels. In this thesis, we propose a converge-cast routing protocol for tree-based WSNs. In particular, a new frame structure is proposed, which is compliant with the IEEE 802.15.4 standard and gives considerable flexibility in scheduling communication between sensor nodes. Importantly, the proposed beacon flooding scheme requires less overhead for network synchronization, compared with traditional hierarchical scheduling schemes. An experimental WSN test bed is used to evaluate the performance of our proposed routing protocol. The results show that our protocol achieves comparative performance to an existing hierarchical routing protocol, but with lower complexity.

We then focus on the issue of extending the battery lifetime for unattended WSN nodes. We propose a systematic design approach for this purpose by utilizing solar energy harvesting and a simple circuit for battery recharging based on the *Harvest-Store-Use* architecture. A 4-step design procedure is used for selecting the appropriate elements in our charge circuit subject to the requirements of load power consumption. Our design approach accounts for variations in environmental conditions. Indefinite

operation of a sensor node can be achieved without the use of any adaptive schemes that require frequent adjustment of the sensor node duty cycle setup. Field experiments are conducted to evaluate the performance of our designed power supply subsystem using a WSN test bed.

Finally, we investigate the feasibility of monitoring soil moisture levels in a field using low-cost imaging sensors. The underlying principle is that plant water stress can be loosely translated to a non-optimum soil moisture level, which also affects a plant photosynthesis indicator called the *Normalized Difference Vegetation Index* (NDVI). Based on this principle, the decision for irrigation scheduling can be made based on the NDVI parameter instead of soil moisture measurements. This enables the use of image-based sensing, which avoids the deployment of a large number of soil moisture sensors across a field, thus significantly reducing the cost. Based on a WSN platform, a series of experimental results are collected to evaluate the feasibility of this approach using low-cost imaging sensors.

Declaration

This is to certify that

i. the thesis comprises only my original work towards the MPhil,

ii. due acknowledgement has been made in the text to all other material used,

iii. the thesis is less than 50,000 words in length, exclusive of tables, maps, bibliographies and appendices.

To my dear family

Acknowledgement

I would like to begin by sincerely thanking my supervisors Dr. Khusro Saleem and Associate Professor Christopher Leckie for their invaluable encouragement, guidance and support during my MPhil research. Khusro and Christopher have been wonderful mentors and advisors, inspiring me with their attitude, enthusiasm and their knowledge for research. I would also like to express my gratitude for the countless hours that they have spent with me in discussing the research subjects, reading my papers and sharing the precious experience of career choice. Without their guidance and help, the completion of this study and thesis would not have been possible.

I would like to thank The University of Melbourne for providing me a pleasant, warm and friendly research environment in the past 2 years. I have benefited greatly from its rich resources in learning and living. The assistance from the services of the laboratory, library and the staff effectively has helped me to complete my MPhil research.

I would like to thank National ICT Australia, the Department of Computer Science and Software Engineering and the School of Land and Environment for providing the experimental facilities, laboratory and funding for conference trips. I kindly appreciate the summer scholarship that I have received from the National Program for Sustainable Irrigation.

I would like to thank the Department of Electrical and Electronic Engineering and Dr. Khusro Saleem for offering me a precious opportunity of being a workshop demonstrator in the subject Embedded System Design during my MPhil research. I have learned an indelible lesson for the preparation of my future career.

I feel grateful to Dr. Kithsiri Dassanayake for his generous help for the installation of wireless sensor networks in the Parkville and Dookie Campuses, as well as assisting in trip arrangement. I also thank Dr. Wanzhi Qiu for his valuable feedback on the verification of the experimental results.

I am grateful to Professor Subhrakanti Dey and Associate Professor Marcus Brazil for teaching the subjects Statistical Signal Processing and Advanced Topics in Communication.

In the days of my MPhil experience in The University of Melbourne, it is an honour for me to interact with wonderful and talented people. I have had an educational and fun experience. I wish to thank Jack Hsu, Guang Wen, Thanh Nguyen, John Li, Cao Do, Jeffrey Spencer, Kevin Yi, Chathurika Ranaweera, Weiyao Zhou, and Senaka Samarasekera for making the EE Engineering RHD office a fun place. I would especially like to thank Jack Hsu for his advice and help in my subject assignments.

I wish to express my gratitude to my parents, Jianguo Liu and Yihong Yang, for their constant support, encouragement and love. They have taught me by personal example the significance of family, responsibility and love beyond the knowledge in one's life.

Finally, my wife, Jingjing, receives my deepest gratitude for her constant understanding, patience, support, encouragement and love, no matter how frustrated and stressed I was during my MPhil research. She has shown me how to be a positive, energetic and optimistic person full of enthusiasm for life.

Table of Contents

List of Figures

List of Tables

Chapter 1

Introduction

1.1 Background

In recent years, there has been an increasing need for connectivity among the distributed devices used for remote real-time monitoring and control. This need and the advancement in electronics and wireless communications have promoted the development of wireless sensor network (WSN) technology [4]. A WSN is a combination of embedded system technology including sensor technology, distributed computing and wireless communication technology. Sensor nodes have the capabilities of sensing, data processing and transmission, which enable real-time monitoring of the phenomenon of interest, and control by actuators within a large-scale region by collaborating with each other. The key features of sensor networks include low cost, low energy consumption, self-organizing operation and cooperative effort [3]. These features make it possible to deploy sensor nodes in harsh and inaccessible environments while achieving long lifetime operation by using batteries and solar panels as the energy supply. The features described above permit a wide range of potential applications for sensor networks, such as industrial control and monitoring [21], home automation [22], precision agriculture [140], health and environmental monitoring [17, 104].

A sensor network usually comprises a set of sensor nodes and one or more base stations (also known as sinks) [2]. In this thesis, we only consider the scenario of a sensor network with one base station, as shown in Figure 1.1. A large number of sensor nodes can be deployed within the designated areas in randomized or predetermined locations and establish a sensor network in a self-organizing fashion.

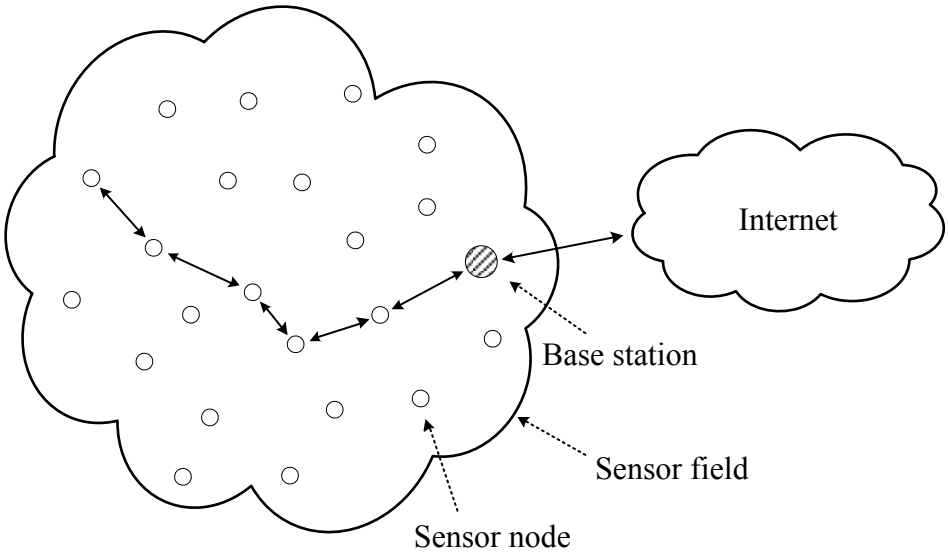

Figure 1.1: An overview of a WSN

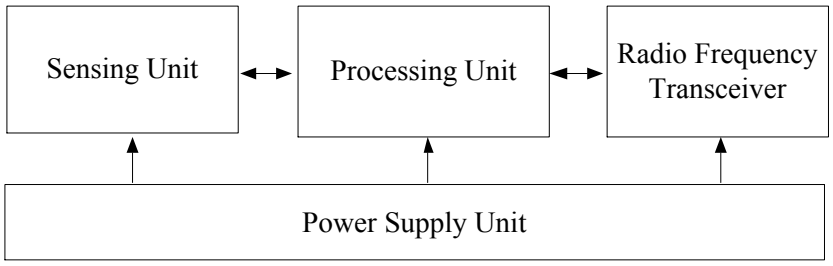

Figure 1.2: The components of a sensor node

Each sensor node senses the physical environment and sends the results to the base station via a certain path. Due to limited energy resources, sensor nodes are restricted to relatively short transmission distances. In this case, data packets must traverse multiple hops to arrive at the base station, and sensor nodes must be capable of forwarding and routing data packets. The base station has more powerful capabilities of computation, storage and communication and is responsible for network maintenance, management and data information exchange between the sensor network and the external world (e.g., the Internet).

A sensor node typically consists of a processing unit, a radio frequency transceiver unit, a sensing unit and a power supply unit. Figure 1.2 shows the component diagram of a sensor node. The processing unit, which usually includes an on-board

microprocessor and memory, controls the operation of the other units and performs simple data processing. In the sensing unit, the sensors are connected to the processing unit through analog-to-digital converters, which convert the analog signals generated by the sensors into digital signals that the microprocessor can interpret. The radio frequency transceiver unit is the gateway that exchanges data with other sensor nodes via a wireless communication channel. The above described components may have different characteristics in terms of input voltage and current consumption, and the power supply unit provides the appropriate voltage and current levels. In the power supply unit, energy storage elements (e.g., a battery) are regulated by the relevant electrical circuitry and energy harvesting elements (e.g., a solar panel). Depending on the specific application, other units can be also added to the sensor node, such as a location finding system and a mobilizer [3, 6], which support the request for accurate geographical information and the mobility of a sensor node, respectively.

Sensor networks can be utilized for applications requiring low cost, low data rates and low power consumption. For example, consider a set of soil moisture sensors deployed densely in a monitored field. These sensors need to send the measurements at a low frequency (e.g., a few reports per hour) to a data center, where each measurement is only a few bytes. For such applications, the use of traditional wireless communication protocols, such as wireless local area network (WLAN) standards (i.e., IEEE 802.11) [59] or Bluetooth (i.e., IEEE 802.15.1) [60] may not be cost-effective, due to their high complexity and excessive data transmission rates, which accordingly increase the overall cost and power consumption [22].

To address the need for low-cost, low-rate and low-power applications, the IEEE working group and ZigBee Alliance proposed the IEEE 802.15.4 [61] and ZigBee [153] standards for low-rate wireless personal area networks (LR-WPANs). The IEEE 802.15.4 specification defines standard protocols in the physical (PHY) and media-access-control (MAC) layers, and specifies a classic frame structure called the *superframe* in a *beacon-enabled* mode. In a superframe period, the operation of a sensor node alternates between the wake and sleep states. This periodic alternation is known as the *duty cycle*. Using a low duty cycle enables energy consumption to be lowered considerably. Compared with wired communications, there is challenge of detecting packet collisions in the wireless channel, in the case where multiple sensor nodes transmit simultaneously. IEEE 802.15.4 specifies a mechanism called *carrier*

sense multiple access with collision avoidance (CSMA/CA) in the MAC layer, which is used to reduce the probability of packet collision by utilizing a *random exponential backoff time* scheme. The ZigBee specification is built upon the IEEE 802.15.4 standard and defines a suite of communication protocols in the higher layers. It allows a number of devices to communicate among themselves through a mesh network topology, and also provides extra features such as device maintenance, discovery, management and security. The protocol stack specified by the IEEE 802.15.4 and ZigBee standards lays a solid foundation for further development of low-cost, low-power, low-rate and low-complexity WSNs.

1.2 Overview of the Problem

In this thesis, we address three challenging problems related to WSNs. First, we focus on the design of low-complexity protocols for converge-cast tree-based WSNs. Second, we tackle the issue of extending battery life in unattended WSNs. Third, we investigate the application of WSNs for precision irrigation in agriculture based on the measurement of soil moisture over large areas. In investigating the relevant solutions for these problems, we also take into account the key factors of cost and complexity, whilst attempting to satisfy the design objectives. In the rest of this section, we give a detailed description of the problems outlined above.

An important challenge in WSNs is the design of low-complexity and robust protocols that enable the efficient transmission of data packets from a large number of sensor nodes to a central base station. This is called converge-cast communication [5]. Efficiency refers to low latency and a high successful delivery ratio, where the delivery ratio is usually calculated as the ratio of received to total transmitted packets. In practice, the difficulty in achieving highly efficient converge-cast communication varies greatly, depending on the network topology. In a star network, each sensor node is directly connected to the base station. The simplicity and robustness of a star topology greatly reduces the complexity of network establishment, communication and maintenance, and data delivery efficiency can be improved considerably by using efficient schemes for collision avoidance, e.g., CSMA/CA [61]. In contrast, efficient converge-cast communication in tree-based WSNs is more challenging, where a packet may need to traverse multiple hops to the base station. In this topology, protocol complexity and robustness become the main concerns. In addition to the use

of a scheme for minimizing the collision probability of packet transmission, sophisticated network synchronization schemes are required. Moreover, data forwarding and routing techniques are needed in order to select the optimal source-destination path. In the case of node failures, the network topology and frame structure may need to be reorganized. A major challenge is to complete this process in a short period while minimizing the associated overhead in the protocol. By considering the issues described above, our aim is to design an efficient converge-cast protocol with the capabilities of robustness, low complexity and high performance for tree-based WSNs.

Extending the lifetime of nodes is another key concern in the design of WSNs. This is of particular significance for unattended WSNs in outdoor applications, where the sensor nodes are usually powered by batteries [4, 9, 126]. In this thesis, we focus on the study of power management for unattended WSNs and address the problem of node lifetime extension. The main challenge is to achieve the extended lifetime operation of a sensor node given the constrained battery capacity and the node power requirements. Low duty cycles can significantly reduce power consumption of a sensor node, hence resulting in an extended lifetime. The main issue with this approach is a reduction in the duration of a node's active period. As a result, sensor nodes may have insufficient time to complete operations including data sensing, processing and transmitting. Energy-efficient routing techniques are capable of minimizing the overall energy consumption for packet transmission by utilizing appropriate routing strategies (e.g., using shortest path routing) [52, 78]. This kind of routing usually requires knowledge of the location of the sensor nodes. Implementing such techniques increases network cost and protocol complexity. There is an inherent trade-off between power consumption and performance. An alternative approach of extracting energy from the environment, known as energy harvesting, gives the possibility of achieving unattended operation without sacrificing network performance [91]. A classic problem for WSNs using energy harvesting is how to select the appropriate harvesting component (e.g., a solar panel) and energy storage based on the given power requirements of a sensor node under varying environmental conditions. Other key concerns for the design of energy harvesting WSNs include matching the voltage and current characteristics among the different sensor node components, and the additional costs resulting from the energy harvesting component. In this thesis, we develop a design procedure for this problem.

Soil moisture is a key variable in the management of irrigation, since using such knowledge can help to improve the efficiency of water usage [116, 142]. We focus on the study of precision irrigation by using real-time soil moisture measurement. A challenge is how to obtain field-scale indications of soil moisture in a cost-effective way for making optimal decisions on irrigation scheduling. The remote sensing approach [16, 71], which uses imaging satellites equipped with the spectral filters to measure electromagnetic energy from the surface soil, can give direct field-scale measurements of soil moisture. The main issues with using remote sensing are the limitations on the measurement accuracy and depth as well as the extremely expensive implementation cost. Another well-known approach is to use soil moisture sensors that provide measurements at a single location [24, 74, 107]. To obtain accurate moisture gradient indications in a large field, a large number of soil moisture sensors and appropriate soil water models are needed. This results in a substantial cost of the measurement system, even though the use of the WSN technology greatly reduces the costs of implementation and maintenance. In addition, irrigation scheduling decisions based on point-scale measurements may not be optimal, since the variations of soil moisture are significantly influenced by factors such as the micro-climate and crop conditions. In this thesis, we examine the feasibility of using low-cost image-based sensors for soil moisture estimation over large areas.

1.3 Outline of Proposed Solutions

This section outlines potential solutions to the problems described in Section 1.2.

Chapter 3 proposes a converge-cast protocol for tree-based WSNs based on the IEEE 802.15.4 standard. Our proposed protocol operates in the nonbeacon-enabled mode where there is no defined superframe structure and no periodic beacon broadcasting scheme in the MAC layer. Instead, we define a framing structure, which gives more flexibility in adjusting the duty cycle of a node. The proposed protocol leverages the CSMA/CA mechanism to minimize the probability of packet collision in the transmission of data as well as the overhead required by network coordination. A *beacon flooding* scheme is used for network synchronization. In beacon flooding, the base station initiates a beacon frame and broadcasts it at the beginning of the frame structure. When a node receives the beacon frame, it immediately rebroadcasts this frame only once. This beacon forwarding scheme ensures all the network nodes

can be synchronized, even when they are not all located within the coordinator's broadcasting domain. In addition, our protocol implements a standard first-in-first-out (FIFO) buffering scheme in the higher layer for data storage and forwarding, and all the data transmissions are handled by CSMA/CA. Our proposed converge-cast tree-based protocol has lower complexity than the protocol [20] that use a time scheduling hierarchy (refer to Chapter 3.2), due to the use of a standard-based frame structure and a simple synchronization scheme. The protocol also improves network robustness and resilience to node failures by using a beacon flooding scheme, and eliminates the artificial delay resulting from time scheduling.

Chapter 4 proposes a systematic approach to designing a low-cost power supply subsystem for unattended WSNs. This subsystem provides energy to a sensor node by using the solar energy harvesting technique. In our design, a classic system architecture termed *harvest-store-use* [126] is applied, which corresponds with the components of the solar panel, rechargeable battery and load in the circuit [58, 67]. To reduce the cost of the overall subsystem, we use a simple and robust battery recharge circuit. The energy-balanced operation of a node can be achieved by following a systematic design procedure for the selection of the appropriate components in our charge circuit. In particular, three key issues related to solar harvesting WSNs are addressed in our design approach. First, we propose a simple and practical method for matching the voltage and current levels of the components. Due to the simplicity of our charge circuit, the solar panel is not required to operate at the maximum power point for all time. As a result, our approach ensures that the sensor node can still operate in varying solar conditions. Second, we use a sunlight motion model to calculate the energy variations in the power supply subsystem. Based on this model, a threshold condition for energy-balanced operation is yielded by considering the load requirements and the varying solar conditions. Third, we limit the system parameters to a safe range to avoid damaging the circuit components by excessive current and overcharging. Our design of the power supply subsystem for unattended WSNs does not require the use of any schemes that adapt the duty cycle to the real-time solar conditions during the network operation. This significantly reduces the implementation complexity of the protocol and conserves the energy resources consumed by such schemes.

In Chapter 5, a scalable approach to measuring field-scale soil moisture is proposed. In contrast to traditional sensing approaches, we investigate an image-based

technique that measures the plant leaf surface light reflectance to determine soil moisture levels. A fundamental principle of the proposed approach is that the plant needs water and light energy in a particular spectral region for photosynthesis [142]. This consequently leads to a correlation between soil moisture levels in the plant root zone and the light reflectance in the leaf surface. Soil moisture sensors are used for actual measurements, and a numerical indicator called the normalized difference vegetation index (NDVI) is measured to indicate the light reflectance by using low-cost image sensors. Based on this idea, we present an experimental methodology to investigate the feasibility of the correlation between soil moisture and NDVI using low-cost imaging sensors in different environments.

1.4 Structure and Contributions of the Thesis

The structure and contributions of this thesis are outlined as follows.

In Chapter 2 ***A Survey on Wireless Sensor Networks: Routing Protocols, Power Management and Applications***,

- We conduct an extensive survey on routing protocols, power management and applications of WSNs. We highlight the main high-level challenges when designing WSNs. We then focus on a particular sensor network application for soil moisture monitoring.
- We classify the existing routing approaches in the literature by considering the network architectures as data-centric, hierarchical and location-based. In power management, the solutions to extending network lifetime are categorized as energy-efficient approaches and environmental energy harvesting techniques. For soil moisture monitoring, we compare traditional methods for soil moisture measurement and collection using WSNs.
- We illustrate the benefits and limitations of the surveyed approaches, and summarize the main techniques in each category.

In Chapter 3 ***Performance Evaluation of a Converge-cast Protocol for IEEE 802.15.4 Tree-Based Networks***,

- We propose a robust and low-complexity protocol for converge-cast WSNs with a tree topology based on the IEEE 802.15.4 standard. Our protocol leverages the MAC-layer communication and maintenance schemes specified by IEEE 802.15.4.

- We propose a high-layer framing structure that specifies the periods of a node's operation in a beacon interval.
- We introduce a beacon flooding scheme for network synchronization and a FIFO scheme for data storage and forwarding in our framing structure.
- We demonstrate the simplicity of our proposed protocol in the stages of network implementation and operation, the ability for quick network synchronization and recovery in the face of node failures, and performance by using an experimental WSN test bed.

In Chapter 4 ***Power Management for Unattended Wireless Sensor Networks***,

- We propose a systematic approach to the design of a power supply subsystem for unattended WSNs. Our design approach is based on the solar energy harvesting technique, which ensures the energy-balanced operation of a sensor node.
- We utilize a simple and robust charge circuit in the design of the power supply subsystem.
- We propose a 4-step design procedure for selecting the appropriate elements in our charge circuit by considering the given load energy requirements and the varying solar conditions.
- We formulate the energy variations in the subsystem by using a sinusoidal sunlight motion model, and give a threshold condition for energy-balanced operation and parameter constraints in a safe operating range.
- We conduct comparative experiments using a WSN test bed in an outdoor environment to evaluate the robustness and performance of our proposed approach.

In Chapter 5 ***Low-cost Plant-based Sensing for Irrigated Agriculture***,

- We propose an image-based sensing approach for measuring field-scale soil moisture. Our approach is to sense the light reflectance in the leaf surface of the observed plant to determine soil moisture levels.
- We investigate the feasibility of using low-cost imaging sensors to measure NDVI, which indicates the light reflectance in the particular spectrum where plant photosynthesis occurs.
- We present an experimental methodology to investigate the correlation between NDVI and soil moisture by conducting experiments under controlled environmental conditions.

In Chapter 6 ***Conclusions***,

- We summarize the major results that have been concluded in the previous chapters.
- We discuss some possible directions of future research.

1.5 List of Publications

The following publications arising from this thesis appeared during the period of being a Master of Philosophy candidate.

- X. Liu, C. Leckie, and S. K. Saleem, "Performance evaluation of a converge-cast protocol for IEEE 802.15.4 tree-based networks," in *Proceedings of the 6th International Conference on Intelligent Sensors, Sensor Networks and Information Processing*, 2010, pp. 73-78.
- X. Liu, C. Leckie, and S. K. Saleem, "Power management for unattended wireless sensor networks," in *Proceedings of the 7th International Conference on Intelligent Sensors, Sensor Networks and Information Processing*, 2011, pp. 329-334.

Chapter 2

A Survey on Wireless Sensor Networks: Routing Protocols, Power Management and Applications

Wireless sensor network technologies offer a promising solution to a range of applications in remote monitoring and control. The design and use of wireless sensor networks are quite application-specific. This chapter outlines the high-level design challenges and issues for the use of wireless sensor networks, and reviews the key techniques in the literature, specifically in terms of the routing protocols and power management approaches. We outline how wireless sensor networks can be used for soil moisture monitoring and discuss the benefits compared with traditional methods. Finally, we describe an experimental platform for wireless sensor networks called NICTOR. NICTOR is used for the purpose of experimental evaluation in the subsequent chapters.

2.1 Introduction

Recent advances in micro-electro-mechanical systems (MEMS), wireless communication technologies and digital electronics have led to a rapid development of wireless embedded devices [2, 4, 6, 134]. The key features of such devices, such as low cost, low power, small size and high performance, make it feasible to utilize large numbers of wireless devices for remote monitoring in a self-configurable and energy-efficient way. In fact, wireless sensor networks (WSNs) are designed and implemented particularly for this objective. The WSN is normally comprised of a large number of sensor nodes, which are deployed in a spatial area that contains the phenomena of interest. The main functions of the sensor nodes are to sense the relevant phenomena

of interest, perform simple data processing, and receive and/or send data via the radio transceiver. The sensor nodes also have self-organizing and cooperative capabilities, which enables them to be deployed in complex environments (e.g., inaccessible regions) and quickly recover from network faults. The benefits of such sensor nodes ensure a wide variety of applications, e.g., environmental monitoring and vehicle tracking [4, 10, 112].

Power supply design is a major concern for the deployment of untethered sensor nodes, since they are often powered by batteries with a finite energy capacity [4, 9, 126]. Once sensor nodes are physically deployed, it is not cost-effective to replace batteries regularly to extend each node's lifetime. Considerable research has focused on addressing such challenges in WSNs. In this chapter, our aim is to specify the key high-level design challenges for WSNs and survey the relevant solutions in the literature, particularly in the scope of routing protocols and power management. In addition, the specific sensor network applications of soil moisture monitoring and a case study of a wireless embedded device for WSNs are discussed.

The rest of this chapter is organized as follows. In Section 2.2, we outline the high-level design challenges and relevant issues for WSNs. In Section 2.3, the main state-of-the-art routing protocols are categorized into data-centric routing, hierarchical routing and location-based routing, and we survey each class individually. In Section 2.4, key power management techniques for WSNs are reviewed. In Section 2.5, we survey sensor network applications in soil moisture monitoring and highlight the main practical system designs and implementation. In Section 2.6, a typical wireless embedded device for WSNs is presented. Section 2.7 summarizes this chapter.

2.2 High-level Design Challenges and Issues

The design challenges for WSNs depend on the specific application requirements. For different application tasks, the design objective and network architecture may not be the same. For example, sensor networks for healthcare applications usually require high reliability and accurate data delivery. Low transmission latency is a key concern in applications for fire detection [4, 145]. In this section, we summarize the key high-level design challenges for WSNs.

Node deployment – Depending on the application, the deployment of sensor nodes can be either pre-determined or random. Deterministic node deployment refers to

sensor nodes that are located and connected with each other in a pre-configured pattern. Data is also routed to the base station via a pre-determined path [2, 6]. In random deployment, sensor nodes are randomly distributed in the monitoring field. In these deployments, sensor nodes self-organize by forming an ad hoc WSN using a peer-to-peer approach [122]. In applications with a large number of nodes, the WSN can be divided into several clusters to achieve larger coverage and higher performance. Each cluster contains several sensor nodes and a central *access point* (AP) called the *cluster head*. In the case that the nodes are not distributed uniformly, how to optimally cluster the sensor network and position the base station and cluster heads based on the limited resources in the sensor nodes becomes a critical issue in order to achieve efficient operation in terms of data routing and energy utilization [66, 150].

Data aggregation – In propagating data to the base station, duplicate messages may be generated by the intermediate nodes. Data aggregation can be used to reduce data flow in the network. In general, data aggregation eliminates duplicate or similar data packets received from different sources and/or combines the rest of them by using appropriate aggregation functions, such as *duplication suppression* [79] and *opportunistic data aggregation* [49]. It has been indicated in [51] that there is a significant reduction in energy consumption of the sensor nodes by aggregating data before transmission. It also suggests an alternative data aggregation through signal processing approaches, which is referred to as *data fusion*. For instance, the seismic signals from different sensors can be translated into a composite signal in the cluster head by using *beamforming* algorithms [147]. The transmission of this composite signal achieves a substantial energy saving.

Although data aggregation reduces traffic load and node energy demand, it potentially increases the data transmission delays because data from some nodes may have to be held at the cluster head in order to be aggregated with data from other sources [51]. In addition, the head node in each cluster may require more powerful processing and storage capabilities than the regular sensor nodes, thereby increasing the total cost.

Data delivery models – The methods of data delivery in WSNs are application-dependent. Data delivery can be categorized as *continuous*, *event-driven*, *query-driven* or *hybrid* [133]. In the continuous model, sensor nodes periodically sense the environment and transmit the data messages to a network coordinator at constant time intervals. This model is particularly suitable for applications where continuous

reporting of environmental conditions is required, such as weather monitoring. Clustering techniques are claimed to be most efficient for static WSNs using periodic data reporting methods [50]. In the event-driven models, the observer is only concerned with phenomena that meet specific conditions. Sensors transmit information to the coordinator only if the events of interest occur. Similarly, in the query-driven model, sensors perform data sensing and transmission when a request is generated by the coordinator or intermediate node (e.g., cluster head). It is also feasible to combine one or more methods in the same network. This is referred to as a hybrid model.

Network performance may be greatly affected by the interoperability of the data delivery model and the routing protocol employed in WSNs [143]. For example, in a WSN application for the detection of radioactive materials [133], the event-driven model and flooding routing scheme are used, such that if the radioactive material is detected, the sensor broadcasts the emergency signal to its neighbors who rebroadcast this message until it reaches the remote center. In this scenario, multiple sensor nodes may sense this event and send the message simultaneously, which potentially increases the likelihood of packet collisions in wireless communication and the loss of this critical information. The latency of information reporting in this scenario is also a critical concern.

Network dynamics – WSNs can be classified by considering the mobility of the sensor nodes or the monitored phenomena. In static WSNs, there is no motion of the sensor nodes or coordinator. Otherwise, it is referred to as a dynamic WSN [82]. In contrast to the fixed-node configuration, the mobility of sensor nodes gives more flexibility and efficiency in many applications, such as in environmental monitoring [33]. However, introducing mobile nodes in WSNs also increases the difficulty of data transfer from or to the moving nodes, since the varying geographical locations of a sensor node may cause changes of network topology and traffic route. In this case, extra energy and communication bandwidth may be required for network coordination and data path recalculation.

In many studies, the sensed phenomena are stationary, known as static events, such as temperature monitoring. However, in some applications they can be mobile. A target positioning, navigation and tracking application is one example [44]. In general, for the purpose of timely updates in the conditions of the phenomena, it requires more frequent reporting to the network coordinator for monitoring dynamic events than

static ones.

In the design of WSNs, the mobility of network components – either sensor nodes or the sensed phenomena, has a direct influence on the deployment of the infrastructure framework, routing protocol, data aggregation method, data delivery mode, and so forth. This affects network performance and energy efficiency. For example, a typical scenario of mobile phenomena is studied in [25], where an approach called a *Frisbee model* is used to minimize the power of sensor nodes and achieve the sensing goals (e.g., accuracy and latency) through activating the sensors inside a Frisbee circle in an event-driven model.

Lifetime extension – In WSNs, the lifetime is an application-dependent performance metric, which can be measured by the time until either a pre-specified number of nodes fail or the network stops providing the results of interest [133]. Sensor nodes are commonly powered by batteries with finite energy. In this case, the utilization of energy-efficient protocols [51, 87, 117, 149] becomes essential in order to prolong the WSN lifetime. Moreover, *energy harvesting* techniques [91] are also widely used in many applications, e.g., the use of solar power [110]. However, this type of approach strongly depends on the ambient conditions around the sensor nodes (e.g., the solar irradiance).

Fault tolerance – Sensor nodes in WSNs may not function correctly or fail due to communication interference, hardware damage, energy depletion and malicious network attacks. It is likely that node failure causes deferred data reporting or missing critical events. To minimize the effects of interruption in the face of sensor node faults, it is essential to enhance the fault tolerance of the WSN by predicting the potential faults and applying appropriate recovery mechanisms.

Here are two typical scenarios of fault tolerance. In the case of strong interference in wireless channels, a popular approach to ensure successful data delivery to the coordinator is the use of *retransmission* and *replication* schemes [8, 75]. However, the major issue with these approaches is that they increase network traffic load and require higher resource consumption (e.g., energy and bandwidth). In response to node failure, one of the most common approaches is to use *multipath routing*. In this approach, a primary path for data delivery between each sensor node and the coordinator is established during network initialization. Once any links or nodes fail on this path, an alternative path is constructed based on a least-cost or balanced rule [55]. Normally, the use of alternative paths causes much higher energy consumption

and longer latency. Furthermore, for the construction of alternative paths, sensor nodes need knowledge of the network topology.

Network cost – A WSN is comprised of a large number of nodes, such as sensor nodes, actuators, routers and the base station. In such an installation, even a small change in the cost of a single node can significantly affect the total cost of the sensor network. In addition, for many applications, sensor nodes are unable to be recycled and reused, once they are physically deployed in the particular environments (e.g., a forest or ocean). As a consequence, designing low-cost sensor nodes has great significance for the practical deployments of sensor networks.

2.3 Routing Protocols

The network protocol is one of the most significant elements of WSNs, and is dependent on the underlying network architecture, requirements and applications. The protocol stack presented in [4] includes the *physical layer*, *data link layer (MAC)*, *network layer*, *transport layer* and the *application layer*. In this section, we focus on the state-of-the-art network-layer protocols for WSNs, known as the *routing protocols*, and highlight some representative approaches.

A taxonomy of routing protocols for WSNs has been developed in several different ways. For example, the protocols in [6] are classified as *multipath-based*, *query-based*, *QoS-based*, *coherent-based* and *negotiation-based*. Mobile ad hoc WSN routing protocols can be categorized into *topology-based* and *position-based* routing, and the latter can be further divided into *proactive*, *reactive* and *hybrid* [80, 92]. In our survey, we classify the routing protocols as *Data-centric*, *Hierarchical*, and *Location-based routing* by considering the network architectures. Converge-cast routing is another classic technique for scheduling data transmission in WSNs. It can be achieved by using one of the routing protocols classified above, or some hybrid of those protocols. Chapter 3 gives a detailed description of converge-cast routing.

2.3.1 Data-centric Routing

In many sensor network applications, it is not feasible to propagate the global network topology to every sensor node. In this case, data dissemination in WSNs cannot be

performed using traditional *address-based* routing, where the source uses a route discovery scheme to find a particular path to the destination for data transmission. In data-centric routing, the sensed data is delivered to the coordinator by using broadcasting and querying mechanisms, which do not require the propagation of the global knowledge among sensor nodes, and consequently leads to a substantial reduction in the network traffic load. Below we survey some protocols based on this approach.

Flooding is a classic technique widely used for data delivery in communication networks including WSNs [90, 152]. The key concept of flooding is summarized as follows. The coordinator broadcasts a request to the entire WSN. If a sensor node can respond, it will broadcast the message to its neighbors. The nodes receiving this message forward it by rebroadcasting. In this manner, the message sent to the coordinator is eventually received or discarded when a pre-specified number of re-broadcast attempts are reached.

From the process described above, flooding is a simple scheme for data dissemination in WSNs. There is no need for costly cooperation mechanisms, e.g., topology maintenance and routing discovery. However, the major drawback is the significant redundancy caused by the re-broadcasts.

Gossiping is an improvement of the flooding protocol [47]. Unlike forwarding the incoming packet by broadcasting, a receiver randomly selects a neighbor to whom to send the message. Once it is received, the neighbor repeats the same process of random node selection and forwarding. The gossiping protocol reduces the probability that a packet traverses a node more than once. However, there can be a long latency in the propagation of the packet from the source to the coordinator, which makes gossiping unsuitable for delay-sensitive applications.

Sensor Protocols for Information via Negotiation (SPIN) are a family of adaptive protocols that are developed to overcome the drawbacks of the flooding protocol [52]. The key idea is to use a high-level attribute-based naming method that describes the sensing data and generates the corresponding meta-data. The exchange of meta-data allows the coordinator to query the data of interest from a selected set of sensor nodes. There are three types of messages specified by SPIN, namely ADV, REQ and DATA. DATA is a message that includes the actual sensing data, and ADV and REQ are signaling messages containing the meta-data of DATA, which are used to advertise and request DATA to and from the neighbors.

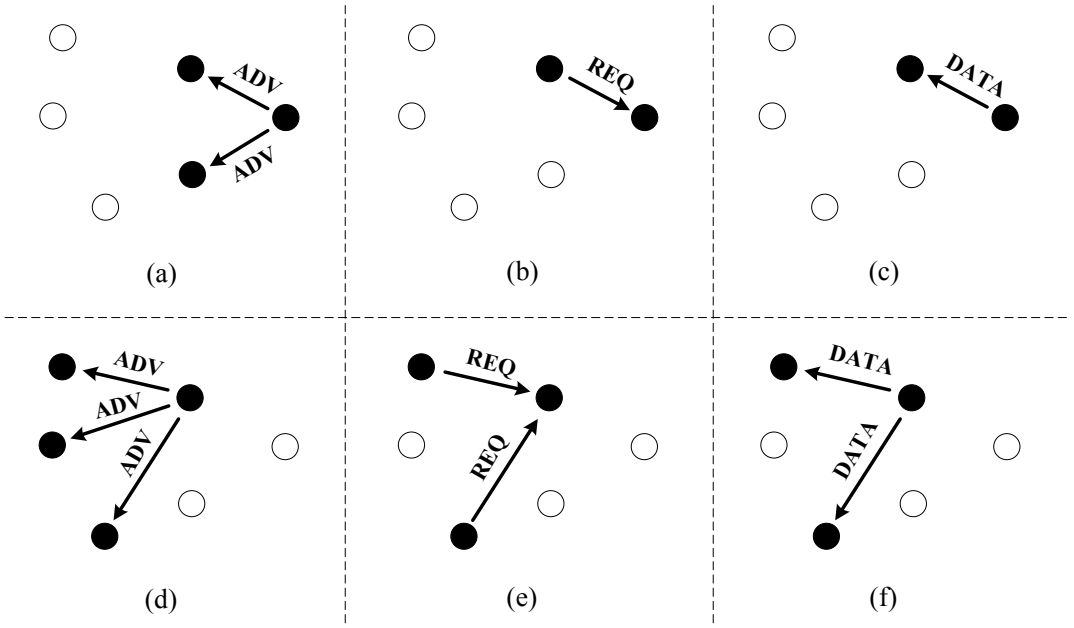

Figure 2.1: The SPIN protocol [52]

Figure 2.1 illustrates an example of the SPIN protocol. As shown from Figure 2.1(a) to (c), a sensor node broadcasts an ADV message to its neighbors. The neighbor that is interested in the DATA sends a REQ message back to request it. Once the DATA message is received, the same procedures are repeated as illustrated from Figure 2.1(d) to (f). This advertise-request mechanism of the SPIN protocol ensures that every sensor node can receive a copy of the data of interest.

The meta-data negotiation of the SPIN protocol among the senor nodes prior to data transmission significantly reduces redundant information compared to flooding. Moreover, the energy efficiency of sensor nodes is improved by adjusting the operating states based on energy resource information included in the meta-data. However, in the case of data delivery along multi-hop paths, the DATA message may not be delivered to the destination if the intermediate nodes are not interested in this DATA. As a result, assigning the appropriate interests to sensor nodes is critical for the SPIN protocol.

Directed Diffusion is a key breakthrough in data-centric routing protocols [62]. It is developed based on two ideas. First, sensed data is named by using the *attribute-value pairs* that describe the sensing tasks. Second, nodes can request sensed data by broadcasting the attribute-value pairs to the entire sensor network. Figure 2.2 shows three steps (a) – (c) in directed diffusion. In Figure 2.2(a), the coordinator propagates

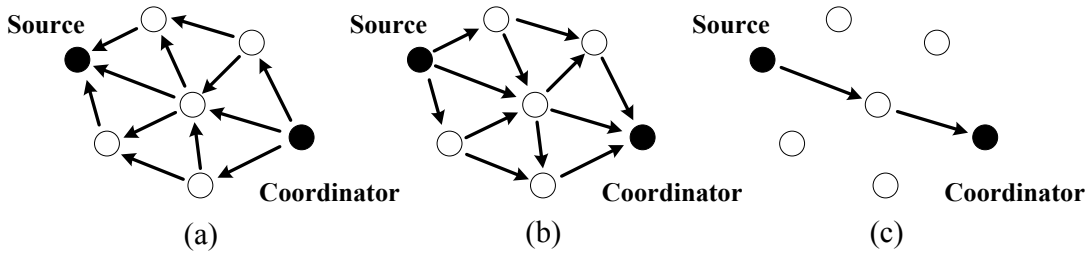

Figure 2.2: The directed diffusion protocol [62]

the interest using the attribute-value pairs throughout all the sensor nodes. Each node caches both the interest information and its entry including a timestamp and several gradient fields. The gradient is defined as the reverse link of the interest propagation between the neighbors. Once this propagation is completed, several paths from the source to the coordinator are established by using the gradient information as shown in Figure 2.2(b). In the final step, the *reinforcement* scheme is used to select an optimal path with the least hops, as in Figure 2.2(c). The periodic refreshment and retransmission of the interest along the selected path is necessary in order to reinforce the node from which its neighbor receives an unseen data message before.

In the case of path failures, directed diffusion enables path repair by reinitiating the reinforcement scheme to establish an alternative path. This feature enhances fault resilience. In addition, data caching and aggregation effectively reduce the redundant traffic flow and achieve energy-efficient routing without consideration of the global topology maintenance. Compared to SPIN, directed diffusion performs the queries in the global scope (rather than the local neighbor-to-neighbor scope) by flooding the interests, and overcomes the issue of unreliable data delivery via the multi-hop paths in SPIN by the reinforcement scheme. Note that, in essence, since directed diffusion is a routing protocol based on the query-driven data delivery model, it may not achieve efficient operation in applications that require continuous data delivery, e.g., environmental monitoring.

2.3.2 Hierarchical Routing

The data-centric routing protocols described in Section 2.3.1 are mostly applied in so-called single-tier WSNs, where there is only one gateway or cluster head. When the number of sensor nodes exceeds a maximum value that the coordinator is capable of

coping with, overall performance of the WSN deteriorates rapidly due to message overload. Consequently, this limited scalability of single-tier architectures restricts the growth in network size and the use of WSNs with a large number of sensor nodes.

The consideration of routing and energy efficiency in large-scale WSNs has led to the development of a multi-tier architecture, known as *cluster-based* or *hierarchical* routing approaches. In hierarchical routing, sensor nodes are grouped based on geographical position and each group is referred to as a cluster. Inside a cluster, the higher-energy node is normally selected as the cluster head, which is responsible for performing data aggregation and communicating with other clusters. For large-scale WSNs, hierarchical routing is an efficient way to reduce the energy consumption of sensor nodes inside the clusters and the volume of data transmission between clusters. Interestingly, in addition to routing, cluster formation is the other significant part in hierarchical architectures. Based on the available energy resources and geographical distribution of sensor nodes, how to cluster a WSN and select cluster heads have become critical problems [13, 51, 89]. In this section, several routing protocols using hierarchical approaches are described.

Low-Energy Adaptive Clustering Hierarchy (LEACH) is one of the early cluster-based protocols for WSNs [51]. The main idea of LEACH is to avoid direct communication from sensor nodes to the coordinator by forming local clusters, thus lowering energy consumption. The operation of LEACH is segmented into *rounds*, similar to the concept of the *beacon interval* in the MAC layer, which is described in Chapter 3.4. In each round there are two phases: the *set-up phase* (cluster formation) and the *steady-state phase* (data aggregation and dissemination).

To form clusters in the set-up phase, the cluster head is selected first by comparing a threshold $T(n)$ with a number between 0 and 1 chosen randomly by sensor node n. If this random number is less than $T(n)$, the node becomes the cluster head for the current round. The threshold $T(n)$ is defined as:

$$T(n) = \begin{cases} \dfrac{P}{1 - P * \left(r \bmod {}^{1}/_{P}\right)} & \text{if } \ n \in \mathrm{G} \\ 0 & \text{othrwise} \end{cases} \qquad (2.1)$$

where P is the desired percentage of cluster heads, r is the count of the current round, and G is the set of sensor nodes that have not been selected as the cluster heads in the last $1/P$ rounds. Once the cluster heads are selected, they broadcast advertisement

messages with the same transmit energy to the remaining sensor nodes, which decide to join the cluster head based on the largest received signal strength of the advertisement for this round. After completing the involvement of sensor nodes, the cluster head broadcasts a schedule message to all the sensor nodes in the cluster to allocate a dedicated time period to each of them for data transmission using *Time Division Multiple Access* (TDMA) scheduling.

The steady-state phase usually has a longer duration than the set-up phase in order to avoid excessive overhead for cluster formation. In this stage, sensor nodes execute sensing tasks and send data to the cluster head. The radio of a sensor node can be shut down to conserve energy until the scheduled transmission period arrives. In contrast, the cluster head must keep its radio on all the time for data reception. Before transmitting data to the coordinator, the cluster head performs the necessary data processing, i.e., aggregation and compression. After this stage finishes, the WSN enters into the next round of the LEACH protocol and repeats the same set-up and steady-state phases as described above.

It has been indicated in [51] that LEACH achieves a considerable extension of WSN lifetimes, which gives a factor of 7-8 and 4-5 reduction in overall energy consumption compared with direct communication and minimum-transmission-energy routing (MTE) [96, 120], respectively. In LEACH routing, data is propagated from a sensor node to the coordinator only via a cluster head. The 2-hop transmission path limits the WSN deployed in large regions, since each sensor node has limited radio power and transmission distance. LEACH assumes that all the nodes begin with the same amount of energy and the cluster head consumes approximately the same amount of energy as non-cluster-head node in each round. This assumption may not be the case in practice. Moreover, the dynamic clustering technique specified in LEACH periodically changes the topology, which requires substantial overhead for network reorganization and synchronization.

Threshold sensitive Energy Efficient sensor Network protocol (TEEN) is an energy-efficient hierarchical routing protocol [89]. The major purpose of TEEN is to achieve rapid and accurate data reporting in response to changes of the monitored phenomena in time-critical applications. The hierarchical clustering scheme in TEEN is developed based on the LEACH hierarchy model [51] and allows for multi-level cluster formation. An example of 2-level clustering in TEEN is given in Figure 2.3. In TEEN, each sensor node senses the phenomenon continuously, but only transmits

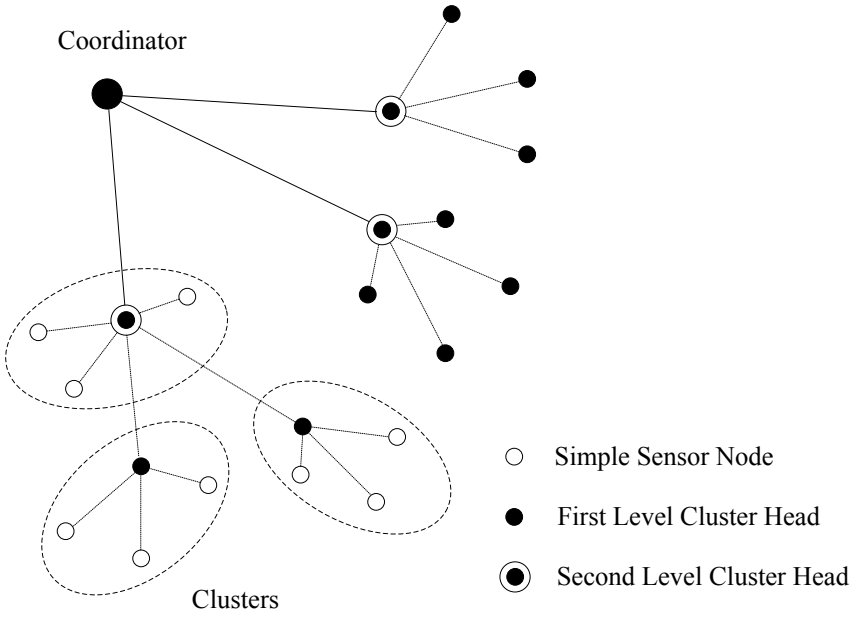

Figure 2.3: An example of hierarchical clustering in TEEN [89]

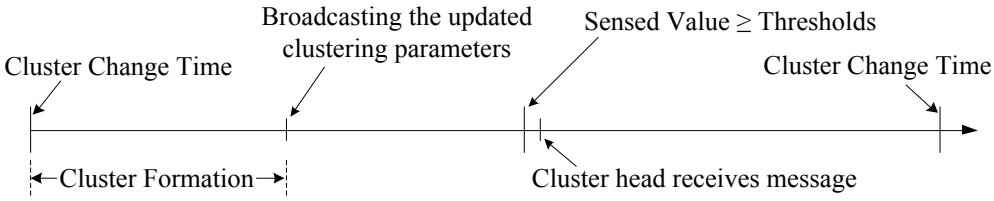

Figure 2.4: Time line for TEEN [89]

sensed data in particular conditions specified by two threshold values, the *Hard Threshold* and the *Soft Threshold*, which are broadcast by its immediate cluster head. The hard threshold specifies the absolute value of the attribute for the monitored phenomenon, while the soft threshold specifies the difference between two consecutive sensed values. The sensor node turns on its transmitter and sends data to its immediate cluster head only when both the current sensed value and the difference from the previous one are greater than or equal to the hard and soft thresholds, respectively. Since cluster heads need to perform additional data processing and transmitting over a longer distance than sensor nodes, TEEN suggests that cluster heads are re-selected after a certain time period T, called the *cluster period*, in order to balance overall energy distribution in WSN. After cluster heads are selected, relevant clustering information is broadcast to all sensor nodes. Figure 2.4 shows a typical time line for TEEN in a cluster period.

The conditional data transmission scheme in TEEN significantly lowers network traffic and the probability of packet collision, which provides low delay for data propagation from sensor nodes to the coordinator. A multi-level clustering hierarchy effectively expands the WSN coverage. These key features make the TEEN protocol well suited to time-critical applications. Furthermore, TEEN provides large-scale flexibility to trade-off energy consumption and sensing accuracy by selecting the adequate soft and hard thresholds. However, the use of large thresholds may cause key events to be missed or uncertainty about the availability of sensor nodes from which no data has been received over a long period. At the other extreme, using very small thresholds leads to excessive node energy consumption due to frequent data reporting. Therefore, TEEN is not suited for applications where continuous data reporting is needed. The proper selection for the thresholds in TEEN is critical, particularly in the case where non-uniform thresholds are required for different types of monitored phenomena.

Two-Tier Data Dissemination (TTDD) is a grid-based data dissemination routing protocol for WSNs, which is designed to support data transmission from sensor nodes to mobile base stations [148]. TTDD assumes that every sensor node in the network located in a fixed position (static), except for the coordinator that moves dynamically over time, and there is no overlap such that the sensed data for each phenomenon is reported only by one sensor node.

Data dissemination in TTDD can be done in three stages, *Grid Construction*, *Query Forwarding* and *Data Forwarding*. In constructing the grid, each source node divides the network plane into a *grid* of square cells and positions itself at one crossing point of the grid. The nodes closest to other crossings are selected as the *dissemination nodes* by recursively propagating the data announcement messages using a greedy geographical forwarding algorithm. After constructing the grid, the mobile coordinator sends a query to source node via two tiers. Low-tier path is established within the grid cell where the coordinator is located, and the high-tier is the path comprised by dissemination nodes. In query forwarding, the query is flooded to the immediate dissemination node in the local cell, and then is forwarded through upstream dissemination nodes until it reaches the source. Afterwards, the data forwarding stage begins. The source node sends data back along the path that the query traverses. Once data arrives at the immediate dissemination node, it is further relayed to the coordinator via the low-tier path by using the *Trajectory Forwarding*

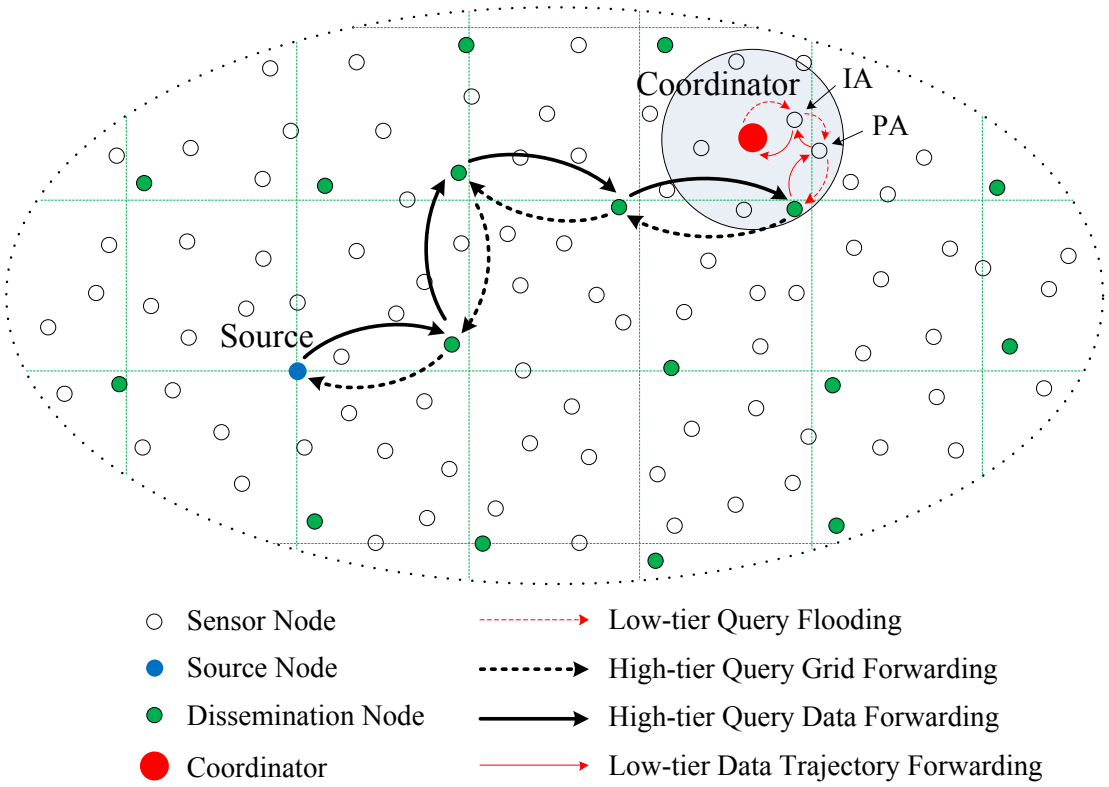

Figure 2.5: Two-tier query and data forwarding in TTDD [148]

scheme. This scheme dynamically selects the transit nodes, called the *Primary Agent* (PA) and *Immediate Agent* (IA), to accommodate location changes of the coordinator. Figure 2.5 gives an illustration of two-tier query and data forwarding in TTDD.

TTDD is an efficient routing protocol for large-scale WSNs and also supports data delivery to multiple mobile coordinators. The experimental results in [148] demonstrate that TTDD achieves performance comparable with the popular directed diffusion protocol in terms of the successful data delivery ratio and energy consumption, but with shorter data delivery delays. The operation of TTDD is based on the assumption that nodes are location-aware. However, the availability of accurate position information in all the sensor nodes may not be feasible in some WSN applications. Moreover, the overhead associated with grid maintenance is substantial for a large number of nodes.

2.3.3 Location-based Routing

In wireless communications, the energy consumption of sensor nodes is mainly affected by the communication distance among them. In order to find the optimal

source-destination path in which there is minimum total energy consumption, some routing protocols require knowledge of location or geographical information in all or part of the sensor nodes. This kind of protocol is referred to as *location-based routing protocols* [92, 124]. The distance between two adjacent nodes commonly can be estimated based on received signal strengths. In contrast, the use of a positioning device (e.g., a low-power GPS receiver) can provide more accurate location information, but also increases total cost.

Location-based routing protocols allow the coordinator to query sensor nodes in designated regions. Nodes that are not involved in data sensing and propagation can be switched into sleep mode to conserve energy. Based on location information stored in the sensor nodes, query and data propagation can be achieved through several routing strategies, e.g., minimum transmission hops [56, 128], minimum spatial distance [78] and restricted directional flooding [14, 151]. In this section, we review some important location-based routing protocols in the literature.

Greedy Packet Forwarding utilizes a set of greedy routing algorithms to achieve source-destination data propagation based on geographical position information provided by location services, e.g., quorum-based services [45, 125] and grid location services [84, 98]. In greedy routing, a packet initiated at the source is forwarded hop-by-hop by following a certain strategy until it reaches the destination. Popular forwarding strategies include *Most Forward within Fixed Radius* (MFR), *Most Forward within Variable Radius* (MVR), *Nearest with Forward Progress* (NFP) and *Compass Routing*. An example of these greedy routing strategies is shown in Figure 2.6.

In Figure 2.6, all the nodes are assumed to be identical. Each node has a maximum radio transmission radius r, and multiple paths exist between the source and coordinator.

In MFR [128], packet is always forwarded to the node that is closest to the destination. The aim of this strategy is to find source-destination path with minimum number of hops. By applying the MFR method in this example, a packet is propagated to the coordinator via intermediate nodes C and F.

MVR [56] is similar to MFR except that the transmit power is dynamically adjusted based on distance between two communicating nodes, unlike the fixed transmission radius (r) applied by MFR. As a result, MVR has the same source-destination path, but achieves lower energy consumption and a smaller packet conflict

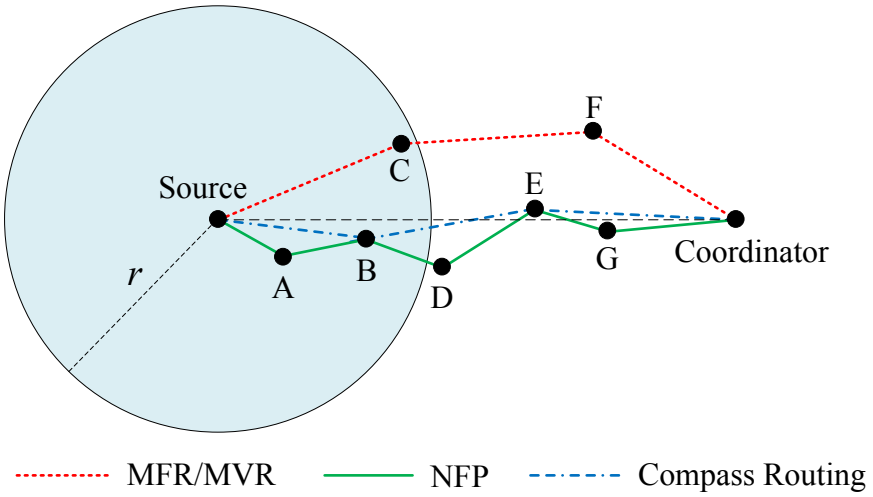

Figure 2.6: Greedy routing strategies [92]

domain.

In NFP [56], the same power adaptive scheme for packet transmission is used as in MVR, and the source or intermediate node transmits a packet to its nearest neighbor towards the destination. NFP minimizes the probability of packet collision and consequently decreases node energy consumption. By using this nearest forward strategy, the source-destination path in Figure 2.6 is comprised of the intermediate nodes A, B, D, E and G.

Compass routing [78] is an efficient greedy strategy that tries to minimize the spatial distance of data transmissions between the source and destination, which effectively lowers overall energy consumption. In compass routing, a packet is transmitted to the neighbor that is closest to the straight line from current node to the destination. In this way, the route to the coordinator in Figure 2.6 traverses the intermediate nodes B and E.

The major challenges associated with greedy routing protocols described above are to overcome the failure of route discovery and avoid the occurrence of routing loops. For example, a typical scenario where the greedy algorithm discussed in [92] terminates is when the current node is closer to the destination than other nodes in its maximum transmission range and the destination is located outside this range. This problem can be solved by using the *least backward progress* method proposed in [128]. However, this may cause a looping problem. Loop-free greedy routing protocols with guaranteed delivery in WSNs are further studied in [56, 124].

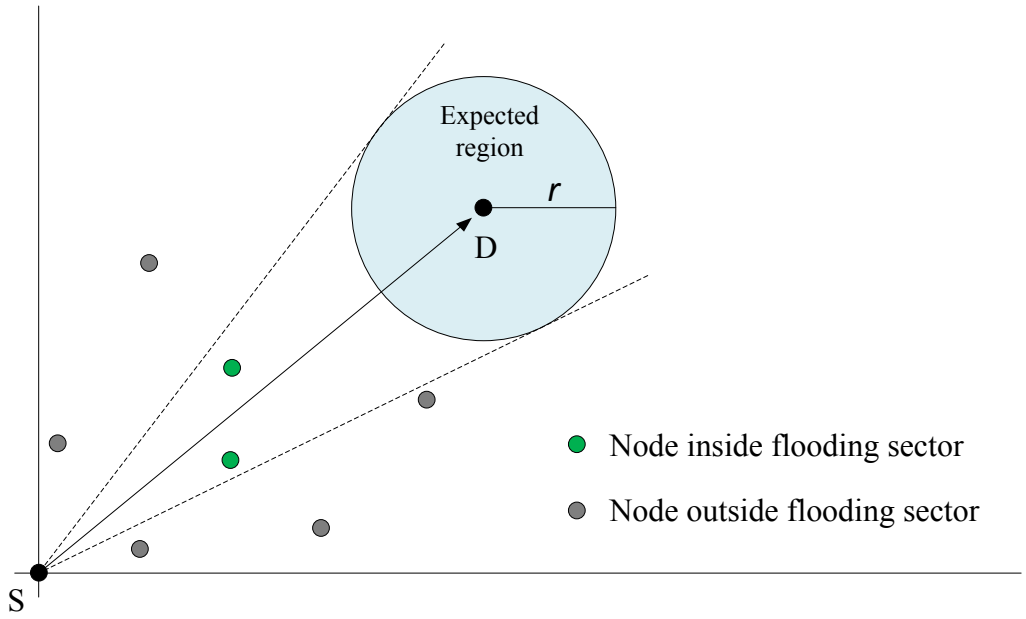

Figure 2.7: The diagram of directional flooding in DREAM [14]

Distance Routing Effect Algorithm for Mobility (DREAM) is a robust routing protocol for data dissemination to static or mobile nodes in ad hoc networks by using a directional flooding scheme [14]. This protocol is designed based on two basic concepts. One is the so-called *distance effect*, which refers to "the greater the distance separating two nodes, the slower they appear to be moving with respect to each other". This fact demonstrates that up-to-date location information can be propagated less frequently to the parent nodes without losing routing accuracy. Second is the *node's mobility rate* upon which the update frequency should be adapted. The faster the node moves, the more frequently location information is updated.

In DREAM, each node locally maintains location information for all other nodes in the network and regularly floods its own up-to-date position message to them. In propagating a packet to the destination, the source first multicasts this packet to the neighbors located in the direction toward the destination. Neighbors then use their own location information to repeat the same multicasting process. By such directional flooding, the packet is eventually forwarded to the destination. The flooding direction mentioned above can be determined as follows. In Figure 2.7, the source S has position information about the destination D with timestamp t_0, and the maximum travelling speed of a node in the network is known as v_{max}. The possible new positions of D at time t_1 can be predicted by drawing the so-called *expected region*,

which is a circle around its old position at time t_0. The radius r of this circle is equal to $(t_1 - t_0)v_{max}$. With respect to S, the flooding direction toward to D is defined by the sector enclosed by two tangents from S to the given expected region, as depicted in Figure 2.7.

The benefits of DREAM are high robustness and resilience to node and path failures, since duplicated packets are produced and forwarded to the destination via multiple routes by using the directional flooding mechanism. DREAM gives the flexibility to control the overhead used for route maintenance by adjusting the update message frequency based on the node distance and mobility rate. Although the use of a lower updating frequency can effectively reduce the overhead, it increases the flooding domain, which in turn may result in a heavier traffic load. Therefore, updating frequency must be selected properly in order to minimize the network traffic and the probability of packet collision. Given that the operation of DREAM requires regular propagation of up-to-date position messages among all the nodes for route calculation, the overhead grows substantially even if there is a slight increase in the number of nodes. The poor scalability means that DREAM may not be applicable to large-scale ad hoc WSNs.

Geographical and Energy Aware Routing (GEAR) is a recursive data dissemination location-based routing protocol for ad hoc WSNs [151]. The development of GEAR is mainly motivated by the need for disseminating queries to sensor nodes lying in the geographical regions of interest in many WSN applications. GEAR assumes that sensor nodes are static and location-aware.

Unlike directed diffusion that directly floods a query to the whole network, GEAR propagates a packet to the target region in a routing- and energy-efficient way by using a two-phase forwarding process – forwarding a packet towards the target region and then disseminating the packet within the region. In the first phase, a heuristic neighbor selection approach is used to route the packet. GEAR selects the neighbor closest to the target region as the next-hop node. In the case that all the neighbors are farther away than the current node, the next-hop node is selected based on the cost associated with its neighbors, e.g., residual energy. Cost values are frequently updated by a simple *Neighbor Hello Protocol* [151]. When a packet reaches the region, either the so-called *Recursive Geographic Forwarding* algorithm or restricted flooding is used to disseminate the packet within the region. GEAR suggests using restricted flooding in low-density networks. In high-density conditions, the proposed recursive

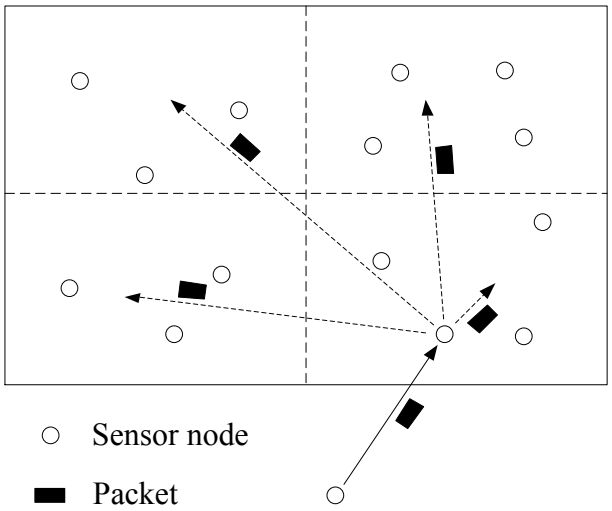

Figure 2.8: Recursive geographic forwarding in GEAR [151]

geographic forwarding scheme can give less energy consumption, and its operation is summarized as follows. As shown in Figure 2.8, the target region is divided into four sub-regions, and a copy of the packet is sent to each of them separately. This splitting and forwarding procedure is repeated until the sub-region only contains one node. When there are no nodes in the sub-region, the packet is discarded.

In GEAR, sensor nodes do not need to maintain location information for other nodes and broadcast their own location message. This results in lower overhead and greater scalability compared with DREAM. In query-driven routing protocols, the query is propagated to the sensor nodes that store the data of interest. GEAR can request data from the sensor nodes that are located within a certain geographical region. The use of energy-aware metrics and unicast forwarding with geographical information makes GEAR perform energy-efficient routing. The comparison results in [151] show that GEAR achieves lower energy consumption for route calculation and data transmission than a similar non-energy-aware geographical routing protocol [70].

2.3.4 Summary

In this section, we classify state-of-the-art routing protocols for WSNs into data-centric, hierarchical and location-based routing, and survey the key routing technologies in each category separately. Table 2.1 summarizes the protocols that have been reviewed in this section and compares them based on several relevant

Table 2.1: Summary and comparison of routing protocols for wireless sensor networks

Routing Protocols	Data-centric	Hierarchical	Location-based	Static node	Mobile node	Mobile sink	Event-driven	Query-driven	Continuous	Energy efficiency	Data aggregation	Fault tolerance	Scalability
Flooding [90, 152]	✓				✓				✓			✓	
Gossiping [47]	✓			✓					✓				✓
SPIN [52]	✓			✓				✓		✓	✓		
Directed Diffusion [62]	✓			✓				✓		✓	✓	✓	
LEACH [51]		✓		✓					✓	✓	✓	✓	✓
TEEN [89]		✓		✓			✓			✓		✓	✓
TTDD [148]		✓	✓			✓		✓				✓	
MFR & MVR [56, 128]			✓	✓					✓				✓
NFP [56]			✓	✓					✓	✓			✓
Compass Routing [78]			✓	✓					✓	✓			✓
DREAM [14]			✓		✓		✓					✓	
GEAR [151]			✓	✓				✓		✓			✓

metrics related to the design challenges discussed in Section 2.2, namely network dynamics, data delivery models, energy efficiency, data aggregation, fault tolerance and scalability.

Some key comments from Table 2.1 are outlined as follows. Data-centric protocols are essentially designed for small sensor networks and have simpler routing schemes than hierarchical and location-based routing. For large sensor networks, hierarchical protocols usually achieve better performance, but need more sophisticated routing strategies. Location-based protocols are more efficient in route discovery, particularly in the case when nodes move continuously. However, the need for frequent location information updates across the network in location-based routing results in substantial overhead. This limits the network dimension and scalability. In addition, data aggregation is an effective approach used to reduce redundancy in data dissemination and improve energy efficiency, but introduces a data delivery delay. The periodic re-selection of cluster heads in hierarchical routing manages to balance energy distribution in the sensor network and enhance the resilience to node failures, but requires additional common overhead. Flooding is another simple scheme to improve fault tolerance, but causes poor scalability.

Clearly, there is not a routing protocol that can solve all high-level requirements. Trade-offs need to be made among several design considerations, e.g., transmissions, energy consumption, latency and data processing, according to the specific application requirements.

2.4 Power Management Approaches

Energy efficiency is a major concern in WSNs, because using a tethered energy supply usually is not cost-effective in outdoor applications. Due to the limited energy in batteries, the challenge of achieving sustainable operations for sensor nodes has been discussed widely in the research community [4, 9, 126]. The solutions can be separated into two main categories, *energy-efficient approaches* and *environmental energy harvesting*. The remainder of this section gives a detailed review of these two types of power management methods.

2.4.1 Energy-Efficient Approaches

In this case, energy efficiency is improved by optimizing the internal operations of sensor nodes and the manner of interactions between them. Data transmission in wireless communication consumes much more energy than other operations in sensor node, e.g., data sensing and processing. Using energy-efficient routing protocols can significantly reduce energy consumption. As described in Section 2.3, the greedy forwarding algorithms utilized in [56, 78] can minimize neighbor-to-neighbor and source-destination route distance, which gives the minimum energy consumption in terms of the sensor node and overall network, respectively. The routing protocols in [120, 151] use energy-aware metrics to determine the optimal routes based on the residual energy of sensor nodes, which effectively balance the energy distribution of the sensor nodes in the whole network. In the process of data dissemination, aggregating data from different sources is another efficient way to reduce the number of transmissions. For small WSNs, the method of data negotiation is used for data aggregation in [52, 62]. In large-scale WSNs, several variants of the clustering hierarchy presented in [13, 51, 89, 150] greatly lower energy consumption by selecting the appropriate cluster heads to shorten the transmission distance and aggregate data.

Matching the wakeup/sleep duty cycles of sensor nodes to real-time traffic loads is another energy-efficient approach, which is usually implemented by the MAC-layer. The aim of adaptive duty-cycling schemes is to reduce the substantial energy waste associated with idle listening. To minimize the duration of idle listening, the MAC protocols in [31, 149] allow the duty cycle to be adjusted based on a data schedule by specifying time parameters included in a special frame in a synchronous way. Improved versions are proposed in [19, 108] by adopting asynchronous communications, where the so-called *preamble sampling* technique is used between the transmitter and receiver to negotiate the schedule of data transmission and thereby limit idle listening. In [87], a similar MAC protocol for tree-based WSNs is presented, which achieves significant energy conservation by using a staggered duty cycle schedule to shorten the wake-up duration.

In [36], *adaptive fidelity* algorithms are explained to extend network lifetime. This approach trades the quality of data delivery against battery lifetime, network bandwidth or the number of active sensor nodes. By following this concept, [146]

proposes a *geographical adaptive fidelity* (GAF) mechanism that is independent of the underlying ad hoc routing protocol. GAF achieves energy savings by selectively turning off sensor nodes while maintaining network fidelity at a constant level. Task migration and remote processing, which are similar to data aggregation, are ways to achieve overall energy savings in a cluster-based network hierarchy. A stochastic decision-based approach in [113] minimizes overall energy consumption by transferring the tasks from sensor nodes to the server (i.e., cluster head) with the appropriate power management policy.

2.4.2 Energy Harvesting

It can be seen that the energy-efficient approaches are designed based on the considerations of optimizing the utilization of residual energy in sensor nodes. In contrast, *energy harvesting* takes into account energy availability and extraction from the environment around sensor nodes for lifetime extension. Perpetual operation can be accomplished by applying appropriate energy harvesting approaches that equalize the rate of energy supply and consumption. However, energy harvested from the environment may not be maintained at a constant level over time, unlike battery energy, since it varies according to environmental conditions. In poor conditions, environmental energy may be insufficient to power the sensor nodes. Thus it is challenging to sustain the operation of nodes by utilizing energy harvesting techniques in time-varying environmental conditions.

There are many potential sources of environmental energy that can feasibly power sensor nodes. These have been comprehensively reviewed in [102, 114]. In [91] the authors have outlined the primary sources for which positive research outcomes have already been achieved, including solar, thermal gradients, vibrations and human movement. The study in [91] also compares typical values of energy levels extracted from energy sources listed above, and concludes that the available amount of solar energy is much greater than the rest within a unit area or volume. In [126], it was demonstrated that using solar energy harvesting techniques can substantially prolong the lifetime for WSNs. In our survey, we focus on solar energy and highlight the key approaches.

Of the early work addressing the energy harvesting problem, [69] proposed a distributed framework for sensor networks, called the *environmental energy*

harvesting framework (EEHF). The key motivation of developing EEHF is based on the principle that environmental energy is distributed heterogeneously across the WSNs and there is a need to exploit the relationship between the spatio-temporal characteristics of energy availability and the task allocation in order to extend network lifetime. EEHF adaptively learns the properties of environmental energy through local measurements and uses this information to align task assignment in each sensor node with its energy availability. The performance of EEHF is evaluated by using a solar-powered WSN, and the experimental results show a significant improvement (i.e., up to 200%) in network lifetime compared with an energy-aware scheme [120].

The development of energy harvesting leads to another way for route selection for data dissemination in WSNs. This is referred to as the *environmental energy aware routing* protocol. The related work is outlined as follows. Solar-aware routing protocols are presented in [139] for WSNs that consist of both battery-powered and solar-powered sensor nodes. Solar-aware routing is similar to standard directed diffusion [62], except that the source-destination route is selected by preferably involving the intermediate nodes that are powered by solar energy. The protocol in [81] presents low-latency routing strategies by considering energy harvesting sensor nodes. Three kinds of costs are specified to determine the optimal route in a certain topology, namely the costs of a single hop, two hop and full path. From the experimental results, these routing strategies have better performance in high-density and low duty-cycling energy harvesting WSNs. Furthermore, [1] proposed a data collection scheme called *Green Diffusion* (GD) for solar-powered WSNs. In GD, a sensor node is dynamically identified as either a *solar-rich* (SR) or *solar-deprived* (SD) node based on the availability of solar energy, and SR nodes are used as much as possible to forward data from SD nodes in the vicinity. GD achieves greater battery energy savings and thus extends the lifetime by adopting a dynamic topology construction scheme, which adaptively adjusts the number, placement and distribution of SR and SD nodes.

Energy harvesting makes it possible for WSNs to operate in the so-called *energy-neutral* mode (i.e., perpetual operation), where the available supply from environmental energy or energy storage (e.g., batteries) is always sufficient for energy consumption. For this, a typical method is to adaptively adjust node's duty cycle to its energy harvesting rate. There have been numerous adaptive duty-cycling schemes proposed for energy harvesting WSNs, and several representative approaches are

reviewed below.

A comprehensive study of power management for energy harvesting WSNs is presented in [57, 67, 68]. The objective is to maximize the use of harvested energy and achieve energy-neutral operation. In these works, a series of analytical models are proposed based on so-called *harvesting theory* to characterize the energy harvesting sources, availability, prediction and relevant workload allocation. Based on these models, duty cycles are dynamically adjusted by observing the deviations between the predicted and actual node energy measurements, to ensure energy-neutrality. Rather than modeling the energy sources, [136] utilizes adaptive control theory to perform duty cycle adaptation based on the measurements of battery energy level, which is related to the dynamics of harvested energy from the environment. In this harvesting-aware duty-cycling approach, the considerations in achieving energy-neutral operation, minimizing the variation of duty cycles and maximizing task performance are formulated as a linear-quadratic tracking problem. Compared with the approaches in [58, 67, 68], [136] does not require a priori knowledge of the environmental energy sources for achieving energy-neutral operation and gives more stability in terms of the duty cycles.

Designing the harvesting system for WSNs is also a significant part of efficient utilization of environmental energy. An energy-harvesting node mainly comprises a harvesting component (e.g., solar panel), an energy storage component (e.g., batteries) and the load (e.g., the node). Due to the nature of time-varying environmental energy sources, the harvesting component sometimes may not provide sufficient energy to the load. In this case, the energy storage component plays a primary role in supplying energy. To achieve sustainable operation, selecting harvesting energy storage components is based on the load energy requirement, in order to make sure that the energy storage component can be recharged before it is depleted. Moreover, two key factors must be considered in designing energy-harvesting WSNs. First, the voltage-current characteristics must be matched among the components in energy-harvesting node. Second, the overall efficiency of energy conversion, transfer and storage in the harvesting system may vary widely when different materials and techniques are used. Next, we highlight some important designs and implementations of solar-powered sensor nodes.

Raghunathan *et al.* [110] presented an extensive study of the system design for solar-powered sensor nodes in terms of the underlying framework, harvesting module

and design considerations. A solar harvesting sensor node termed Heliomote is prototyped by equipping an off-the-shelf node – a Mica2 mote [54] with a custom harvesting board, a small-size solar panel and rechargeable NiMH batteries. The experimental results illustrate that Heliomote is capable of near perpetual harvesting-aware operation in outdoor applications. Minami *et al.* [97] described the design and implementation of battery-less senor nodes called Solar Biscuits, which interestingly utilize a small solar cell and a super capacitor (i.e., a high-capacity capacitor) as their energy source. The performance of Solar Biscuit is evaluated by several experiments. By utilizing both the battery and capacitor as energy storage, Jiang *et al.* [63] presented an architecture using a multi-stage energy transfer system for solar-powered WSNs. A prototype called Prometheus is designed and implemented based on the Telos Mote [109] with a small solar panel, super capacitors, a Li-ion battery and a DC-DC regulator. From the evaluation results, Prometheus allows near perpetual operation by using low duty cycles (e.g., < 1%).

Other solar energy harvesting designs and implementations, such as HydroWatch [129], Fleck1 [29], Everlast [119], Sunflower [123] and AmbiMax [103], use the same system architecture as those described above, referred to as the *Harvest-Store-Use* architecture [126]. It has been indicated in [29, 63, 97, 103, 119, 123] that the use of super capacitors as energy storage is a more feasible option for long-term operations (i.e., more than a few years) than rechargeable batteries, since the capacitors have almost unlimited charge cycles and their lifetime would not be reduced by frequent recharging and discharge. However, the capacitors have several drawbacks, e.g., higher current leakage, cost and larger size. Therefore, using rechargeable batteries is still recommended for short-term deployments.

In energy harvesting, many approaches to improving the efficiency of utilizing environmental energy have been presented. Alippi *et al.* [7] proposed an adaptive system design for a low-power *maximum power point tracker* (MPPT) circuit, which is used to optimally transfer solar energy to rechargeable batteries in various solar conditions. Krüger *et al.* [80] introduced a model that predicts harvested solar energy over long periods by taking into account several key impact factors in energy harvesting. Empirical studies of solar energy harvesting systems are presented in [38, 83].These studies suggest several methods for selecting the most appropriate system parameters, e.g., the duty cycles, in different seasons and geographical locations. Noh *et al.* [99] proposed a hybrid routing protocol for energy harvesting WSNs by

adopting both MAC-layer duty cycle adaptation and higher-layer geographical routing. This routing protocol enables extended network operation and low latency in end-to-end data propagation.

2.4.3 Summary

In this section, we have discussed the main power management approaches for extending the lifetime of sensor networks. Figure 2.9 summarizes these approaches by using a 2-level hierarchical classification, and outlines the related methodologies. The level-1 classification is based on the energy availability from energy sources. Energy-efficient approaches are used to maximize the utilization of residual energy in a node's energy storage component, while energy harvesting maximizes the energy extraction from the environment. In the level-2 classification, the approaches are further categorized according to several key aspects, including data routing, duty cycle setup, design and implementation.

Unlike energy-efficient approaches, energy harvesting offers a potential opportunity to achieve sustainable operation without sacrificing network performance. However, adding an energy harvesting component to sensor nodes increases the total cost of the network. It is very challenging to maintain harvested energy at stable levels, since it is strongly affected by the environmental conditions.

2.5 Sensor Network Applications for Soil Moisture Monitoring

There has been increased interest in field-scale measurement of soil moisture. In this section, we discuss the main deficiencies of traditional methods for soil moisture monitoring, focus on sensor network applications for this purpose, and survey the important design approaches and implementations in the literature.

2.5.1 Main Shortcomings of Traditional Methods

Soil moisture is a key spatio-temporal variable in the hydrology cycle. It helps explain the hydrological behavior of the water exchanges occurring at the boundary between the air and the ground [142]. Field-scale indications of soil moisture [23, 116, 142] are powerful tools used in a variety of multidisciplinary studies, such as the study of

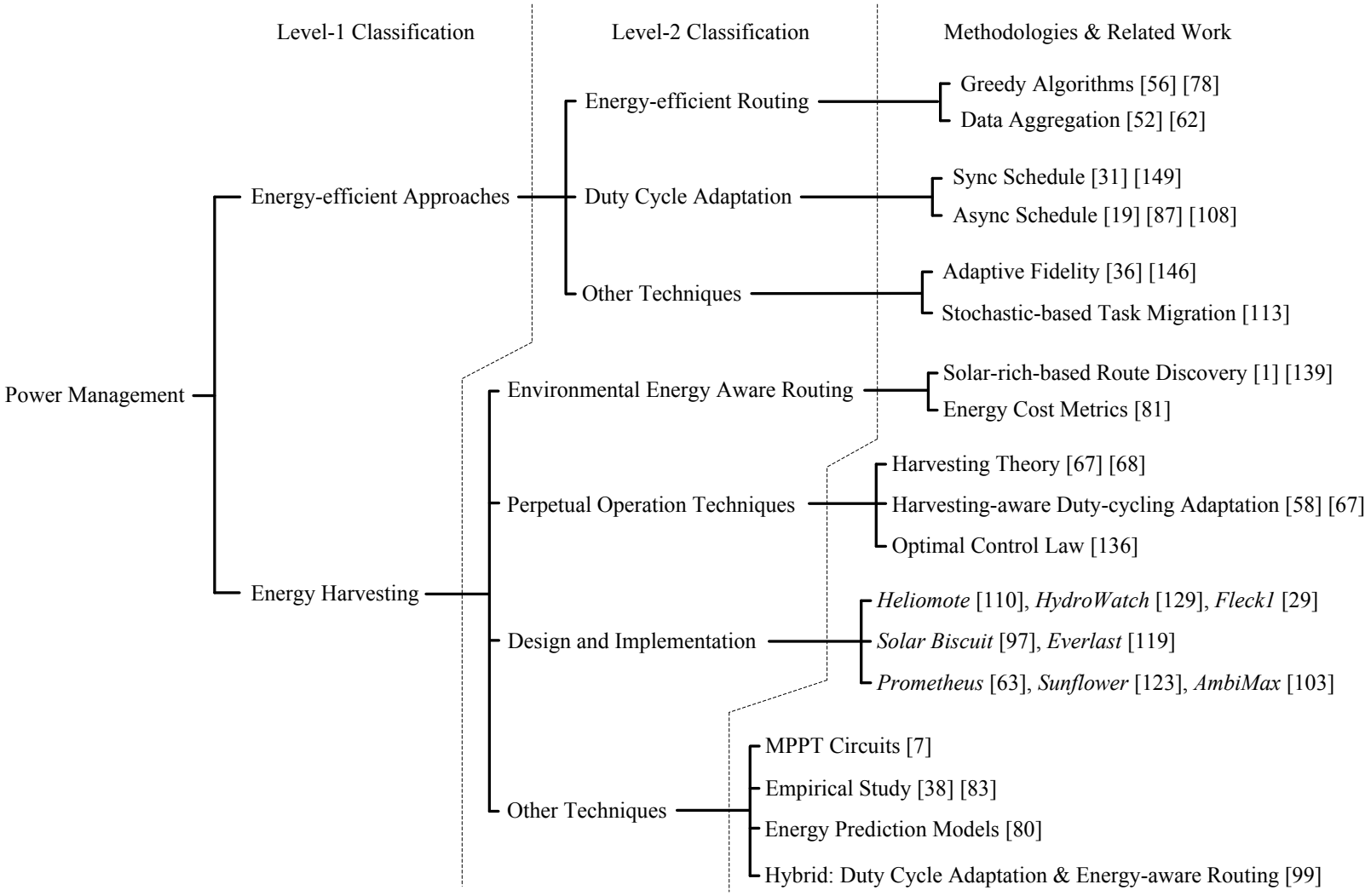

Figure 2.9: Classification and methodologies in power management for wireless sensor networks

global climate change [53], hydrology and vegetation monitoring [15], and precision irrigation in agriculture [121, 140]. In this sense, a suitable method for measuring soil moisture is necessary. The general methods can be classified as remote sensing and point (in situ) measurements [116].

In remote sensing, soil moisture is determined by measuring the electromagnetic energy that is reflected or emitted from the soil surface in particular portions of the spectrum. This approach can directly provide the large-scale gradient indications of surface soil moisture without using point sampling techniques and soil water models [116]. However, the accuracy of remote sensing is highly sensitive to the land surface structure and vegetation, and the measurement depth is restricted to only 2 to 5 centimeters from the soil surface [16]. Moreover, the cost of deploying such a measurement system is extremely expensive, since professional imaging devices with special spectral filters and aerial platform (e.g., satellites [71, 142]) are needed.

In point measurements, several types of sensors are developed to measure point-scale soil moisture based on different physical principles, e.g., capacitance, tensiometric and hydrometric methods [16, 116]. Compared with remote sensing, soil moisture sensors have lower costs and can yield multi-depth measurement [32]. However, a major challenge in using point measurement methods is to efficiently manage soil moisture sensors distributed across a large-scale region and collect the sensed measurements to a central data center.

2.5.2 Sensor Networks for Soil Moisture Monitoring

The use of sensor network technology can overcome the functional limitations of traditional electronic moisture sensor systems as discussed in Section 2.5.1. The basic idea is to equip the soil moisture sensors with low-cost and low-power wireless devices. By utilizing self-organizing network protocols, sensor networks can provide automatic management of soil moisture sensors without the need of any human intervention. Other key features include flexible scheduling of data measurement and transmission, large-scale and high-density deployments, reliable data delivery and long-term operation. Importantly, sensor networks operate in an untethered manner. This substantially reduces the total cost for the system installation and maintenance. Next, several key sensor network applications for soil moisture monitoring are surveyed.

Cardell-Oliver *et al.* [24] presented the design and implementation of a WSN to monitor the spatial-temporal variations of the surface soil moisture. Battery-powered *Mica2* motes [54] equipped with *Echo20* sensor probes [34] are used to measure and collect soil moisture measurements. Based on the observation that soil moisture changes rapidly during rainfall periods, a reactive method termed *Event-Condition-Action rules* is utilized to adapt the measurement frequency to the real-time events (e.g., rainfall). In this application, the sensor network is used to achieve variable measurement intervals for soil moisture without losing resolution, and eliminates the energy waste related to traditional measurement systems using constant measurement intervals.

Pierce *et al.* [107] developed regional and on-farm solar-powered WSNs for use in agricultural systems, which are capable of monitoring real-time environmental conditions (e.g., soil moisture and air temperature) and controlling important farming operations. According to the application requirements (e.g., the coverage area), regional and on-farm WSNs use different network architectures, namely *master-repeater-slave* and *star* architectures, respectively. For soil moisture monitoring in this application, the configuration of the sensor probes deployed at three different depths is used to make optimal irrigation decisions. For example, measurements collected in [107] show that irrigation events affect only the content of surface soil moisture and the overall tendency in the upper and middle soil layers keeps decreasing over the experiment's duration. This illustrates that the amount of irrigated water is not sufficient to maintain soil moisture levels and hence normal crop growth. In this application, the use of sensor networks provides the opportunity for precision agriculture in a large-scale region (approx. 60×90 km), and reduces potential water wasted in irrigation.

Kim *et al.* [74] presented an extensive study of remote monitoring and control of a precision irrigation system using WSNs. Six in-field sensor nodes are deployed across a farm according to a soil map. Sensed data is periodically transmitted to a central base station, and solar energy harvesting is used. In this application, electronic relays and logic controllers are added to the irrigation facilities, and irrigation operations are remotely controlled via wireless communications. The proposed *site-specific precision linear-move irrigation system* allows the operation of variable rate irrigation based on the real-time analysis of the soil moisture and weather condition measurements. Such sensor network applications for irrigation systems give a

potential solution to maximizing crop production while saving water.

2.5.3 Summary

In this section, we discussed the use of sensor network applications for soil moisture monitoring. In contrast to traditional methods, sensor networks enable automatic control and management of soil moisture sensors distributed in large-scale monitoring areas. Sensor nodes are capable of transmitting soil moisture measurements in real-time to a remote data center via wireless communications. In addition, sensor networks have lower costs and energy consumption than wired electronic systems or manual operation. Real-time soil moisture monitoring based on sensor network platforms offers great opportunities to carry out precision agriculture by adaptively scheduling the irrigation events.

2.6 Case Study of a WSN Platform

The availability of a real experimental platform is critical for research studies of WSNs, since it is very difficult to simulate the behavior of sensor nodes in a wireless environment. Even minor differences between the simulation models and real conditions can lead to different outcomes [48]. To overcome the limitations of the simulation method, many WSN platforms have been designed and prototyped. In this section, we present the NICTOR WSN platform (see Figure 2.10).

NICTOR is a wireless communication and actuation platform for remote monitoring and control, which was developed by a research group in National ICT Australia (NICTA). As illustrated in Figure 2.11, the main components of the NICTOR hardware include a microprocessor, a radio frequency transceiver, a power supply unit and a set of I/O interfaces (i.e., digital, analog and serial communications).

The microprocessor is the core element that controls other modules to perform calculations, access memory, handle interrupts, manage clock synchronization and communicate with the peripherals via I/O interfaces. A low-power and low-cost Atmel ATmega128L processor [11] is used in the NICTOR platform. It is designed based on an 8-bit AVR RISC architecture, and can achieve up to 8 MIPS throughput at 8MHz. Its built-in memories include 128 Kbytes of programmable Flash, 4 Kbytes

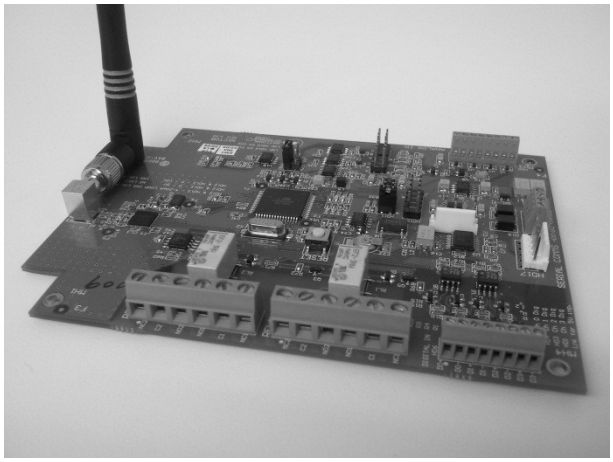

Figure 2.10: NICTOR hardware

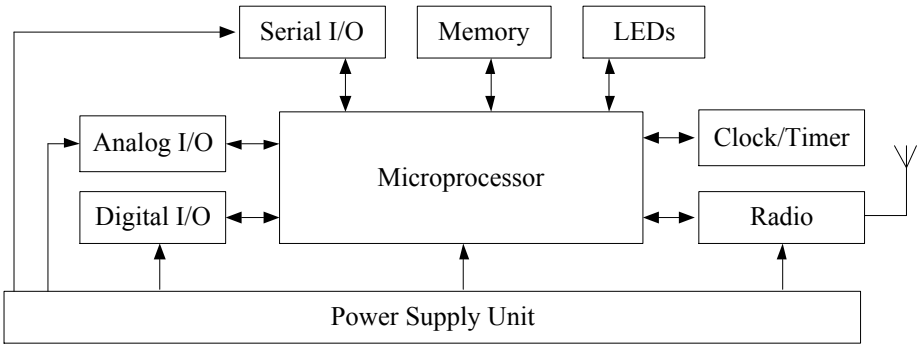

Figure 2.11: NICTOR framework

of EEPROM and 4 Kbytes of SRAM. It also provides a range of features to enhance flexibility and scalability, such as the on-chip timers and counters, standard JTAG interface, analogy-to-digital converter (ADC) and programmable UARTs.

NICTOR uses the CC2420 [131] radio frequency transceiver, which is a 2.4 GHz IEEE 802.15.4/ZigBee [61, 153] compliant radio. The power supply unit is responsible for converting the input voltage and providing the appropriate voltage levels to each module. In addition, several LEDs give the convenience for debugging and status indications. The standard I/O interfaces allow NICTOR to be connected with a wide range of peripherals without hardware modifications.

The software operating in the NICTOR nodes has been previously developed by the NICTA research group, and is not a contribution of this thesis. It is compiled with the standard libraries of the ATmega128L microprocessor and the IEEE 802.15.4 MAC-layer protocol. For the WSN test bed used in Chapter 3, the application of our

proposed network-layer routing protocol is developed based on this original software platform. In Chapter 4, the same software is applied, and an additional peripheral charge circuit is designed and integrated (see Figure 4.1). The sensor node described in Chapter 5 has the same software and hardware configuration as described in Chapter 3.

2.7 Summary

The remarkable progress in sensor network technologies has created potential applications for remote monitoring and control in many areas. Due to constrained resources and harsh environmental conditions, the design of sensor networks is highly dependent on specific application requirements. In this chapter, we have outlined the key high-level design challenges and related issues for sensor networks, and give a comprehensive survey of existing solutions related to the routing protocols and power management approaches. We classified the routing protocols as data-centric, hierarchical and location-based according to the network architecture. These important routing techniques are summarized and compared. We summarized power management approaches by using the proposed 2-level hierarchical classification, and discussed the related methodologies and existing work in each category. We highlighted the key shortcomings of traditional methods for soil moisture monitoring, and surveyed sensor network applications in this field. Finally, a typical WSN platform called NICTOR was outlined, and the key functionalities and features were highlighted.

In the rest of this thesis, several open issues to be addressed are outlined as follows. In Chapter 3, we focus on the problem of converge-cast communication in tree-based WSNs. Our aim is to design a higher-layer protocol that is capable of achieving efficient and reliable data delivery from sensor nodes to a central base station, while having low complexity and high resilience to node failure. In Chapter 4, we address the issue of supplying sustainable energy for unattended WSNs. In particular, we propose a systematic design approach for the energy supply subsystem of a sensor node by utilizing solar energy harvesting technique. It can provide energy-balanced operation for a sensor node in varying environmental conditions. In Chapter 5, we focus on the issue of monitoring soil moisture levels in a field by using an image-based sensing technique based on WSNs, and investigate the feasibility of utilizing

low-cost image sensors for the measurement of soil moisture with our experimental methodology in practical deployments.

Chapter 3

Performance Evaluation of a Converge-cast Protocol for IEEE 802.15.4 Tree-Based Networks

In this chapter, we focus on the subject of routing protocol design and performance in converge-cast IEEE 802.15.4 wireless sensor networks (WSNs). Specifically, we consider the case of converge-cast communication in tree-based network topologies. A key challenge in this scenario is how to design a converge-cast protocol with high performance and low implementation complexity. Network robustness is another significant issue that the protocol has to deal with in the face of node failures. We present a new converge-cast routing protocol for tree-based WSNs to address the above issues. The performance of the proposed protocol is evaluated using an experimental WSN test bed.

3.1 Introduction

A major factor underlying the growth in interest in WSNs is their ability to provide a reliable and cost-effective way to collect and disseminate data in a distributed setting [134]. To facilitate standardization of platforms and protocols, the IEEE 802.15.4 standard defines the physical and medium access control (MAC) layer specifications for low-complexity wireless personal area networks (WPANs) [61]. Overlaid on top of IEEE 802.15.4, the ZigBee standard includes a set of network and application layer specifications for creating, maintaining and utilizing WSNs [153]. Three network topologies are supported: star, tree and peer-to-peer. In practice, star and tree networks are more often used due to their simplicity and robustness [137].

A classic problem in WSNs is the transmission of data from a large number of nodes to a central collection point or coordinator. Depending on the network topology, a completed transmission may require multiple hops. This process is known as *converge-cast* communication. The MAC and network layer protocols, physical network topology and network size directly affect the performance of converge-cast WSNs. For example, there is a reduction in the proportion of packets that are successfully delivered as the network size increases, and a star topology can decrease the packet delay in contrast to a tree topology [20].

Protocol complexity and robustness are other key concerns for converge-cast WSNs. As discussed in Chapter 2, WSN protocols that support a time scheduling mechanism are an efficient approach for data transmission and collision avoidance (e.g., [77]). However, in the case of node failures, the complexity associated with this scheme may lead to substantial transmission overhead at the network coordinator in order to reorganize the superframe structure [137]. This can significantly reduce network performance (e.g., packet delay).

In this chapter, we propose an alternative converge-cast routing protocol for tree-based WSNs. The main motivation for the proposed protocol is to achieve comparable network performance while overcoming the complexity and latency associated with a hierarchical transmission scheme as in [20]. Importantly, the proposed scheme is compliant with the IEEE 802.15.4 standard. The performance of the proposed protocol is evaluated using an experimental WSN test bed.

The rest of this chapter is outlined as follows. Section 3.2 outlines the existing protocols in the literature. Section 3.3 outlines the problem addressed in this chapter. Section 3.4 presents a detailed description of the proposed protocol. In Section 3.5, the performance of the protocol is evaluated. In particular, we outline the evaluation objective, an experimental test bed and methodology, and present the experimental results that are compared with the protocol in [20]. In Section 3.6, this chapter is summarized.

3.2 Current Protocols

The standard IEEE 802.15.4 specification lays a solid foundation for the further development of WSN protocols in various applications. It proposes a standard protocol stack in the physical and MAC layers, and specifies a series of operating

mechanisms and parameters associated with both layers. The superframe structure in the MAC layer is the most significant proposal in the IEEE 802.15.4 standard protocol, which provides an efficient solution to common issues that arise in WSN environments. For example, the network is synchronized by a beacon broadcast by a coordinator at the beginning of the superframe. In the contention period, the CSMA/CA algorithm is utilized to avoid collision if multiple WSN nodes attempt to transfer data simultaneously. In addition, an inactive period is specified at the end of the superframe. In this period, no data transmission is allowed and all the WSN nodes are switched into sleep mode. This awake/sleep feature in the superframe significantly reduces the energy consumption of a WSN node. In contrast to the IEEE 802.15.4 specification, the ZigBee standard specifies a protocol stack in the network and application layers, and provides for more flexibility in the protocol and application development for WSNs, especially for large-scale WSNs in a tree topology.

Based on the IEEE 802.15.4 and ZigBee specifications, considerable research has focused on the context of the protocol development and improvement of the reliability, robustness, performance and energy efficiency in WSNs. Common performance metrics include throughput, packet delay and delivery ratio. The network topology is a key factor that may affect the attributes listed above. As discussed before, star and tree networks are the most common topologies used in WSN applications. However, due to the differences in the structure of the two network topologies, the relevant problems in each type of WSN become very different, which results in the variation of the implemented protocols as we describe below.

In a star network, there is only one hop between each end node and the coordinator. A packet from each node can be directly transmitted to the coordinator without any intermediate nodes. The low complexity of a star topology greatly simplifies the procedure of network establishment as well as the protocol complexity, and gives a high tolerance in the face of the node failure. For instance, the failure of any WSN node does not affect the communication between other nodes and the coordinator. In star-based WSNs all the nodes are assumed to be able to reliably receive the coordinator's broadcasting transmissions. In other words, they all share the same contention domain and have to compete with each other in order to transmit packets successfully. The avoidance of packet collision is handled by the CSMA/CA algorithm. In this topology, packet delay and network synchronization usually are not a major concern in the WSN protocol design. The study in [111] suggests an

improvement of the protocol performance in a star network in terms of the throughput and energy consumption by disabling the MAC-level acknowledgements. The adjustment of the protocol parameters specified by IEEE 802.15.4 is another typical approach to improve the performance, outlined by [76].

In contrast to star-based WSNs, centralized data collection is more challenging in WSNs with a tree topology. In this topology, the transmitted packet may traverse multiple hops via a certain routing path to a central coordinator. In addition to the node-to-node data transmission, the protocol for tree-based WSNs has to deal with receiving and forwarding data in transit nodes that are located in the middle level of the tree. Unlike a star topology, the WSN nodes in a tree may be located outside the coordinator's broadcasting domain, which means that they cannot receive the beacon frame directly. In this case, it is necessary to implement a scheme in the protocol for network synchronization. If multiple contention domains exist in a tree network, the WSN nodes sitting in different domains can transmit packets simultaneously. However, due to the multiple levels of the tree, a packet from tree level j has to be transmitted and forwarded j times to the coordinator in level 0. To collect the same amount of data, the traffic load in tree-based WSNs is much heavier than that in star-based ones, which leads to a higher collision probability during the contention period. Like the network synchronization problem discussed above, packet collision is another critical issue in tree-based WSNs.

It is widely claimed that time scheduling is an efficient approach for collecting data in converge-cast IEEE 802.15.4 WSNs. There is an improvement in terms of the efficiencies of data transmission and collision avoidance by applying a time scheduling scheme in tree-based WSN protocols [27, 73, 127], and the study in [26] uses the same scheduling approach to propose an energy efficient protocol for cluster-tree based WSNs. The study in [20] outlines a commonly used converge-cast communication protocol that leverages built-in features in the IEEE 802.15.4 and ZigBee standards. The scheme employs a hierarchical transmission scheme for scheduling transmission. It is summarized as follows. Nodes operate in beacon-enabled mode. The active period of the parent superframe is only used for data transfer between a parent and its children. During the inactive period, each child router broadcasts its own beacon at a pre-defined offset, and the same hierarchical superframe structure is applied within each time slot partitioned by child beacons. There is no overlap between the active portions of child superframes.

One of the benefits of this algorithm is a reduction in the level of competition for transmission in large multi-level tree-based WSNs. However, this mechanism artificially introduces packet delay, which means that packet transmission via more than one hop requires two beacon intervals at least. Under heavy traffic load, it may require more. A second significant disadvantage is the complexity associated with the scheme. In the case of node failures the entire superframe structure may need to be reorganized. This responsibility falls to the network coordinator. The overhead associated with this process is substantial. A similar well-known protocol for converge-cast transmission in tree-based networks is the DMAC protocol [87]. A key disadvantage associated with DMAC is a lack of interoperability with the IEEE 802.15.4 standard.

3.3 Problem Definition

As described in Section 3.2, time scheduling is an efficient way to reduce the packet collision probability, particularly in the deployment of a large number of nodes. However, it also artificially introduces transmission delay. Routing protocols like DMAC [87] have a lack of interoperability with the IEEE 802.15.4 standard. This may limit the use of standard vendor products and integration with other networks. Protocol complexity and fault resilience are also key factors that impact network performance. In this chapter, we focus on the routing protocol design for converge-cast tree-based networks. The aim is to overcome the issues associated with the existing protocols discussed earlier, while reducing the complexity of the routing protocol as well as network reorganization in the case of node failures. To address this problem, we introduce a new frame structure in the network layer based on the standard IEEE 802.15.4 MAC protocol. The non-beacon mode is used to increase the flexibility of arranging frame periods. The synchronization of the nodes across multiple tree levels is achieved by using the beacon flooding and waiting schemes in our frame structure, which also eliminates the artificial packet delay related to typical time scheduling mechanisms (e.g., [20]). In terms of complexity and fault resilience, the benefits of our protocol compared with time scheduling are discussed and listed in Section 3.4. To evaluate our protocol, we use the performance metrics of throughput, packet delay and successful transmission probability as defined and analyzed in Section 3.5.

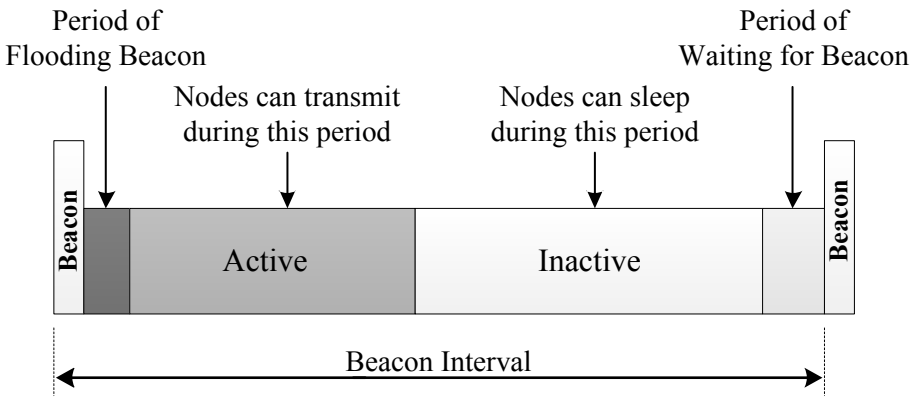

Figure 3.1: Frame structure

3.4 Proposed Protocol

In this section, we propose a converge-cast protocol for WSNs with a tree topology based on the IEEE 802.15.4 standard, such that our protocol is less complex compared to a popular time scheduling protocol [20].

As specified by the IEEE 802.15.4 standard, in the so-called beacon mode, the MAC layer broadcasts a periodic beacon transmission to synchronize the entire network. The time span between two consecutive beacons is called the beacon interval (BI). Each beacon interval consists of active and inactive periods. The length of the active period is known as the superframe duration (SD). Typically SD is less than BI. Nodes in the network can communicate during this active period. The remainder of BI is an interval during which nodes may sleep to conserve power. When SD is equal to BI, there is no inactive period. The IEEE standard also specifies a non-beacon mode. In this case the MAC layer does not broadcast a periodic beacon, and there is no defined superframe structure; the higher layers are free to impose a custom framing structure. Our proposed protocol exploits this flexibility and operates in the IEEE 802.15.4 non-beacon mode. Figure 3.1 outlines the frame structure of the proposed protocol.

Note that in IEEE 802.15.4 beacon enabled mode the MAC layer is responsible for generating and broadcasting beacon frames that include all the relevant information for the structure between two beacons, like the beacon interval and the superframe duration. The duration of the active/inactive period in this structure is determined by the standard parameters (e.g., beacon order (BO) and superframe order (SO)) within a

specified range of values. This results in a limited number of choices for the ratio of the duration of the active period to the duration of the beacon interval, which is known as the duty cycle. Note that if the duty cycle is too high, there is a significant impact on energy consumption in the WSN. Our proposed protocol imposes its own framing structure (Figure 3.1) and is similar to the standard beacon-mode superframe described above. However, in our case the tasks of generating and broadcasting beacon frames are handled in the higher layer, rather than the MAC layer. This gives greater flexibility to organizing the frame structure in each beacon interval without the duration restriction.

Our proposed framing structure consists of five main periods, namely (1) the period of broadcasting a beacon, (2) the period of the flooding beacon, (3) the active period, (4) the inactive period and (5) the period of waiting for a beacon. The detailed functionalities for each period are described in the following.

At the beginning of the frame structure, the network coordinator broadcasts a beacon frame. The beacon frame payload contains the frame timing structure and possibly other information including data transmissions to individual nodes in the network. Following the beacon frame is a period called the *flooding beacon*. During this period, when nodes receive a beacon broadcast frame, they re-broadcast the frame once only. Much like the standard IEEE 802.15.4 beacon frame, nodes receive the framing timing structure as a payload in the custom beacon. By this relaying scheme, every node is guaranteed to receive the beacon frame including those outside the coordinator's broadcasting domain, and the entire network can be synchronized within a very short time period. After a node has re-broadcast the beacon frame, in the active period it is free to commence transmissions to its parent by using the unslotted CSMA/CA algorithm as specified by the IEEE 802.15.4 standard. During the inactive period, there is no transmission and nodes operate in sleep mode for energy conservation. Given that the beacon frame plays a significant role in providing network synchronization, a fixed time slot is provided prior to the next beacon interval, called the *waiting beacon* period. This period gives nodes sufficient processing time to turn back to the normal operating state from the sleep mode before the beacon frame is broadcast. Without the allocation of this short period, a beacon frame may be missed, which causes a node and its children to lose the network synchronization until the receipt of the next beacon frame.

The protocol is compliant with the nonbeacon-enabled IEEE 802.15.4 standard framework. It permits a far simpler network synchronization mechanism than the beacon-enabled mode outlined in Section 3.2, since the flooding mechanism is designed to ensure that every node in the tree receives the beacon frame containing all network timing information within a very short time slot once it is broadcast by a coordinator, without the implementation of any sophisticated time scheduling schemes.

In addition, the protocol also allows a more flexible arrangement for the duration and proportions of each period in the frame structure. The reason for this is that the beacon interval (BI) and superframe duration (SD) in the beacon-mode can be calculated by using the following equations [61].

$$BI = aBaseSuperframeDuration \cdot 2^{BO} \tag{3.1}$$

$$SD = aBaseSuperframeDuration \cdot 2^{SO} \tag{3.2}$$

$$for\ 0 \leq SO \leq BO \leq 14 \qquad SO, BO\ \in \mathbb{Z}$$

In equations (1) and (2), SO and BO denote the *beacon order* and the *superframe order*, respectively; *aBaseSuperframeDuration* represents the minimum superframe duration of 15.36 ms as specified in the IEEE 802.15.4 standard, when $SO = 0$.

From equations (1) and (2), the maximum beacon interval is approximately 252 seconds, and the available number of choices for the duty cycle (the ratio of SD/BI) is also constrained by the parameters SO and BO. Our protocol eliminates such limitations on the frame structure by deploying the nonbeacon-enable IEEE 802.15.4 mode. In this mode, the higher layer is responsible for managing the frame structure, where the custom beacon frame is allowed to contain the unrestricted timing information. This is a significant improvement, since short beacon intervals may result in reduced energy efficiency. All the network activities in WSNs can only occur within the pre-defined active period, including network construction, synchronization, data collection and transmission, maintenance signaling etc. To meet the minimum requirements in terms of performance, reliability and robustness in WSNs, this time period usually needs to be fixed above a certain length. On the other hand, to prolong the lifetime of a WSN node, a lower duty cycle is necessary. In this case the only way to get lower duty cycles is to extend the beacon interval. Tree network formation is achieved as specified by the ZigBee standard.

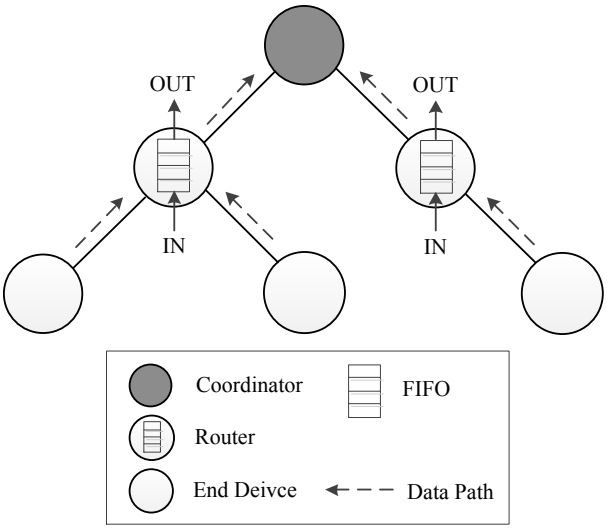

Figure 3.2: Transmission diagram with FIFO scheme

Converge-cast communication is achieved without any further scheduling. Any data packets received by a parent (router) node from a child node are stored and then forwarded using a standard first-in-first-out (FIFO) buffering scheme that is implemented in the higher layer. The transmission diagram with FIFO scheme is shown in Figure 3.2. As indicated above, all such transmissions are carried out by using unslotted CSMA/CA.

As for the existing protocols with time scheduling schemes, there is a dedicated time slot in the active period allocated to a group of nodes (e.g., nodes in each tree branch or level), during which they conduct a local competition to transmit the data. In this case, if a router node can always successfully transmit the packet to its parent before the receipt of the next one from its child, the implementation of the FIFO buffering scheme is not necessary. However, in our proposed protocol every node performs a global competition within the entire active period, which means that a router node may need to temporarily store multiple packets from its child nodes within a certain time. The higher a router node is located in the tree, the greater the probability this scenario will occur. Therefore, to avoid packet loss, the FIFO buffer with an appropriate size is required in our router nodes.

In the following example, we illustrate the operation of the proposed protocol by six stages and its benefits in contrast to existing protocols. Assume that there is a converge-cast WSN with a multi-level tree topology. Some nodes are geographically located outside the radio area covered by the network coordinator. Every node has

already connected with the coordinator directly or via multiple hops, and is waiting for the beacon frame.

Stage 1. The network coordinator generates a beacon frame in the higher layer by attaching a beacon overhead to a payload, which includes the pre-defined timing information indicating the frame structure outlined in Figure 3.1. This beacon frame is then encapsulated in the lower layers (MAC and PHY) and broadcast.

Stage 2. The nodes within the coordinator's broadcasting domain are the first to receive the beacon frame. Once it is received, they will immediately re-broadcast it within their own broadcasting domains in the same way as described in Stage 1. The same procedure is repeated by their child nodes, and eventually every node in the WSN receives the beacon frame.

Stage 3. After re-broadcasting a beacon frame, a node constructs the frame structure based on the relevant timing information in the beacon payload. After that, nodes perform data collection and transmission in a pre-defined task routine. A router node temporarily stores the received packets in its FIFO buffer, and forwards them to its parent node packet-by-packet by using the unslotted CSMA/CA algorithm. In this manner, the packets initiated in any level of the tree can be delivered to the coordinator via one or more hops.

Stage 4. When a node's active period reaches the time span specified by the frame structure, it stops all activities and enters sleep mode. The remaining packets in the router's FIFO buffer are kept for the next active period.

Stage 5. Nodes switch back to normal operating mode from sleep before the network coordinator broadcasts next beacon frame. In this stage, nodes only monitor the channel for the receipt of beacon frame.

Stage 6. Next beacon interval starts over from Stage 1.

Based on the example above, the benefits of the proposed protocol over existing ones are summarized as follows.

Benefit 1. The proposed protocol achieves higher energy efficiency than beacon-enabled IEEE 802.15.4. This is because not only do the nodes switch to sleep for energy conservation in Stage 4, but also the protocol gives more flexibility for constructing the frame structure, such as the beacon interval and duty cycle. As discussed earlier, a lower duty cycle can significantly extend a node's lifetime.

Benefit 2. The proposed protocol has a lower complexity than protocols with hierarchical time scheduling schemes as described in Section 3.2. First, our protocol deploys a universal frame structure defined by the network coordinator, which is much simpler than those in time scheduling protocols where nodes in different tree levels may correspond to different frame structures. Second, time scheduling protocols need a mechanism for the reorganization of the frame structure in the case of node failure, but this is not necessary in our protocol. Third, there is a difference in synchronizing the network between our protocol and time scheduling protocols. For the latter, it is carried out by a series of local synchronizations between the adjacent tree levels in scheduled time slots. In comparison, our protocol deploys a global synchronization scheme of re-broadcasting the beacon that can be performed in only one time slot as in Stage 2.

Benefit 3. The proposed protocol enhances network robustness. The beacon flooding scheme in Stage 2 enables the network to be synchronized in a very short time slot. During beacon flooding, a node may receive multiple copies of the beacon. This reduces the probability of losing synchronization due to interference. An early wake-up of the nodes in Stage 5 leads to a further reduction of this probability. In the case of a node failure (e.g., a router node), its child nodes are temporarily disconnected from the network. The reconnection of these nodes to the network is handled by the IEEE 802.15.4 MAC layer protocol inherited by our protocol. After that, the higher layer takes responsibility for re-synchronizing.

Benefit 4. The proposed protocol eliminates the artificial delay associated with hierarchical time scheduling schemes. For protocols with such schemes, a group of nodes are allocated with one or several dedicated time slots for data transmission in each beacon interval. In this case, a packet may traverse more than one time slot belonging to different groups to the network coordinator. In this progress, the packet is artificially delayed when it waits for the next scheduled time slot. For example, if the nodes in each tree level have only one time slot to transmit the packets and a higher level is scheduled prior to a lower level in each beacon interval, a packet transmitted from level j to level 0 requires at least j beacon intervals. In

contrast, there is no such limitation in our protocol.

Benefit 5. The proposed protocol is compliant with the standard nonbeacon-enabled IEEE 802.15.4 protocol in the MAC and PHY layers. The protocol overcomes a limitation of the existing protocols (e.g., DMAC protocol [87]) in terms of lack of interoperability. In terms of the higher level ZigBee protocol, our proposed protocol is developed based on the standard IEEE 802.15.4 protocol, and thus provides the same services as required by the ZigBee protocol.

The next section outlines the experimental evaluation of our proposed protocol and a comparison with a time scheduling protocol [20] in terms of the reduction in packet delay (Benefit 4). The other benefits listed above are not experimentally tested in this thesis, but are highlighted as directions for future work.

3.5 Protocol Evaluation

In this section, the proposed protocol is evaluated using an experimental approach based on a WSN test bed. In Section 3.5.1 the aim of the evaluation is outlined. Section 3.5.2 explains the WSN test bed. Section 3.5.3 outlines the experimental methodology including the WSN node configuration, relevant parameter settings, network topologies and performance metrics used. In Section 3.5.4, four sets of experimental results are presented and discussed. We also compare the performance of our protocol with a time scheduling protocol [20] by applying the same experimental configuration.

3.5.1 Aims

In contrast to existing protocols, the key benefits of our proposed protocol have been illustrated in terms of energy efficiency, network robustness and protocol complexity in Section 3.4. However, network performance, which is another significant concern on protocol design, has not been addressed yet. The objectives of this section are to evaluate the performance of our protocol using common experimental setups in terms of the WSN parameters and network topologies (e.g., star and tree), and compare the outcomes of the protocol evaluation with an existing protocol.

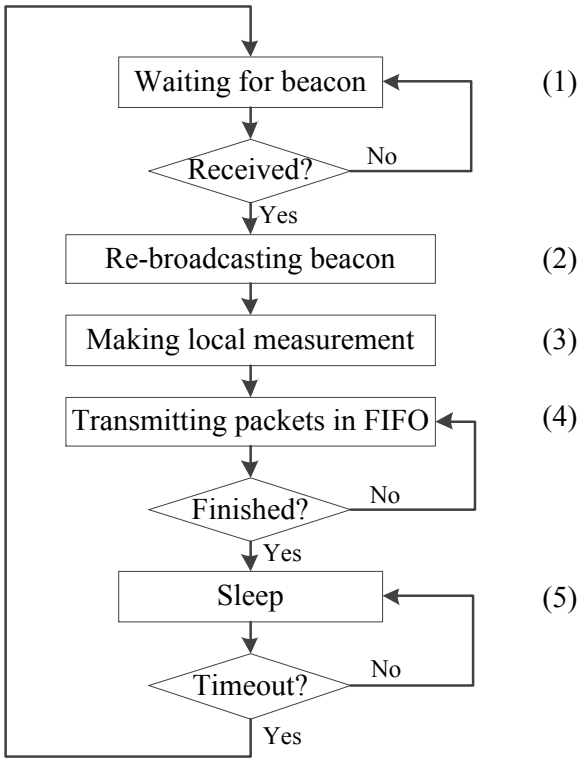

Figure 3.3: Flowchart of a node's state

3.5.2 Wireless Sensor Network Test Bed

In the experimental evaluation, the WSN is implemented using the NICTOR test bed described in Chapter 2. For the results presented in the experiments, all nodes are collocated to ensure a worst-case mutual interference scenario. For convenience, all the nodes are powered by a mains DC source.

3.5.3 Methodology

The state diagram shown in Figure 3.3 summarizes a node's state in the experiments. There are five key states of a node in the experiments, which correspond to the periods specified by the frame structure (Figure 3.1). State (1) corresponds to the period of waiting for a beacon. When a beacon frame is received, the node enters state (2) in the beacon flooding period. During the active period, a node first makes a local measurement (e.g., soil moisture or temperature) in state (3), and then transmits the measured data as well as the received packets stored in its FIFO buffer in state (4).

Table 3.1: Experimental parameters

Radio Frequency	2.4 GHz
macMinBE	3
macMaxBE	5
macMaxCSMABackoffs	5
macMaxFrameRetries	3
Packet Length (with Overhead of PHY & MAC)	41 Bytes
Length of Beacon Interval	5 Seconds
Length of Beacon Flooding Period	see comment[#] below
Length of Beacon Waiting Period	1 Second
Length of Inactive Period	0 Second

[#]This was measured and is a very short period, on average a few milliseconds.

State (5) corresponds to a node entering sleep mode for energy conservation. When the inactive period finishes, a node returns to state (1) to start the next beacon interval.

Table 3.1 lists the key experimental parameters applied in our proposed protocol. According to the IEEE 802.15.4 specification [61], the parameters of *macMinBE*, *macMaxBE*, *macMaxCSMABackoffs* and *macMaxFrameRetries* are defined as follows.

- ***macMinBE***: The minimum value of the backoff exponent in the CSMA/CA algorithm
- ***macMaxBE***: The maximum value of the backoff exponent in the CSMA/CA algorithm
- ***macMaxCSMABackoffs***: The maximum number of backoffs the CSMA/CA algorithm will attempt before declaring a channel access failure
- ***macMaxFrameRetries***: The maximum number of retries allowed after a transmission failure

Note that the backoff exponent, known as *BE*, is defined as the number of backoff periods a node needs to wait before attempting to access a channel. *BE* is initialized to the value of *macMinBE*, but no more than *macMaxBE*, during the iterations of the CSMA/CA algorithm.

Each node in the NICTOR test bed has the capabilities of automatically scanning the wireless channels and joining the network by selecting a node with maximum signal strength as its parent node. The feature of dynamic router selection substantially increases the network robustness when there is a need for network

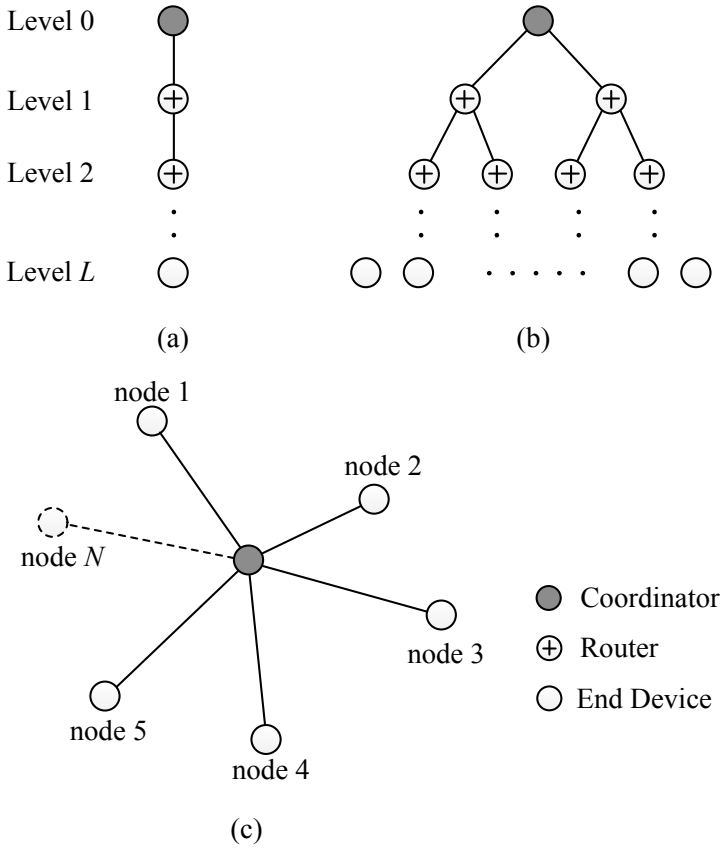

Figure 3.4: Topologies

reorganization. The attribute *maxChildren* is used to specify the maximum number of direct children that a node can have. When this attribute is set to 0 in each node except the coordinator, a star network is formed eventually. Likewise, a tree network can be formed with a non-zero attribute setting.

In the experiments, each node generates only a single local measurement packet during each beacon interval. A node's local sensor measurement is stored in the local FIFO first. To increase the reliability of data transfer, acknowledged transmissions are employed. To mitigate the effect of finite FIFO buffer size, the experiment employs buffer sizes large enough to ensure there are no buffer overruns. Further, in evaluating the throughput metrics described below, a long active period is selected (approximately 4 seconds) to avoid losses associated with the beacon forwarding and beacon waiting periods. Since energy efficiency is not addressed in the experiments, the nodes do not operate in a sleep mode after the active period and there is no inactive period (0 second) in the frame structure.

Figure 3.4 illustrates three topologies evaluated in this study: (a) Single branch tree, (b) Binary tree, and (c) Star. For all topologies the network size is varied up to 30

nodes (excluding the network coordinator). The maximum level for the binary tree is 4, and 30 for a single branch tree.

The proposed protocol is evaluated using the performance metrics listed below:

- **Throughput**: The number of bits received by the network coordinator per unit time, calculated as:

$$\text{Throughput} = \frac{8P_L \sum_{i=1}^{m} N_i}{\sum_{i=1}^{m} T_i} \tag{3.3}$$

  where P_L is the packet length; N_i denotes the number of packets received within the i^{th} beacon interval; T_i represents the delay for the last arrival packet for the i^{th} beacon interval; and m is the total number of beacon intervals that the experiment occupied.
- **Packet delay**: The time interval between a node transmitting a packet and receipt at the network coordinator. In our experiments, an approach to measure the packet delay is described below. Due to a very short period (a few milliseconds) for the flooding beacon, we neglect the impact of this period on the packet delay and assume that a node starts the transmission attempt when it receives a beacon frame. Therefore, the time interval between transmitting a beacon frame and receiving a packet in the network coordinator is measured as the packet delay.
- **Successful transmission probability** (P_{ST}): The ratio of the number of received packets and the number of transmitted packets. This metric is measured in the network coordinator by counting the received packets within a fixed number of beacon intervals. Note that this metric reflects the success of final delivery of packets to the network coordinator, and does not attempt to measure the number of retries required to successfully deliver a packet if unsuccessful on the first or second attempt.

Note that in measuring packet delay and the successful transmission probability, a packet received at the network coordinator can be identified through its header, which contains the source node information.

As mentioned before, acknowledged transmissions are employed. There is of course a low probability the child node will not receive the acknowledgement frame due to interference, even though the packet was successfully transmitted to its parent. In such circumstances, the coordinator sometimes will receive multiple copies of a

Table 3.2: Overview of experiments

Experiment	**Topology**	**Network Size**	**Metrics**
Set 1	Single Branch Tree	30 Nodes	P_{ST}, Delay
Set 2	Binary Tree	30 Nodes	P_{ST}, Delay
Set 3	Star	2 – 30 Nodes	P_{ST}, Delay, Throughput
	Binary Tree		
	Single Branch Tree		
Set 4	3-Level Tree (3 Nodes at L=1)	3 – 30 Nodes	P_{ST}, Delay

packet from a node. In the experiments, any duplicated packets received by the coordinator are ignored. Although we do not use an inactive period in our experiments, this does not affect the performance metrics of throughput, packet delay and successful transmission probability. This is because even if a non-zero inactive period was used, all nodes would still be able to complete their tasks before the sleep period.

3.5.4 Results and Discussion

In this section, the experimental results are presented. Table 3.2 lists the overview of our experiments.

In the first experiment, a single branch tree topology is used with a total of 30 nodes, and the maximum tree level is 30. This is the most challenging tree topology that is often neglected in other studies, but nonetheless is an important case that can arise in many applications, such as a WSN application in a tunnel. Figure 3.5 shows the probability of packets being successfully transmitted to the coordinator as a function of the tree level. It can be clearly seen that successful transmission probability decreases substantially as the tree level increases. Even a node at L=1 exhibits a relatively low successful transmission probability (less than 28%), and this probability quickly converges to approximately 7% in the node at L=30. This asymptotic behavior results from the characteristic of the multi-level tree topology discussed in Section 3.2, such that a packet initiated in level j has to be transmitted j times to the coordinator. As the tree level j increases, the successful probability of transmitting a packet from this level to the coordinator decreases exponentially, since the packet can be discarded in any level if the number of its transmission attempts

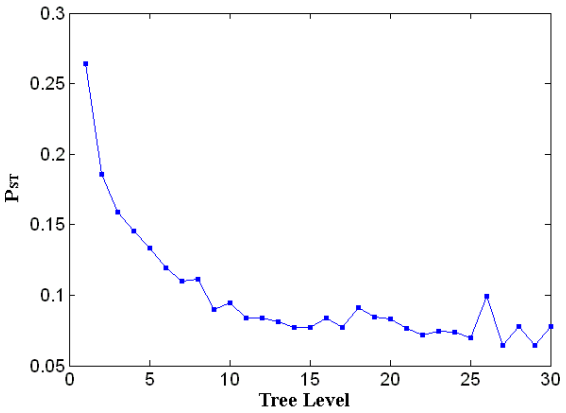

Figure 3.5: Successful transmission probability for 30-node single branch tree

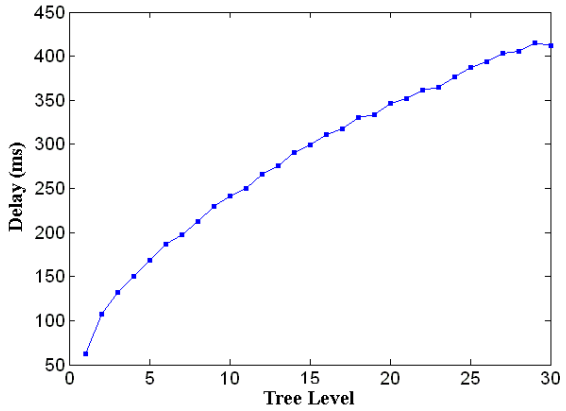

Figure 3.6: Packet delay for 30-node single branch tree

reaches the maximum number of retries specified by the parameter *macMaxFrameRetries*. While the observed successful transmission probabilities are quite low, recall that in our experiments we are testing worst-case operating conditions where all the nodes are co-located (maximizing interference) and all nodes attempt to transmit at the start of the active period.

Packet delay is measured as well. In Figure 3.6, the latency between the coordinator and each node is presented, and the curve's slope gradually decreases, suggesting the average delay per-hop converges to a constant value as the tree level increases. The most likely reason for this behavior is that the node's capacity in higher levels, especially for the node at L=1, is saturated. In this case, the received packets from lower tree levels cannot be immediately forwarded and have to be stored in their FIFO buffers first. This causes an almost fixed hop delay as the tree level increases. With this challenging tree topology, packets transmitted from the bottom of

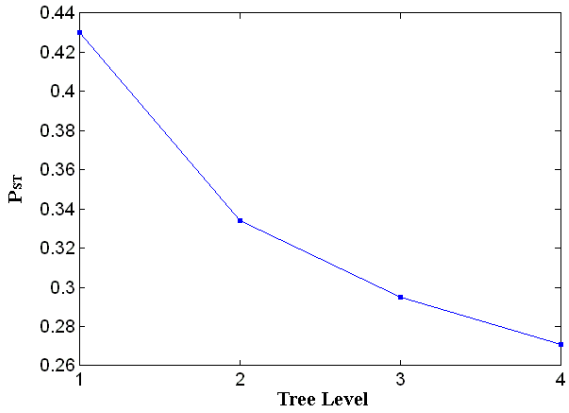

Figure 3.7: Successful transmission probability for 4-level binary tree

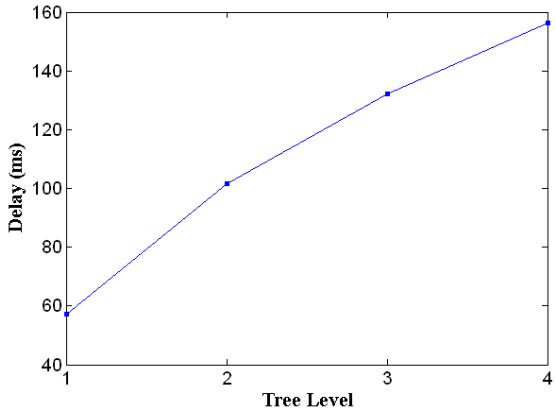

Figure 3.8: Packet delay for 4-level binary tree

the tree to the top have to go through all parent nodes, and there is an increasing likelihood that a transmission will be unsuccessful due to the CSMA/CA scheme being unsuccessful at obtaining a successful transmission slot.

Next, we discuss the results for a 4-level binary tree. In this case each parent node has two children, and there are 30 nodes in total. Figures 3.7 and 3.8 show the successful transmission probability and delay, respectively. The results show the same tendency as the single branch tree. However, since the depth of the tree is reduced significantly for this scenario, better performance is achieved, although both tree topologies deploy the same number of nodes.

To evaluate the impact of network size on performance and compare with different topologies, the number of nodes is varied up to 30 for each topology, namely a star, binary tree and single branch tree. For the binary tree, the maximum number of children is limited to 2 for each parent, and the maximum tree level is 4. Nodes are

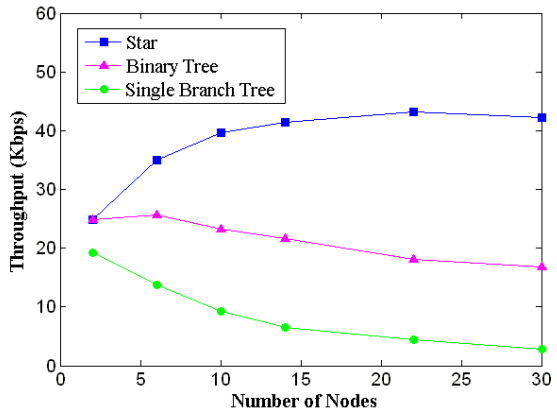

Figure 3.9: Throughput vs. number of nodes with three topologies

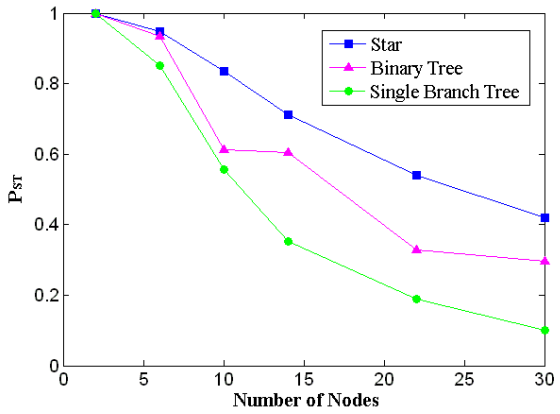

Figure 3.10: Successful transmission probability vs. number of nodes with three topologies

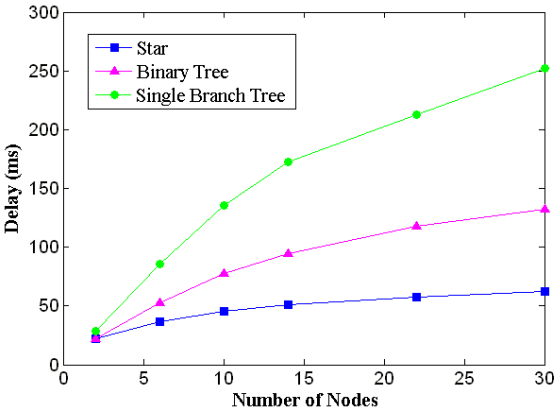

Figure 3.11: Packet delay vs. number of nodes with three topologies

distributed into the next tree level as evenly as possible until the upper levels are full. From Figures 3.9, 3.10 and 3.11, it can be observed that the star network has the best

performance. In contrast, the single branch tree exhibits the worst performance and the binary tree is located between the two extremes. Throughput curves in Figure 3.9 highlight a notable distinction for the star topology. As network size increases, throughput for the star grows first and eventually becomes saturated, but it keeps decreasing for the tree topologies. According to Figure 3.10, the successful transmission probability for a binary tree degrades substantially with increasing tree depth. However, the degradation does not change much for the same depth but increasing number of nodes. Hence we infer that the tree depth has a greater impact on the successful transmission probability than the number of nodes in the tree. In terms of packet delay illustrated in Figure 3.11, tree networks are more sensitive to changes in network size than a star network, and the delay increases with depth in a tree network, as expected.

We now compare the performance of the proposed protocol with that described in [20] and highlight its key advantage. The results outlined herein use the same topology, a 3-level tree with 3 nodes at tree level 1. The results for our proposed protocol are shown in Figures 3.12 and 3.13. The reader is referred to Figures 11 and 12 in [20] for comparison and specifically for the case (Tree: SO=1, BO=3). The compared curves are briefly summarized as follows.

In Figure 11 in [20], the success probability is evaluated as a function of the number of nodes (from 20 to 50). The value of the success probability for 20 nodes is approximately 60 percent, and it decreases linearly to 52 percent for 30 nodes.

In Figure 12 in [20], the packet delay is evaluated as a function of the number of nodes (from 3 to 50). The delay increases substantially from 10 ms for 3 nodes to 100 ms for 15 nodes, and afterward it grows slightly to about 122 ms for 50 nodes.

In the case of the success probability, our performance is 10 to 20 percent lower than the best-case performance for a tree network in Figure 11 of [20]. This is expected since our protocol does not impose any form of transmission time scheduling and allows CSMA/CA to resolve all medium access contentions. With regards to delay, our protocol achieves between 25 percent improvement for 20 nodes to 10 percent improvement for 30 nodes. From the results for both protocols, there is a trade-off between delay and successful transmission probability. This can be simply tuned by increasing or decreasing the number of transmission retries. The key advantage is that our proposed protocol delivers comparable performance but with a much simpler protocol as described in Section 3.4. If a node fails in our network,

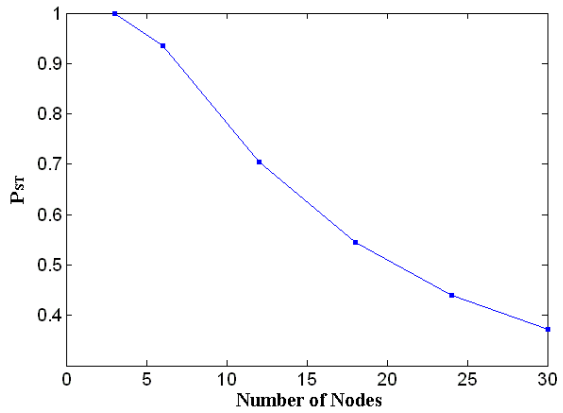

Figure 3.12: Successful transmission probability vs. number of nodes

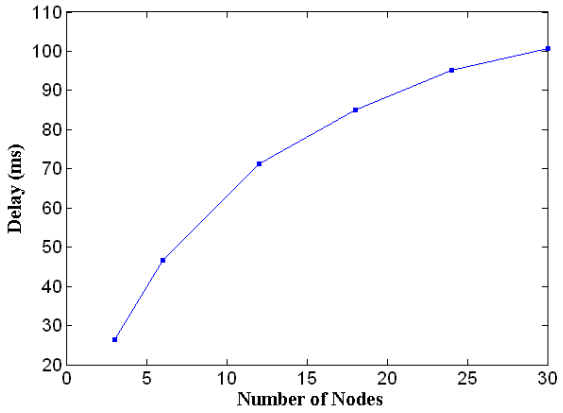

Figure 3.13: Packet delay vs. number of nodes

there is no need to reorganize the superframe structure.

3.6 Summary

A converge-cast protocol for IEEE 802.15.4 tree-based WSNs has been proposed. Our protocol uses beacon flooding and leverages CSMA/CA to minimize the amount of network coordination overhead required, which is typical of tree-based networks. We have used a wireless sensor network test bed to evaluate the protocol's performance. Our proposed scheme is compliant with the IEEE 802.15.4 standard, which makes it readily applicable to existing devices and platforms.

A comparison is conducted against an existing hierarchical scheduling scheme [20] in Section 3.5.4. It is shown that our protocol delivers comparable performance in the deployment of small and medium-size networks. Our proposed converge-cast protocol

does not use any scheduling schemes to reduce the probability of packet collision in wireless communications, thus having lower complexity. When network size grows to a large number of nodes (e.g., hundreds), the collision probability increases substantially. In this case, the beacon flooding scheme in the broadcast period may not work efficiently, which means that some nodes may fail to receive the beacon, thus losing the synchronization. This failure also could happen frequently during periods of data sampling and transmission, and therefore results in a significant reduction in the performance in terms of throughput, delay and successful transmission probability. Due to this limitation of our proposed frame structure, the use of hierarchical scheduling may still be needed in the case of dense deployment of a large number of nodes.

Several potential benefits of our proposed converge-cast protocol have been highlighted in Section 3.4. A direction for future work is to verify these claimed benefits using appropriate experiments. For example, protocol robustness can be evaluated in terms of measuring the resources (e.g., time and energy) required for network reorganization or failure recovery.

Chapter 4

Power Management for Unattended Wireless Sensor Networks

A reliable power supply is one of the most critical issues in the design of wireless sensor networks, especially for unattended WSNs in outdoor applications. The main challenge is how to extend battery lifetime given the constrained battery capacity and the WSN node power requirements. In this chapter, we address this challenge by focusing on the design of the WSN power supply subsystem. We propose a systematic approach to designing low-cost power supplies that can act as a reliable current source for unattended WSN applications. Our proposed design approach improves reliability under varying environmental conditions, regardless of the specific duty cycle parameters. The performance of our designed power supply is evaluated by an experimental WSN deployment.

4.1 Introduction

A substantial research effort in energy management in WSNs has been dedicated to the development of *energy-efficient* protocols for the medium-access-control and network layers. The underlying approach in the majority of these studies is the use of a non-unity duty cycle, in which nodes alternate between *wake* and *sleep* states. A low duty cycle, where the node is mostly in the sleep state, can significantly extend a node's operation for a given power supply capacity. The drawback is a reduction in data throughput, as well as an increase in packet delays. This is particularly the case in large converge-cast WSNs with multiple hops [5, 65], which represent one of the

most common WSN architectures. This highlights the needs to balance power consumption and performance (i.e., throughput and delay).

The other key element in energy management for WSNs is the power supply subsystem. A reliable power supply is a key concern for unattended WSN applications. Unattended WSNs are normally powered by a rechargeable battery and solar panel [29]. This is invariably a constrained power supply that results in a significant challenge for reliable data collection and transmission. There has been much attention dedicated to energy harvesting and scavenging technologies in WSNs. However, due to current and voltage level requirements of many common sensors and actuators, this approach is not always practical. The WSN power supply also often constitutes a large cost component of the overall system. Solar panels and batteries do not enjoy the same low cost economics of scale as other CMOS components. This presents another design challenge. How does the WSN designer balance the cost and complexity of the power supply subsystem? This problem has been largely overlooked in the WSN research community. Consequently, the power supply subsystem is often over or under-engineered.

In this chapter, we propose a systematic approach to the design of low-cost power supplies for unattended WSNs. Our approach relies on a very simple and robust battery recharge circuit, while keeping the cost of the overall power supply subsystem to a low level. Importantly, the proposed approach does not involve adaptive schemes that change the duty cycle during the network operation. This greatly simplifies the protocol complexity, saves the processing and energy resources consumed by the adaptive scheme, and overcomes the synchronization issue in tree-based WSNs. We use an experimental WSN test bed to evaluate the power supply subsystem that is designed using our proposed approach.

The structure of this chapter is as follows. Section 4.2 outlines the common design approaches to extending the battery lifetime of a WSN node. Section 4.3 outlines the problems addressed in this chapter. Section 4.4 outlines our approach. Section 4.5 outlines the design evaluation by using an experimental WSN test bed, including the evaluation objectives, the WSN test bed description, the design methodology, and the experimental results and discussion. Section 4.6 summarizes the results and outlines further work.

4.2 Current Approaches

In this section, we outline some typical approaches to the extension of battery lifetime and achieve self-sustainable environmental-powered WSNs, especially for unattended WSNs in outdoor applications. We focus on the approaches where the WSN nodes are powered by solar energy.

As indicated earlier in Section 4.1, a standard power supply subsystem for WSNs consists of a rechargeable battery and a solar panel. Typically the design of this subsystem has relied on rule-of-thumb measures [29, 97]. For example, the battery voltage is selected based on the design of the WSN node's voltage regulator, and the solar panel is designed to ensure it does not overcharge the battery in full sun conditions. However, this process does not consider issues including the variability in the solar panel's voltage and current supply characteristics as a function of solar irradiance as well as irregular load demands (e.g., switching currents when actuating pumps). In addition, the long-term variation of solar conditions is overlooked in this approach, which can cause the solar panel to undercharge the battery in weak solar conditions because the battery capacity has not been selected appropriately.

The approach outlined in [68] models the relationship between solar energy supply and load consumption. This model is used in an adaptive algorithm that achieves energy-balance operation by dynamically adjusting the duty cycle to match solar irradiance. In this operation mode, energy supply is always greater than consumption. However, this adaptive scheme increases the protocol complexity, and requires additional processing and energy resources. In low solar irradiance, the low duty cycles may reduce the reliability of data transmission. Synchronization becomes a significant issue because transit nodes are adjusted to distinct duty cycles in tree-based WSNs [100]. For example, when a parent node goes into sleep mode and its child is still in the wake-up period, a synchronization scheme is required to handle the network maintenance and potential data transfer.

Another approach is to use sophisticated regulation circuitry to maximize the utility of a solar panel. The design in [7] is typical of a maximum power point tracker (MPPT) circuit that optimizes the solar energy transfer to the batteries in WSNs. It is evident that the use of advanced battery management charge circuits in [110] with a sufficiently large solar panel is beneficial. However, it is a significant cost component.

4.3 Problem Definition

Several key approaches to the design of power supply subsystem for WSNs have been described in Section 4.2. The major benefits associated with them are highlighted individually. However, the shortcomings of these approaches still remain. For example, the variation of solar conditions are overlooked in the rule-of-thumb approaches (e.g., [29, 97]), and the adaptive scheme that dynamically adjusts the duty cycle in [68] increases the energy consumption by the additional processing as well as the protocol complexity. In this chapter, we focus on the power supply subsystem design for unattended WSNs. The purpose is to design low-cost solar-powered subsystems without the use of any adaptive schemes to adjust the duty cycle during operation, while considering the variation of solar conditions that impacts the variability of the solar panel's current and voltage outputs. To address this issue, our power supply subsystem is designed to use a simple and robust charge circuit, and a systemic approach is proposed for selecting the appropriate solar panel and battery elements based on the load power consumption. Particularly, our design approach uses a sunlight motion model to calculate the energy variations in our charge circuit, which enables a self-sustainable energy supply with *indefinite lifetime*. The performance of our designed power supply subsystem is evaluated by measuring the battery voltage, which is an indicator of the battery remaining capacity. For the operation of indefinite lifetime, the variation of battery voltage is discussed in Section 4.5.

4.4 Design Procedure

A systematic approach to designing the power supply subsystem for a WSN node is proposed in this section, including the charge circuit, the proposed design procedure and a detailed discussion for each step.

To reduce the cost, we consider a simple yet robust charge circuit (see Figure 4.1) for the WSN power supply subsystem design. The circuit consists of solar panels, a diode, rechargeable batteries and load. The diode prevents the batteries from discharging through the solar panel. Practical WSN nodes may have other ancillary hardware elements such as cellular modems for back-haul data transmission or sensor and actuator conditioning circuitry. We assume that the load element consists of

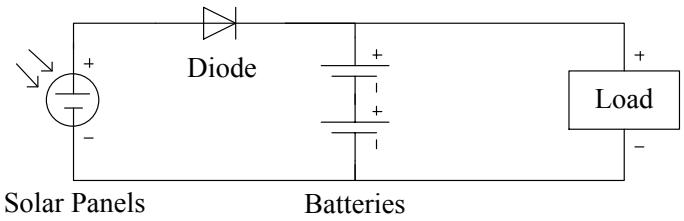

Figure 4.1: Charge circuit

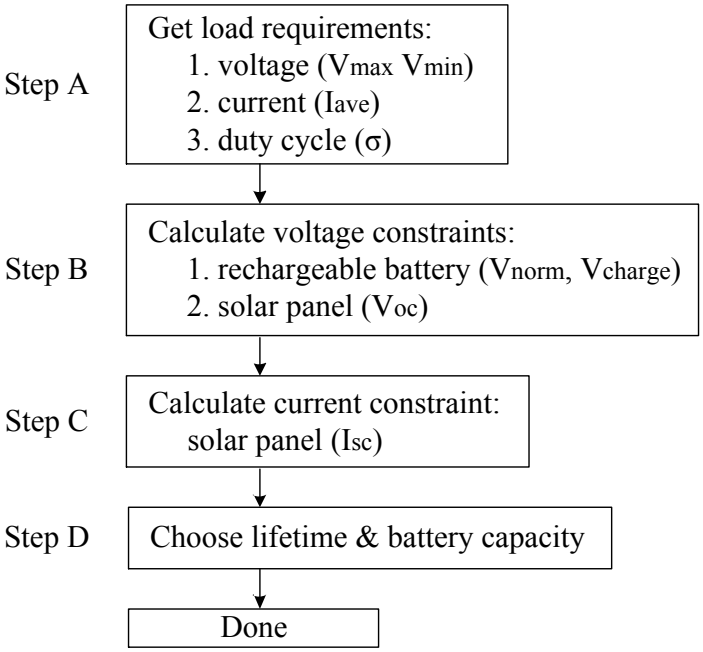

Figure 4.2: Design procedure

multiple devices connected in parallel. This is often overlooked in other studies where all the focus is on the WSN hardware. The circuit in Figure 4.1 is a widely used configuration that has been shown to work well with Sealed Lead Acid (SLA) and NiMH batteries [118]. These batteries offer a significant cost advantage as well as being very reliable in outdoor applications and resilient to constant trickle charging and discharging, as is the case in WSN applications [30, 88].

Figure 4.2 summarizes our proposed power subsystem design procedure. It consists of four key steps. Step A determines the load requirements (voltage, current and duty cycle). Step B calculates the voltage constraints of the batteries and solar panel. In Step C, the current constraint of the solar panel is calculated. In the final step, the required WSN lifetime and battery capacity is selected.

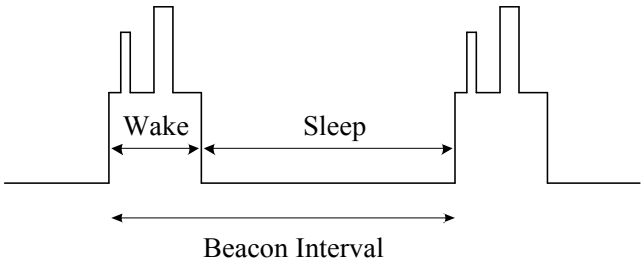

Figure 4.3: Typical current waveform of WSN load

4.4.1 Load Requirements

This section determines the load input voltage and its average input current given multiple load elements and a constant duty cycle configuration.

The load elements discussed earlier may have distinct input voltage ranges, such as a modem [93] that normally operates at a higher input voltage than the WSN hardware. The load input voltage has to lie within their overlapping range. Assume that the load comprises M devices, and the input voltage range of device j is between V_j^{min} and V_j^{max}. The overall load input voltage can be calculated as follows:

$$V_{min} = Max(V_1^{min}, V_2^{min}, \dots, V_j^{min}, \dots, V_M^{min}) \quad (4.1)$$

$$V_{max} = Min(V_1^{max}, V_2^{max}, \dots, V_j^{max}, \dots, V_M^{max}) \quad (4.2)$$

where V_{min} and V_{max} denote the minimum and maximum load input voltage, respectively.

We assume a typical load current waveform in Figure 4.3. Note that the waveform in the wake period can be punctuated by high current spikes related to the WSN activities. These can have a damaging effect on the battery if not properly accounted for in the design procedure. The duty cycle (σ), defined as the ratio of the wake-up duration to the beacon interval, is another key influence factor. In this paper, the average load input current (I_{ave}) is calculated based on this cycle:

$$I_{ave} = i_0 + \sigma(i_1 - i_0) \quad (4.3)$$

where σ is the duty cycle, i_1 represents the average current in the wake period, and i_0 is the current in the sleep period.

Equation (4.3) gives the relationship between the duty cycle and the average load

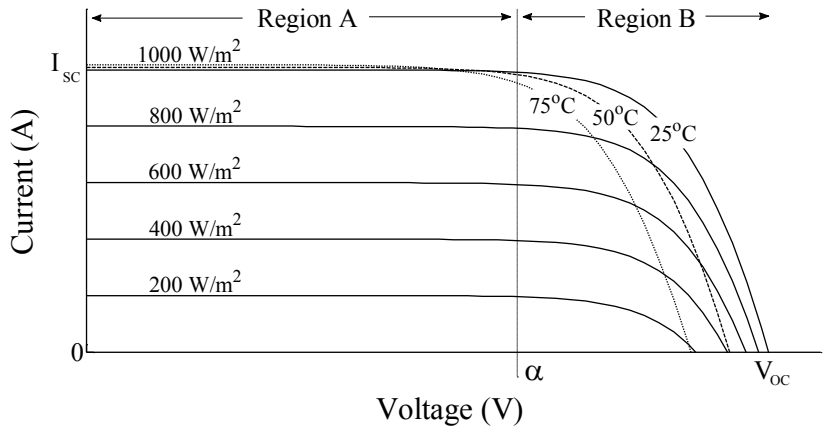

Figure 4.4: I-V characteristic of a solar cell

input current. In the rest of the design, we will use this average current, instead of the duty cycle. All the voltage and current parameters used in equations (4.1) - (4.3) are specified by the relevant device datasheets.

4.4.2 Voltage Constraints

This section outlines the approach to calculating the constraints on the voltage parameters of the battery and solar panel.

Rechargeable Battery – Most WSN design studies are based on the battery voltage in the discharged state, called the normal voltage (V_{norm}). In contrast, its charge voltage (V_{charge}) is often overlooked in these studies. This may cause the battery not to be recharged in the optimal condition. However, our power supply subsystem design is based on both voltage parameters available from the battery datasheet, i.e., V_{norm} and V_{charge}. They are limited by the load voltage requirements referred to in equations (4.1) and (4.2). The constraints on the voltage parameters of the rechargeable battery should satisfy the following inequality.

$$V_{min} \leq V_{norm} < V_{charge} \leq V_{max} \tag{4.4}$$

Solar Panel – The open circuit voltage (V_{oc}) indicates the maximum voltage that a solar panel can supply. From its I-V curve in Figure 4.4, with constant solar irradiance, the output current of the solar panel remains almost unchanged in Region A until its output voltage exceeds a certain value, which is approximated as α percent (e.g., 75%)

of the open circuit voltage. After this point, the output current monotonically decreases to zero in Region B. To achieve the highest output current of the solar panel for the given solar irradiance in our power supply circuit (Figure 4.1), we select an appropriate value of the V_{oc} parameter restricted by the battery's charge voltage so that the solar panel can operate in Region A in most solar irradiance conditions. This can be calculated as follows:

$$V_{oc} \geq \frac{V_{charge}}{\alpha} \tag{4.5}$$

The above approach significantly simplifies the calculation for the current parameter of the solar panel in the next section.

4.4.3 Current Constraints

In this section, a systematic approach to determining the current parameter of the solar panel is presented, and two key constraints of the circuitry component breakdown and battery overcharging are discussed, respectively.

Similar to the parameter V_{oc}, the short circuit current (I_{sc}) reflects the current supply of the solar panel. Our proposed approach to calculating the value of this parameter can be summarized as follows. As described in Section 4.4.2, in most cases, the solar panel operates in Region A in our power supply subsystem. In this region, the output current of the solar panel can be represented as a function of the instant solar irradiance $E(t)$ with a coefficient of the I_{sc} value to the standard test irradiance $1000\ W/m^2$ [94], given by equation (4.6).

$$I(t) = \frac{I_{sc}}{1000} E(t) \tag{4.6}$$

The solar irradiance on the surface of the solar panel obeys a sinusoidal variation during the daytime period [72]. It can be represented by the following equation.

$$E(t) = \begin{cases} E_{peak} \cdot \sin\frac{\pi}{\tau}(t - \tau_1) & \tau_1 \leq t \leq \tau_2 \\ 0 & \text{otherwise} \end{cases} \tag{4.7}$$

and

$$\tau = \tau_2 - \tau_1 \tag{4.8}$$

where τ_1, τ_2 and τ represent the time of sunrise, sunset and the daily sunlight duration in hours, respectively; E_{peak} denotes the daily peak solar irradiance in W/m^2.

Integrating the instant solar irradiance (Equation 4.7) in daytime yields the daily solar radiation in day j, which is

$$\int_{\tau_1}^{\tau_2} E(t)\, dt = Q_j \tag{4.9}$$

By substituting equation (4.7) into (4.9) and unifying the time units to second, the daily peak irradiance E_{peak} in day j is solved as:

$$E_{peak} = \frac{\pi Q_j}{7.2 \times 10^3 \cdot \tau} \tag{4.10}$$

where Q_j denotes the daily solar radiation in $J/(m^2 \cdot day)$ in day j.

According to equations (4.6), (4.7) and (4.10), the instant output current of the solar panel in day j can be represented as a function of the daily solar radiation, which is

$$I_j(t) = \begin{cases} \frac{12\pi\eta I_{sc} Q_j}{\Phi\tau} \sin\frac{\pi}{\tau}(t - \tau_1) & \tau_1 \le t \le \tau_2 \\ 0 & \text{otherwise} \end{cases} \tag{4.11}$$

where the constant $\Phi = 8.64 \times 10^7\ J/(m^2 \cdot day)$, and η is the overall energy conversion efficiency [144] of the solar panel, which is typically 6-40% [43].

The energy conversion capability of a solar cell may be affected by the factors of light reflectance, cell temperature, quantum carrier separation and electrical conduction [144]. In our proposed approach, we consider the overall energy conversion efficiency (η), instead of each of these individual efficiencies.

From equation (4.11), the daily peak output current of the solar panel in day j is

$$I_j^p = \frac{12\pi\eta I_{sc} Q_j}{\Phi\tau} \tag{4.12}$$

The integration of the output current function given by equation (4.11) yields the *daily supplied energy* $C_j(t)$ by the solar panel in day j, as follows:

$$C_j(t) = \begin{cases} 0 & 0 \le t < \tau_1 \\ \frac{12\eta I_{sc} Q_j}{\Phi}\left[1 - \cos\frac{\pi}{\tau}(t - \tau_1)\right] & \tau_1 \le t \le \tau_2 \\ \frac{24\eta I_{sc} Q_j}{\Phi} & \tau_2 < t \le 24 \end{cases} \quad (4.13)$$

The *daily consumed energy* $C'(t)$ by the load can be calculated based on its average current requirement that has been calculated in equation (4.3):

$$C'(t) = I_{ave} t \qquad 0 \le t \le 24 \quad (4.14)$$

By equalizing both one-day energy supply and consumption, the value of the short circuit current parameter of the solar panel in our WSN power supply subsystem can be calculated as follows:

$$I_{sc} = \frac{\Phi I_{ave}}{\eta Q} \quad (4.15)$$

where Q is a system parameter that needs to be selected as described below.

By equation (4.15), the question of how to select the I_{sc} parameter of a solar panel is translated into the selection of the Q parameter, which is a representative value for the local solar conditions. The major benefit of this translation is that the power supply subsystem with the given load in the charge circuit (Figure 4.1) can be systematically characterized by the ratio of the parameter Q and the local measurements of the solar radiation.

Q selection based on 1-day measurement: To achieve the energy-balanced operation of a WSN node in day j, we consider the condition that the daily supplied energy exceeds the daily consumed energy, which is

$$C_j(24) \ge C'(24) \quad (4.16)$$

This yields,

$$I_{sc} \ge \frac{\Phi I_{ave}}{\eta Q_j} \quad (4.17)$$

By substituting equation (4.15) into (4.17), it can be concluded that the I_{sc} parameter of the solar panel must be selected by satisfying the ratio $Q/Q_j \le 1$ in order to maintain the 1-day energy balance.

Q selection based on N-day measurements: The daily solar radiation Q_j varies continuously according to the seasons in a particular geographical location. We assume that its N-day measurements are $Q_1, Q_2, \dots, Q_N$, and Q_{min} and Q_{max} represent their minimum and maximum value, respectively. The mean Q_{ave} is defined as:

$$Q_{ave} = \frac{1}{N}\sum_{j=1}^{N} Q_j \tag{4.18}$$

In this case, the N-day energy-balanced operation of a WSN node can be achieved by satisfying the following inequality.

$$\sum_{j=1}^{N} C_j(24) \geq N \cdot C'(24) \tag{4.19}$$

By simplifying inequality (4.19), it can be rewritten as:

$$I_{sc} \geq \frac{\Phi I_{ave}}{\eta Q_{ave}} \tag{4.20}$$

Similarly, for the N-day energy balance, the I_{sc} parameter of the solar panel must be selected by applying a system parameter $Q \leq Q_{ave}$ in equation (4.15).

There is no scheme to limit the current upper bound in our proposed charge circuit (Figure 4.1). This may potentially damage the components (e.g., the diode or battery) in circuit. The maximum output current (I_{max}) of the solar panel can be calculated by considering the case $Q_j = Q_{max}$ in equation (4.12). We safely limit this value below the current tolerance (I_{tol}) of the charge circuit:

$$I_{max} = I_j^p \Big|_{Q_j = Q_{max}} \leq I_{tol} \tag{4.21}$$

By substituting the equations (4.12) and (4.15) into (4.21), it can be rewritten as:

$$\frac{Q}{Q_{max}} \geq \frac{12\pi I_{ave}}{\tau I_{tol}} \tag{4.22}$$

Inequality (4.22) gives the condition of the system parameter Q with respect to the maximum daily solar radiation in order to prevent the breakdown of the components in the charge circuit.

As discussed above, it requires a system parameter $Q \leq Q_j$ in equation (4.15) to prevent a reduction of the battery energy in day j. However, in such conditions, the battery is inevitably overcharged in our charge circuit, such that the battery is still charged after reaching its full electrical capacity.

Battery overcharging is the other critical issue in our power supply design. It causes deterioration in the battery performance, even by maintaining the charge current at a very small level (e.g., trickle charging rate). In the extreme case, it results in a battery explosion, leakage or irreversible damage. Fortunately, most types of modern batteries (e.g., SLA and NiMH batteries) are designed to avoid gas (e.g., hydrogen) generation and only produce heat when overcharged in low currents [138], which significantly reduces the pressure inside the battery and enhances its tolerance to overcharging. In our design, to reduce the cost of a WSN node, we take advantage of this battery feature and do not deploy any additional schemes for preventing the battery from overcharging. In such circumstances, it is sufficient to calculate the overcharging duration per day and limit it to a safe range. Before moving to this question, we first determine the battery energy variation over time based on the proposed current model in our charge circuit.

The maximum amount of energy that a battery is capable of storing is known as the battery capacity, which is commonly measured in ampere-hours (Ah). In the charging process, the battery stops gaining energy when it reaches full capacity. This battery characteristic can be modeled by an upper limit function $[x]^a$, which is defined as follows:

$$[x]^a = \begin{cases} x & x \leq a \\ a & x > a \end{cases} \tag{4.23}$$

By discretizing the functions of the daily energy supply and consumption given by equations (4.13) and (4.14) at the same sampling rate of $1/T$, the battery energy at time kT can be updated by incrementing the energy at the previous time tick $(k-1)T$ by the difference between the supplied and consumed energy in time interval $[(k-1)T,\ kT]$. Hence, the instantaneous battery energy $\hat{C}_j(k)$ at time $t = kT$ in day j can be calculated by the following recursive equation:

$$\hat{C}_j(k) = \left[\hat{C}_j(k-1) + \Delta C_j(k) - \Delta C'(k)\right]^C \quad 0 < k \leq \frac{24}{T}, k \in \mathbb{Z} \tag{4.24}$$

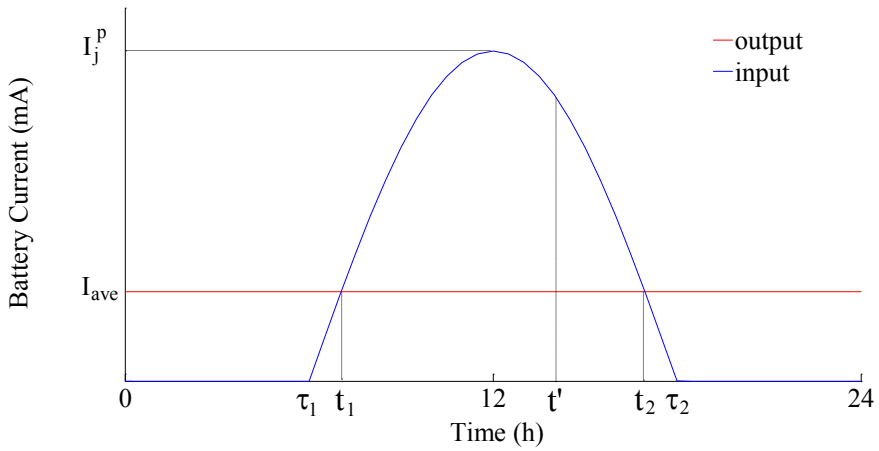

Figure 4.5: The variation of the battery current

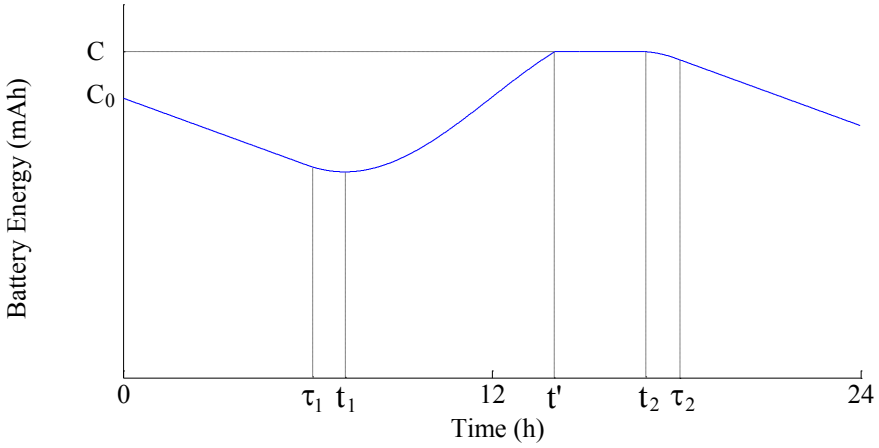

Figure 4.6: The variation of the battery energy

where T is the sampling interval in hours, C denotes the battery capacity, and $\hat{C}_j(0)$ is the initial state of battery energy in day j. The terms $\Delta C_j(k)$ and $\Delta C'(k)$ are the supplied and consumed energy in the sampling interval, which are defined as:

$$\Delta C_j(k) = C_j(kT) - C_j\big((k-1)T\big) \tag{4.25}$$

$$\Delta C'(k) = C'(kT) - C'\big((k-1)T\big) \tag{4.26}$$

Figure 4.5 and 4.6 illustrate the current and energy variations of the battery in our charge circuit with a given WSN load and solar panel in day j, which suggests a typical case of battery overcharging. The condition of energy balance is applied with a ratio of $Q/Q_j < 1$. As outlined in Figure 4.3, the input current of the WSN node may

vary widely in a beacon interval (e.g., between wake-up and sleep periods). The length of a beacon interval is usually about 2 to 3 orders of magnitude shorter than the length of a day. Therefore, the average load current I_{ave} in equation (4.3) is used as an approximation of the battery output current in Figure 4.5, while its input current varies in the daytime as the output current of the solar panel (equation 4.11) and reaches the peak value of I_j^p (equation 4.12) in the middle of the day. In Figure 4.6, the battery energy is calculated by equation (4.24) with a minute sampling interval. C_0 is the battery energy $\hat{C}_j(0)$ at time tick $k = 0$ and C is the battery capacity. The battery starts to gain and lose the energy at time points t_1 and t_2, respectively, which can be solved by equalizing the battery's input and output current:

$$C_j(t) = C'(t) \tag{4.27}$$

This yields,

$$t_1 = \tau_1 + \frac{\tau}{\pi}\arcsin\left(\frac{\tau Q}{12\pi Q_j}\right) \tag{4.28}$$

$$t_2 = \tau_2 - \frac{\tau}{\pi}\arcsin\left(\frac{\tau Q}{12\pi Q_j}\right) \tag{4.29}$$

where t' is the time when the battery is fully charged and starts to be overcharged. The battery overcharge duration δ_j in day j is defined as follows:

$$\delta_j = t_2 - t' \qquad t_1 < t' < t_2 \tag{4.30}$$

Based on the above example, it can be concluded that the occurrence of overcharging the battery is related to both the initial state $\hat{C}_j(0)$ of battery energy and the daily solar radiation Q_j. For the latter, a ratio of $Q/Q_j < 1$ is a necessary condition of the battery overcharge in day j. Its sufficient and necessary condition is given by the following inequality.

$$C_j(t_2) - C'(t_2) \geq C - \hat{C}_j(0) \tag{4.31}$$

The value of $\hat{C}_j(0)$ depends on the battery energy $\hat{C}_{j-1}(k')$ at time $t_2 = k'T$ and the solar radiation Q_{j-1} in the previous day, where k' is an integer value corresponding to the time t_2. The initial energy state $\hat{C}_j(0)$ can be calculated by using

the following equation:

$$\hat{C}_j(0) = \hat{C}_{j-1}(k')\Big|_{t_2=k'T} + \left[C_{j-1}(\tau_2) - C_{j-1}(t_2)\right] - \left[C'(24) - C'(t_2)\right] \qquad (4.32)$$

In satisfying the overcharge condition given by inequality (4.31), the overcharge duration δ_j in day j varies as a function of the parameters Q_j and $\hat{C}_j(0)$, which can be solved by:

$$C_j(t_2 - \delta_j) - C'(t_2 - \delta_j) = C - \hat{C}_j(0) \qquad 0 \le \delta_j < \tau \qquad (4.33)$$

where δ_j approaches to τ when Q/Q_j decreases towards zero ($I_{sc} \to \infty$). When equality holds in (4.31), δ_j just maintains at zero such that the battery energy reaches the full capacity only at time t_2.

In our design, we consider the case of the maximum overcharge duration δ_{max}. According to equation (4.33), this case occurs when both the initial state $\hat{C}_j(0)$ and solar radiation Q_j achieve the maximum, which are equivalent to

a) $Q_j = Q_{max}$
b) $Q_{j-1} = Q_{max}$
c) $\hat{C}_{j-1}(k')\Big|_{t_2=k'T} = C$

where the conditions b) and c) imply the maximum value of $\hat{C}_j(0)$, which is represented as $\hat{C}_{max}(0)$.

To solve the maximum overcharge duration δ_{max}, we first substitute equation (4.32) into (4.33) under the conditions a) – c), which is

$$C_j(\tau_2) - C_j(t_2) + C_j(t_2 - \delta_{max}) = C'(24) - C'(t_2) + C'(t_2 - \delta_{max}) \qquad (4.34)$$

Note that this is a transcendental function in terms of δ_{max}. By substituting equations (4.13), (4.14), (4.15), (4.29) into (4.34), it can be represented as a function of the ratio of Q/Q_{max} and the daily sunlight duration τ:

$$\delta_{max} = F\left(\frac{Q}{Q_{max}}, \tau\right) \qquad 0 \le \delta_{max} < \tau, 0 < \frac{Q}{Q_{max}} \le 1 \qquad (4.35)$$

We apply a root-finding algorithm called Brent's Method [18] for solving the maximum overcharge duration δ_{max} in equation (4.34). Figure 4.7 shows the results

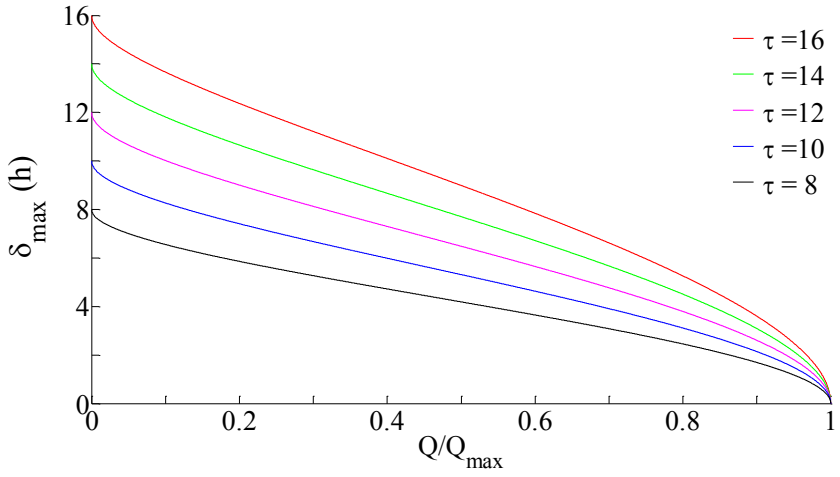

Figure 4.7: δ_{max} versus Q/Q_{max}

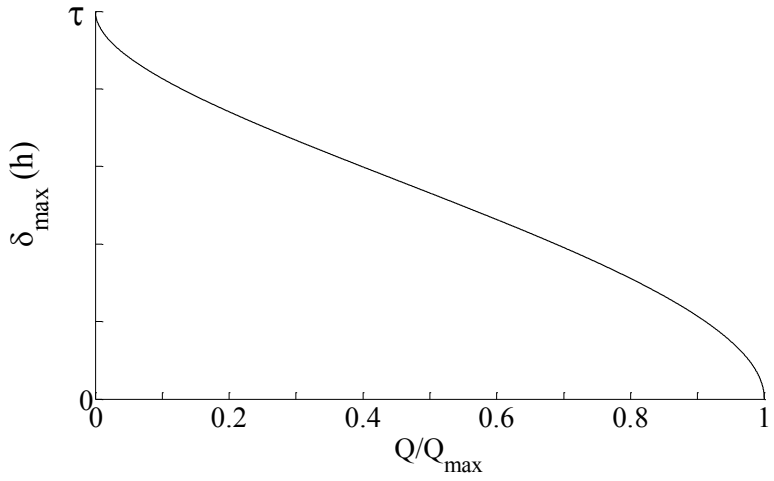

Figure 4.8: An approximation of δ_{max} versus Q/Q_{max}

of δ_{max} versus Q/Q_{max} with different values of the daily sunlight duration τ. It can be seen that the maximum overcharge duration δ_{max} decreases monotonically as the ratio Q/Q_{max} increases for each value of τ. It decreases to zero when $Q = Q_{max}$, and approaches to τ when Q goes towards zero. On the other hand, for a constant ratio of Q/Q_{max}, the duration δ_{max} has an approximately linear relationship with the daily sunlight duration τ. Under such an approximation, a curve of δ_{max} versus Q/Q_{max} is redrawn in Figure 4.8.

Like the current limitation in equation (4.21), we limit the maximum overcharge duration δ_{max} to be below the overcharge tolerance (δ_{tol}) specified by the battery:

$$\delta_{max} = \delta_j \Big|_{Q_j = Q_{max}, \hat{C}_j(0) = \hat{C}_{max}(0)} \leq \delta_{tol} \tag{4.36}$$

The constraint on the Q value corresponding to the overcharge tolerance δ_{tol} can be determined by referring to either Figure 4.7 or 4.8.

In summary, this section presents an approach to select the parameter I_{sc} of a solar panel in order to maintain the energy balance between the supply and consumption in our charge circuit, which is given by equation (4.15). According to this equation, this problem is translated to the characterization of the system parameter Q instead. Equation (4.18) gives a general rule of Q selection based on the historical N-day measurements of the daily solar radiation. Moreover, two constraints of the parameter Q are discussed in regards to the maximum current in the charge circuit and the maximum battery overcharge duration, given by equation (4.22) and Figure 4.7.

4.4.4 WSN Lifetime and Battery Capacity

This section outlines the design goal of achieving a given WSN lifetime in our power supply subsystem, and discusses relevant parameter constraints.

In practice, most WSN node power supplies are designed to be capable of providing the load with energy for an indefinite lifetime. We focus on the same aim for our power supply subsystem design. From our charge circuit (Figure 4.1), the WSN node lifetime is related to the parameter I_{sc} of the solar panel, the load average current requirement and the battery capacity. For these parameters, the battery capacity does not play a predominant role in the indefinite lifetime design, and the effect of the load average current has been accounted for when the parameter I_{sc} is calculated based on equation (4.15). Therefore, selecting an appropriate value of the parameter I_{sc} is critical for the design of a WSN node with an indefinite lifetime. By equation (4.15), this can be translated to the selection of the parameter Q.

A WSN node can operate for an indefinite lifetime by applying $Q \leq Q_{ave}$ as suggested in Step C. In the condition $Q_{min} < Q \leq Q_{ave}$, the solar panel can only provide part of the required energy by the load when the actual daily solar radiation is less than the selected parameter Q. Achieving indefinite operation requires a battery with sufficient capacity that can provide the rest of the required energy during periods of low solar radiation. In the condition $Q \leq Q_{min}$, the solar panel is capable of

providing the energy required by the load in all sunlight conditions in the given location. The minimum battery capacity is the load energy requirement during nighttime.

Many factors have an impact on battery capacity, such as temperature, self-discharge and lifecycle [130]. We use the overall battery efficiency ρ to formulate the effects of these factors. This value mainly depends on the application environment, battery quality and usage.

If the parameter Q is not selected properly (e.g., $Q > Q_{max}$), the WSN node cannot operate with an indefinite lifetime regardless of the battery capacity, since the battery discharge rate always exceeds its charge rate. In this condition, the average lifetime ε of the WSN node can be approximated by

$$C'(\varepsilon) - \frac{C_j(24)\Big|_{Q_j=Q_{ave}}}{24}\varepsilon = \rho C \tag{4.37}$$

This yields,

$$\varepsilon = \frac{\rho C}{I_{ave}(1 - Q_{ave}/Q)} \tag{4.38}$$

Equation (4.38) leads to the well-known formula that is used to calculate the lifetime ε_{min} of a WSN node when the effect of the solar panel is neglected due to its malfunction or poor weather conditions.

$$\varepsilon_{min} = \frac{\rho C}{I_{ave}} \tag{4.39}$$

The WSN lifetime can also be estimated by finding the time tick k that satisfies $\hat{C}_j(k) = 0$ in equation (4.24) with initial energy $\hat{C}_j(0) = \rho C$. Multiple solutions may exist, but the minimum one is appropriate, i.e., the first time point when the battery has completely discharged.

Note that applying an appropriate value of the system parameter Q is the key step in the design of the power supply subsystem of a WSN node using our proposed approach. It can be selected based on either the observation or the prediction for the daily solar radiation. Needless to say, the use of the predicted values has practical significance in anticipating the states of the power supply subsystem (e.g., the battery energy). However, it requires the use of forecasting techniques for the daily solar

radiation based on their historical observations. This problem is beyond the scope of our research, and is not addressed in this chapter. Instead, we use the observed values of the daily solar radiation to evaluate our design performance as outlined in Section 4.5.

4.5 Design Evaluation

In this section, we design the power supply subsystem for a practical WSN node by following the design procedure specified in Section 4.4. An experimental WSN test bed is used to evaluate the design performance. Section 4.5.1 outlines the objectives of the power supply subsystem design and performance evaluation. Section 4.5.2 outlines the WSN test bed used in the experiments. The experimental methodology and design parameters are presented in Section 4.5.3. The experimental results are summarized and discussed in Section 4.5.4.

4.5.1 Aims

Our aim is to design two power supply subsystems for the experimental WSN node with different sets of design parameters based on the proposed design procedure in Section 4.4. The design performance of each power supply subsystem is evaluated individually by using an experimental WSN test bed. Based on the collected measures of battery energy information, the purpose of the first experiment is to present a mismatch case between the load requirements and the WSN power supply subsystem, when this subsystem is not adequately dimensioned. The second experiment shows a node with an indefinite lifetime when its power supply subsystem satisfies the suggested condition in Section 4.4.4 for the given load.

4.5.2 Wireless Sensor Network Test Bed

In this section, we describe the experimental hardware, communication protocol, implementation framework and load requirements of our experimental test bed.

In the experiments, we employ the NICTOR hardware (Figure 4.9) described in Chapter 2 as the wireless communication device. A Beacon Flooding protocol [85]

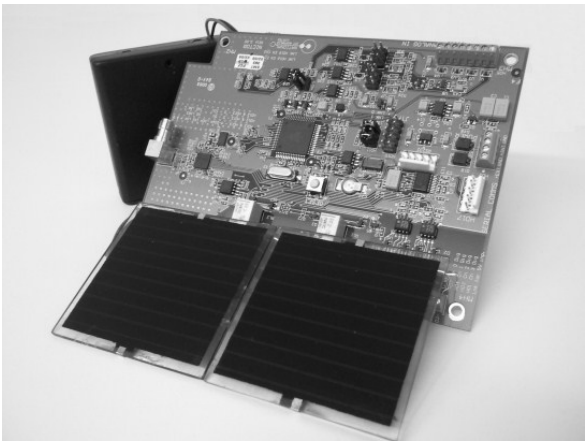

Figure 4.9: NICTOR platform

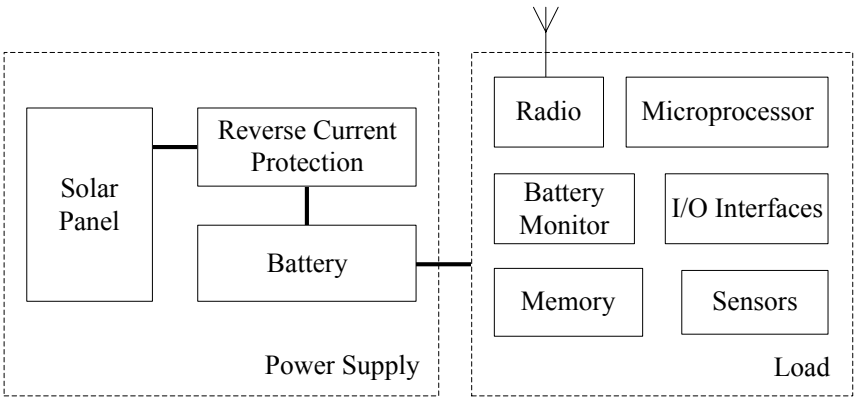

Figure 4.10: Implementation framework

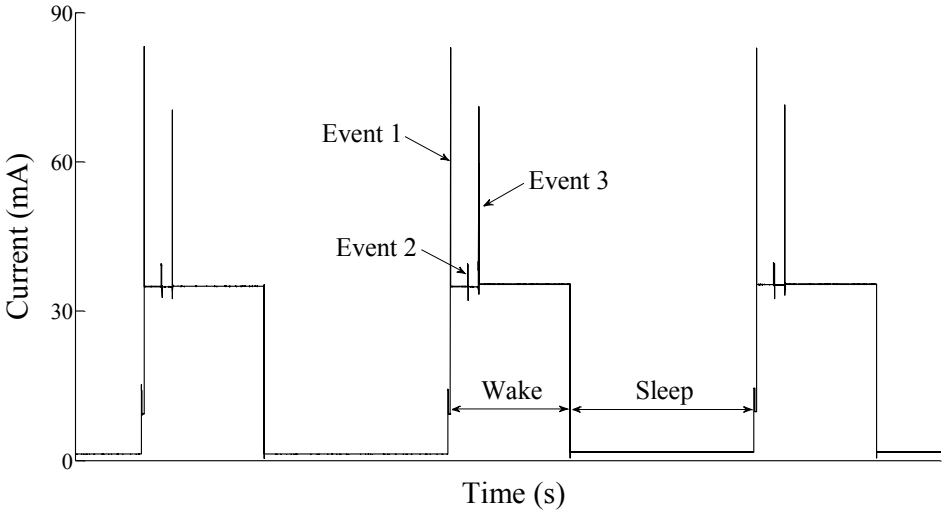

Figure 4.11: Load current measurement for 3 beacon intervals

proposed in Chapter 3 is applied in the coordinator and router nodes. This is a low-complexity converge-cast protocol for WSNs with a tree or star topology. It gives users the freedom to adjust the beacon interval structure, e.g., the duty cycle.

Figure 4.10 illustrates the overall framework of the node implementation. The charge circuit described in Section 4.4 (see Figure 4.1) is deployed in the experiments. The NICTOR platform has a built-in battery monitoring sensor, and also connects with two soil moisture sensors via I/O interfaces. All the measurements are periodically sent to the coordinator.

During the WSN node operation, all the load devices consume energy. However, only the NICTOR platform requires the external power supply, and in turn, it powers the rest. The range of its input voltage is from 3.4V (V_{min}) to 12V (V_{max}). To calculate the average current consumption of our experimental load, its current variation is recorded for several beacon intervals. From Figure 4.11, the current during the sleep period remains approximately 1.6mA (i_0). During the wake period, the current remains almost constant at 35mA, except for three events, which are system wake-up from sleep state (Event 1), beacon re-broadcast (Event 2) and making measurements (Event 3), in chronological order. Although the current jumps suddenly during these events, their durations are quite short in contrast with the entire active period. Hence, the average current in the wake period can still be approximated at 35mA (i_1).

4.5.3 Methodology

This section outlines the deployment setup of the experimental WSN, the battery energy measures, the power supply subsystem design and the selection of relevant parameters.

Two experiments are conducted at Dookie Farm in northern Victoria in Australia ($36^{\circ}22'10''\text{S}, 145^{\circ}42'17''\text{E}$). All the nodes are located in an open field without any obstacles in front of the solar panel, and the surface of the solar panel is adjusted to be perpendicular to the plane of the sun's motion. The coordinator is powered by an energy source with sufficient capacity and remains awake all the time with a duty cycle $\sigma = 1$. Each router node is attached to a power supply component shown in Figure 4.10, including the charge circuit, solar panel and rechargeable batteries.

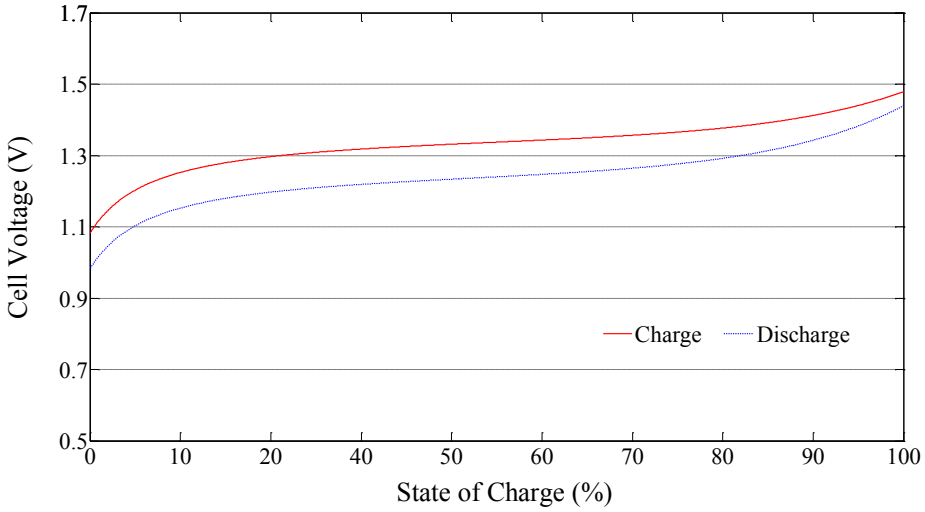

Figure 4.12: Voltage-energy characteristic of a NiMH battery cell

In the experiments, we use the NiMH rechargeable batteries. Figure 4.12 shows a typical charge/discharge curves for a NiMH battery cell. It can be observed that, for either the charge or discharge curve, each energy state corresponds to a unique cell voltage. Based on this voltage-energy characteristic, the energy of the NiMH battery can be estimated by measuring its voltage. In our experiments, we apply this approach to estimate the battery energy in various charge/discharge stages based on the corresponding voltage measured by a built-in battery monitoring sensor in the WSN node.

In our proposed design approach, the selection of the parameter Q in equation (4.15) is affected significantly by the historical N-day measurements of the daily solar radiation applied in equation (4.18). The daily sunlight duration is a necessary parameter in the calculation of the maximum current and battery overcharge duration. To improve the design accuracy and the credibility of the data source, all the historical measurements of the daily solar radiation and the daily sunlight duration used in our design are obtained from the official statistics [41, 132].

The first experiment is conducted in autumn. In this period the sunrise and sunset times vary slightly, and the daily sunlight duration is about 11 hours [41]. According to the measurements based on satellite images [132], the average daily solar radiation is approximately 19 $\mathrm{MJ}/(\mathrm{m}^2 \cdot \mathrm{day})$ in this period from recent 5-year statistics, where the maximum reaches up to $21\mathrm{MJ}/(\mathrm{m}^2 \cdot \mathrm{day})$, and the minimum is only 3 $\mathrm{MJ}/(\mathrm{m}^2 \cdot \mathrm{day})$ in extremely cloudy days (lasting no longer than 2 days). For most days, the

Table 4.1: Design parameters in experiment I

	Parameter	**Value**
Sunlight Conditions	τ	11 hours
	Q	168 $\mathrm{MJ/(m^2 \cdot day)}$
	$Q_{min}/Q_{ave}/Q_{max}$	15/19/21 $\mathrm{MJ/(m^2 \cdot day)}$
Load	i_1/i_0	35/1.6 mA
	σ	1
	I_{ave}	35 mA
	V_{min}/V_{max}	3.4/12 V
Solar Panel	V_{oc}	9 V
	I_{sc}	90 mA
	η	0.2
Batteries (4×NiMH AA)	V_{charge}	5.6-6 V
	V_{norm}	4.8-5.2 V
	C	2500 mAh
	ρ	0.95

daily solar radiation fluctuates between 15 and 21 $\mathrm{MJ/(m^2 \cdot day)}$. Table 4.1 lists all the design parameters in this experiment.

In this experiment, the duty cycle of the WSN node is set to $\sigma = 1$. In this case, the load requires a large average current value of 35 mA calculated by equation (4.3). The voltage parameters of the battery and solar panel are selected to satisfy the constraints given by inequalities (4.4) and (4.5). In Step C, a solar panel with the parameter $I_{sc} = 90\mathrm{mA}$ is selected, which gives a reference parameter $Q = 168\ \mathrm{MJ/(m^2 \cdot day)}$ according to equation (4.15). In considering the current tolerance of the charge circuit, the diode allows a maximum forward current of 1A, while the battery charge current is normally limited below a value of $0.2\mathrm{CmA}$, where CmA denotes the current that is expressed as a multiple of the battery capacity C [130]. Therefore, a limited current of 500mA by the latter is used as the current tolerance. By examining inequality (4.22), it is concluded that the current in the charge circuit varies in a safe range. In this experiment, the parameter Q exceeds the maximum solar radiation Q_{max}, which does not satisfy either the condition of battery overcharge or the condition of indefinite lifetime of the WSN node. In this case, the average lifetime of the WSN node is estimated to be 77 hours by using equation (4.38).

The second experiment is conducted during the summer (Nov-Dec), so the sunlight conditions have to be reconsidered by deploying the same approach as experiment I.

Table 4.2: Design parameters in experiment II

	Parameter	**Value**
Sunlight Conditions	τ	14 hours
	Q	13.9 $\mathrm{MJ/(m^2 \cdot day)}$
	$Q_{min}/Q_{ave}/Q_{max}$	15/27/36 $\mathrm{MJ/(m^2 \cdot day)}$
Load	σ	0.04
	I_{ave}	2.9 mA

In this period, the sunlight duration increases to an average of 14 hours [41] per day, while the daily solar radiation achieves up to a maximum value of 36 $\mathrm{MJ/(m^2 \cdot day)}$ with an average 27 $\mathrm{MJ/(m^2 \cdot day)}$ [132]. Like in autumn, the minimum is around 3 $\mathrm{MJ/(m^2 \cdot day)}$ as well, but for most days, the solar radiation fluctuates above 15 $\mathrm{MJ/(m^2 \cdot day)}$. Table 4.2 lists the parameters that differ from those in experiment I.

In the second experiment, the aim is to achieve an indefinite lifetime of the WSN node. According to the suggested conditions in Section 4.4.4, we apply the condition $Q \leq Q_{min}$ to design the WSN power supply. To satisfy this condition, we deploy the same solar panel and only change the duty cycle to $\sigma = 0.04$, which gives a much lower load average current of 2.9mA, compared to that in experiment I. Under such the load consumption, the parameter Q consequently drops substantially from 168 to 13.9 $\mathrm{MJ/(m^2 \cdot day)}$ and meets our applied condition above in the sunlight conditions listed in Table 4.2. In this experiment, the charge circuit has the same current tolerance of 500mA as in experiment I, and the design still satisfies the current constraint given by inequality (4.22). The battery is overcharged every day in this design because of the applied condition $Q \leq Q_{min}$. According to Figure 4.7, the maximum overcharge duration is approximately 8.5 hours corresponding to the ratio Q/Q_{max}, Note that the maximum charge current I_{max} in this design lies within a typical trickle current range ($< 0.01C$) for a NiMH battery. In this case, the battery normally endures the overcharging for a longer time (total 10 to 20 hours [101]). Therefore, the batteries are able to safely work in their daily charge-discharge process.

4.5.4 Results and Discussion

This section presents two experimental results based on the different designs for the power supply subsystem described in Section 4.5.3 and the relevant discussions.

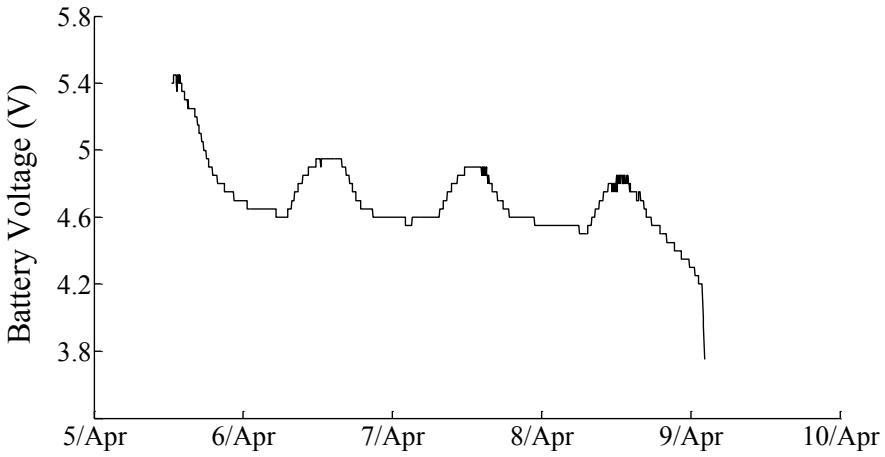

Figure 4.13: The measurements of battery voltage in autumn (experiment I)

Figure 4.13 shows the measurements of the battery voltage in April based on the design parameters for experiment I. According to the voltage-capacity characteristic of the NiMH battery, its energy can be reflected by its overnight voltage in our experiment. Compared with the normal voltage, its output voltage drops rapidly to 4.6V during the night-time, and each cell remains at 1.15V, which reflects that its energy reduces to a very low level. The battery depletes after 82 hours. Recall that our estimated average lifetime under these conditions was 77 hours. This result demonstrates that the power supply subsystem in experiment I is not capable of supplying sufficient energy under the load current requirement and the sunlight conditions listed in Table I. This is to be expected given our analysis in Section 4.4.3, since a large Q value greater than the maximum daily solar radiation Q_{max} is yielded by a large load average current and a small I_{sc} value of the solar panel based on equation (4.15). As discussed in Section 4.4.4, the indefinite lifetime design cannot be implemented in the condition $Q > Q_{max}$, unless the load average current is reduced or a solar panel with a larger I_{sc} value is used.

In the experiment II, we design a power supply subsystem supporting an indefinite lifetime of the WSN node. In this case, the design performance is evaluated by presenting a section of the experimental results and analyzing the battery energy variation during this period. Figure 4.14 depicts the measurements of battery voltage over 25 days in summer. For most days, the battery voltage during the night-time maintains around 5.2V, and each cell corresponds to 1.3V. From the characteristics of the NiMH battery, this indicates that its energy keeps almost its full capacity. It is worth noting that the battery energy decreases to about 5V on 8th/Dec, which results

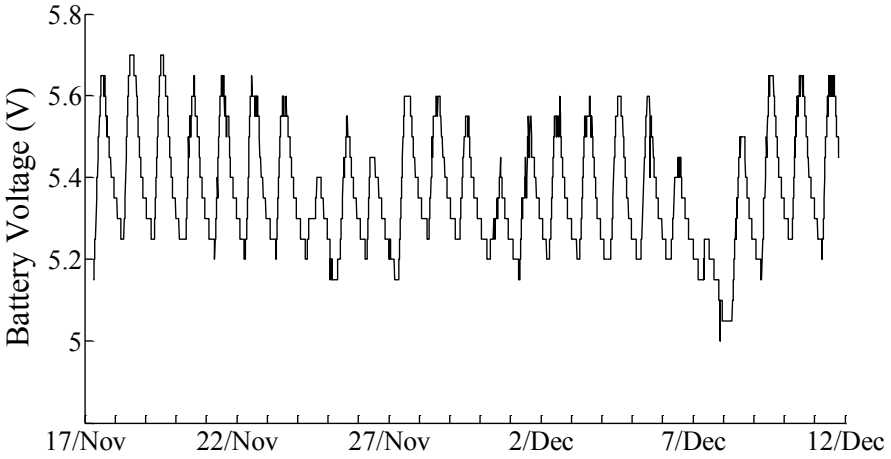

Figure 4.14: The measurements of battery voltage in summer (experiment II)

from a level of solar radiation less than our applied Q_{min}. This is expected because the Q_{min} value selected in this experiment is not the absolute minimum of the historical measurements, but a value less than most of them. There is no period longer than two days where the daily solar radiation is less than our applied Q_{min}. After this day, the battery energy gradually grows back to the level as in most days. According to the high overnight voltage and its small fluctuation in Figure 4.14, it can be concluded that the power supply subsystem in this experiment is able to achieve our design purpose.

4.6 Summary

In this chapter, a systematic approach to designing a low-cost solar power supply subsystem for unattended WSNs is proposed. Based on a theoretical daily solar irradiance model, we calculate the parameter constraints for the elements in our charge circuit, in order to achieve indefinite lifetime operation of a WSN node. An experimental WSN test bed is used to evaluate our proposed design approach. A benefit of our approach is that it accounts for the effects of the load requirements and the environmental sunlight variation on the indefinite lifetime design, while a scheme to change the duty cycle is not required during the WSN operation.

Chapter 5

Low-Cost Plant-Based Sensing for Irrigated Agriculture

The efficient management of water resources has become a major focus of research in recent years due to the increasing frequency of water shortages. A major source of water consumption is irrigation in agriculture. In on-farm irrigation, the control of the water supply to crops is commonly based on the measurement of the water content in the soil, known as the soil moisture level. A typical approach to measuring soil moisture level is to use a sensor probe that is buried in the ground, which gives the measurement at a single point in a field. The major limitation of this approach is that it requires the deployment of a large number of soil moisture sensors in order to make irrigation scheduling decisions over a wide physical area. Accurate sensing over a large area thus incurs a substantial cost. In this chapter, we evaluate the potential for measuring soil moisture over large areas by using image-based sensing techniques. Low-cost imaging sensors and wireless sensor networks (WSNs) can be used to reduce the total cost of measuring moisture levels. Experimental results in two test environments are presented.

5.1 Introduction

Novel approaches to irrigation scheduling are becoming critically important as water resources in agriculture come under increased scrutiny. It has been shown that through increased measurement of plant water requirements, one can substantially improve yield and quality with less water [95]. However, a challenge has been in implementing the measurement of water requirements in a way that is low cost,

sufficiently accurate and easy to use. This remains an open challenge since the current uptake of smart irrigation scheduling systems is low.

Between 2004 and 2008, the Victorian Government funded a joint research initiative called Smart Irrigation between National ICT Australia, The University of Melbourne and Uniwater. The purpose of this project was to develop low-cost wireless sensor networks and irrigation scheduling algorithms for dairy, viticulture and horticulture. This project demonstrated up to 30% water savings in dairy irrigation and up to 75% increases in yield in horticulture [35]. The project laid the foundations for future research in the application of intelligent sensor networks and control algorithms to irrigation science.

Current approaches to irrigation scheduling rely on point-scale measurements of soil moisture [57, 107]. However, due to crop, soil and micro-climate variability, decisions based on point-scale data may not be optimal for a large agricultural field. Overcoming this limitation requires a sensing system with a wider spatial coverage.

In this chapter, we evaluate the probability of monitoring soil moisture levels in a field using image-based sensing. In particular, we investigate the feasibility of using low-cost infrared sensors. We present the outcomes of a series of experiments used to evaluate this scheme. We present the results of our feasibility studies under two practical deployments: in an agricultural field and in a climate controlled plant-house.

The structure of the rest of this chapter is outlined as follows. Section 5.2 presents a method for moisture measurement known as the normalized difference vegetation index. Section 5.3 outlines an experimental method of measuring soil moisture based on this index, and describes our experimental implementation, methodology and results. Section 5.4 summarizes the feasibility of this approach and future work.

5.2 Normalized Difference Vegetation Index

This section outlines a common indicator of plant water stress, the *normalized difference vegetation index* (NDVI). The NDVI can be used as a surrogate for soil moisture, since it has been shown that the NDVI can be affected by the level of a plant's water stress [37, 39, 42, 135]. Water stress loosely translates to a non-optimum soil moisture level. This is how the NDVI parameter could be used as an irrigation scheduling decision parameter.

Photosynthesis of green vegetation requires the light energy within a particular

frequency spectrum. The strong absorption of solar radiation by live green plants occurs in the visible spectral region from 400 to 700 nanometers, also known as the photosynthetically active radiation (PAR) region [40], where part of the energy required by the process of photosynthesis reaction occurs. Therefore, in contrast with other objects, live green plants appear relatively dark in the PAR region. However, they appear relatively bright in the near-infrared (NIR) spectral region (700-1100 nm), because leaf cells have evolved to scatter solar radiation at these wavelengths to prevent the plants from overheating and damaging their tissues and organisms.

The normalized difference vegetation index (NDVI) [12] is a numerical indicator that is used to assess whether there is live green vegetation in an observed region. It is calculated based on the reflectance of the visual and NIR light from the vegetation, which is defined as follows:

$$\mathrm{NDVI} = \frac{\mathrm{LR_{NIR}} - \mathrm{LR_{VIS}}}{\mathrm{LR_{NIR}} + \mathrm{LR_{VIS}}} \tag{5.1}$$

In equation (5.1), $\mathrm{LR_{VIS}}$ and $\mathrm{LR_{NIR}}$ denote the light reflectance measurements in the visible and NIR spectral regions, respectively. Light reflectance is the ratio of the reflected and incoming light, ranging between 0 and 1. Hence, the calculation of NDVI always varies between -1 and 1. An index of zero indicates that there is no vegetation, while an index close to positive one indicates the highest possible density of green leaves.

Figure 5.1 illustrates an example [141] of NDVI calculation for the given reflectance measurements of both visible and NIR light by using equation (1), and the indices are compared between a healthy plant (left) and an unhealthy one (right).

From Figure 5.1, the healthy plant absorbs 92 percent of the energy from the visual light, and reflects a large portion (50%) of the NIR light. In contrast, more visual light (30%) and less NIR light (40%) are reflected by the unhealthy plant. According to equation (5.1), the healthy plant obtains a high NDVI of 0.72, while the latter only achieves 0.14.

From the above example, it can be seen that there are distinct reflectance values of the visual and NIR light for two plants in different health conditions, which leads to a substantial difference of NDVI. The plant with a higher value of NDVI illustrates that it absorbs more light in the PAR region and reflects more in the NIR region. In this case, it normally has a faster rate of photosynthesis that requires more water when

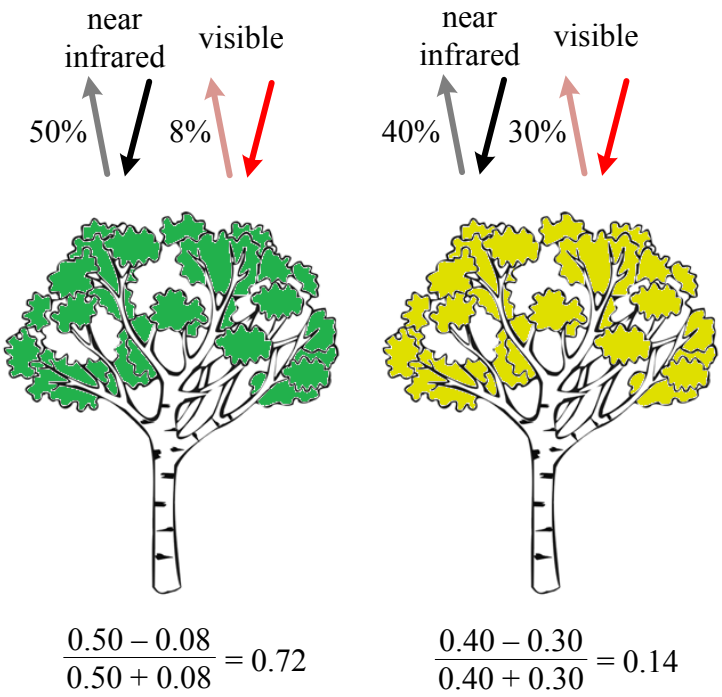

Figure 5.1: Light reflectance and NDVI based on an example from [141]

other influence factors remain constant (e.g., temperature and availability of nutrients) [46]. Plants with different values of NDVI may have an impact on the variation of the soil moisture.

Jordan [64] reported the first use of light radiation in NIR and red spectral regions for measurement of the leaf-area index in a forest. This method is based on the principle that the chlorophyll in plant leaves absorbs more red light than NIR light. Therefore, it is feasible to indicate the leaf areas in a field by measuring the ratio of the NIR/red light reflectance. By following this concept, Pearson *et al.* [105, 106] developed a hand-held spectral radiometer for estimating the biomass index for grass canopy, and a comprehensive study on the measurement of bidirectional light reflectance of vegetation canopies in NIR and red spectrum is presented in [28]. Due to the limitation of a simple NIR/red ratio in monitoring vegetation indices such as biomass, leaf water content and chlorophyll content, Tucker [135] investigated the feasibility of using various linear combinations (including the vegetation index) of NIR and red light radiation for the same purpose. Further, Gamon *et al.* [39] examined the indices of NDVI and NIR/red ratio as indicators of canopy structure, light absorption and photosynthesis by using an in situ measurement method, and discussed the selection of the index for a particular application.

The sensing technology of light radiation in particular spectra is also used for remotely measuring soil moisture levels over a large area. This usually is done by using multi-spectral radiometers that are carried by an aircraft or satellite above the monitored fields. Wigneron *et al.* [142] gave a comprehensive review on various methods for retrieving surface soil moisture using microwave radiometric systems. An inversion "triangle" procedure is proposed in [42] for estimating surface soil water content from measurements of surface soil temperature and NDVI, which are remotely collected by an airborne radiometer with particular spectral filters. By using a similar approach, the experimental results presented in [71, 115] show successful applications of passive microwave technologies for delivering soil moisture over land surface. Farrar *et al.* [37] outlined an extensive study of the relationship between NDVI and moisture levels for different types of soil. A *Lag Correlation* method is used to correlate the measurements of NDVI and soil moisture that are collected over long period. For the spectral sensing approaches described above, a major drawback is the high expense of deploying such measurement systems, which significantly limits their applications in small-scale irrigation agriculture.

In this chapter, we investigate the feasibility of using low-cost image sensors for estimating soil moisture levels from the measurement of NDVI based on green plants. Our proposed experimental approach for measuring NDVI avoids the use of expensive image devices, and consequently reduces overall cost. In the concurrent experimental period, a low-cost moisture sensor based on a WSN is used for collecting real measurements. The relationship between NDVI and soil moisture is investigated by using a simple correlation approach. The next section outlines a detailed description of our proposed low-cost imaging-based experimental methodology for soil moisture estimation.

5.3 Low-cost NDVI Measurement

This section presents an experimental evaluation of making measurements by using a low-cost imaging-based approach. The structure of this section is outlined as follows. Section 5.3.1 is the experimental overview. Section 5.3.2 outlines the hardware devices used in this experiment. Section 5.3.3 outlines the experimental methodology. Section 5.3.4 presents the experimental results and discussion. A concluding summary is given in Section 5.3.5.

5.3.1 Overview

In this experiment, we focus on the study of an imaging-based approach to measuring soil moisture levels by deploying low-cost sensing devices, including a wireless sensor node, soil moisture sensor and low-cost visual and NIR cameras. The light reflectance from a plant with green leaves is measured by the visual and NIR cameras separately, in order to calculate the normalized difference vegetation index (NDVI) (see Section 5.3.3) of a plant under study. The wireless sensor node with a soil moisture sensor is used to collect the true measurements of the soil moisture. The objective of this experiment is to investigate the relationship between the soil moisture and the NDVI of a green plant by correlating both measurements collected using low-cost cameras in the experiment.

5.3.2 Experimental Devices

This section outlines the hardware devices used in the experiment, including the visual and NIR cameras, soil moisture sensor and wireless sensor node.

In imaging-based approaches, the use of professional cameras (e.g., NIR and thermal) significantly increases the total cost. In this experiment, we deploy low-cost webcams (shown in Figure 5.2) to collect the images of the plant.

Webcams are typically designed for the visible spectrum. The lens filter only allows visible light to pass through and filters the NIR wavelengths. A standard webcam is used as the visual camera in the experiment. As for the NIR camera, we have modified a standard webcam by replacing the original filter with a filter that only allows the NIR spectrum through. The webcam used in this experiment has the standard USB interface, and provides the functionalities of manual focus and capturing images with 640 × 480 pixels [86].

The sensor probe called ECH_2O (see Figure 5.3) is deployed to measure the soil moisture in the experiment because of its low cost, high accuracy, low power requirements and easy maintenance [34]. Soil moisture is also known as the volumetric water content, which is defined as the ratio of the water volume and the total volume of water, air and soil. In our experiment, a sensor probe measures the soil moisture based on an initial constant voltage between its two electrodes buried in the soil. It then measures the rate of change of the voltage that is related to the volumetric

Figure 5.2: Low-cost webcam

Figure 5.3: Soil moisture sensor probe

water content in the soil.

In the experiment, the soil moisture sensor is equipped with a wireless device called NICTOR, which has been described in Chapter 2. The NICTOR device is responsible for controlling the sensor to periodically sense soil moisture and transmit sensed data to a remote network coordinator. The use of the sensor network gives a low cost of implementing our experimental system, flexible experimental parameter setup (e.g., the measurement frequency), and efficient and reliable data delivery.

5.3.3 Methodology

This section describes our experimental setup in terms of device placement and interconnection, and presents an image processing approach to calculating the light reflectance from an image in either a RGB or grayscale format.

To ensure a sufficient photosynthesis area for the purpose of image processing, a green leafy plant that belongs to the genus *Passiflora* is used in the experiment. The plant has thin leaves that are approximately 7cm in width and 14cm in length. Figure

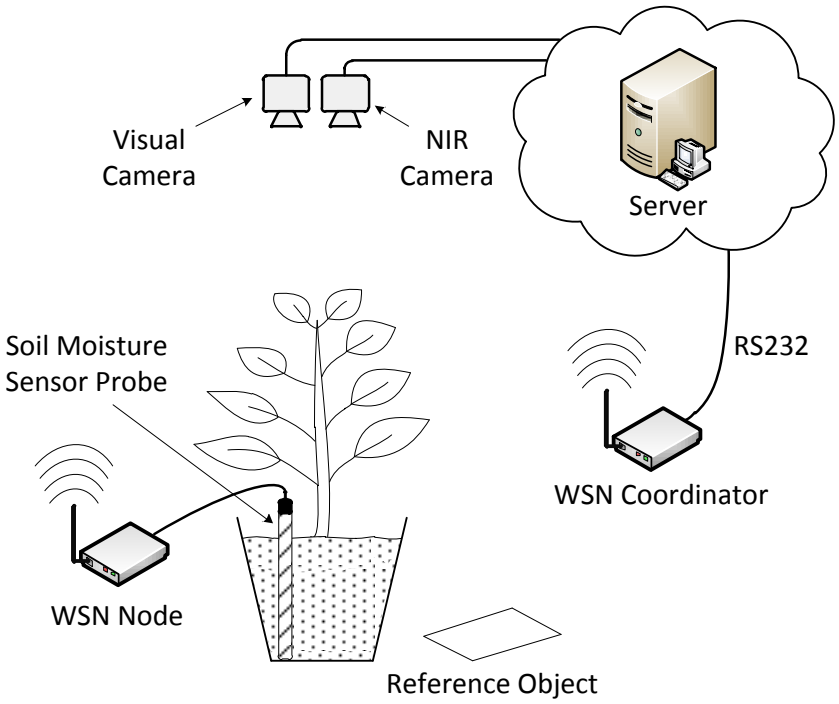

Figure 5.4: Experimental setup

5.4 depicts the experimental setup.

During the experiments, the soil is irrigated when it is observed that the plant starts to wilt. In irrigating a plant, the sufficient amount of water is supplied to fully saturate the soil.

Both the visual and NIR cameras are collocated and placed right above the plant. A piece of white paper is used as a reference object (the red circled region in Figure 5.5), and the incoming light is assumed to be reflected completely in this region. A soil moisture sensor probe is placed vertically in the flowerpot, which gives an average of the moisture values in all the soil levels. By interfacing the sensor probe with a WSN node, the soil moisture is measured periodically and transmitted to a network coordinator. Both the cameras and sensor probe are directly connected to a computer that collects the images and soil moisture every minute.

Figure 5.5 shows two images from visual and NIR cameras, respectively. The visual images are saved in RGB format, and NIR images are in grayscale format. The light intensity in each pixel in a grayscale image is represented as a value ranging from 0 (black) to 255 (white). Each RGB image is composed of three independent channels of red, green and blue primary colors. The image in each color channel can be treated as a grayscale image with a single intensity value in each pixel.

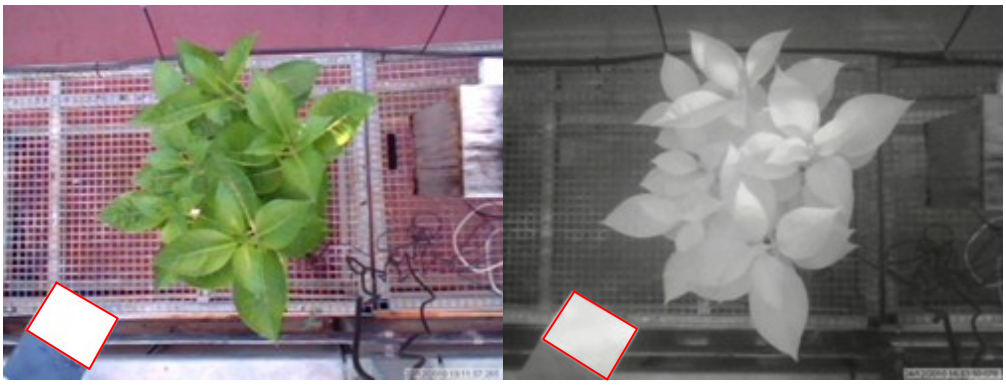

Figure 5.5: Visual and NIR images

Figure 5.6: Leaf images

The light reflectance is calculated as follows. First, a partial image that only contains the plant leaves is extracted from an original image shown in Figure 5.5. We use a set of standard functions provided by the MATLAB software for the leaf extraction. The basic principle is that a layer mask is first generated by detecting the outline of the leaves. Then, the leaf images can be extracted by overlapping both the layer mask and original image. Figure 5.6 presents three extracted leaf images in different formats, namely RGB, red color channel and grayscale. The RGB and grayscale images come from the visual and NIR cameras, while the image in the red color channel is extracted from the RGB image. In our experiment, we use the image in the red color channel and the grayscale image to calculate the light reflectance in the visible and NIR spectrum, respectively.

Second, the average light intensity (I_e) of the extracted image is calculated using the following equation:

$$I_e = \frac{1}{N}\sum_{k=1}^{N} I_e(k) \tag{5.2}$$

where $I_e(k)$ denotes the light intensity for pixel k, and N is the total number of the pixels in the image.

Third, the maximum light intensity (I_e^{max}) in the reference object region is used as the intensity of incoming light that is assumed to be totally reflected into the camera in this region.

Finally, the light reflectance (LR) of the observed plant can be calculated as follows:

$$LR = I_e / I_e^{max} \tag{5.3}$$

Using equation (5.1), the NDVI value can be calculated based on both visual and NIR images.

5.3.4 Results and Discussion

This section presents the measurements of NDVI and soil moisture by using the methodology described in Section 5.3.3. Based on the experimental results, the correlation between NDVI and soil moisture is analyzed. In the process of the experiment, the impact of the environmental variables (e.g., temperature and light) on the measurement results is minimized by changing the experimental environment and device configuration.

The first experiment is conducted in a glasshouse where the plant is subject to natural lighting conditions. During the experiment, it is observed that there is an unexpected variation in behavior of the NDVI measurements. Figure 5.7 presents such a case of the measurements of LR_{NIR}, LR_{VIS} and NDVI in one day (from 5am to 10pm).

In Figure 5.7, the NDVI varies between 0 and 0.4 over most of the period. This differs considerably from the usual range (between 0.8 and 0.9) of the green leaf plant's NDVI suggested in [12]. Moreover, it is notable that the NDVI values decrease below zero around mid-day (approx. 1pm – 2pm). This is caused by a significant increase in the measurements of LR_{VIS} that exceeds LR_{NIR} in this period.

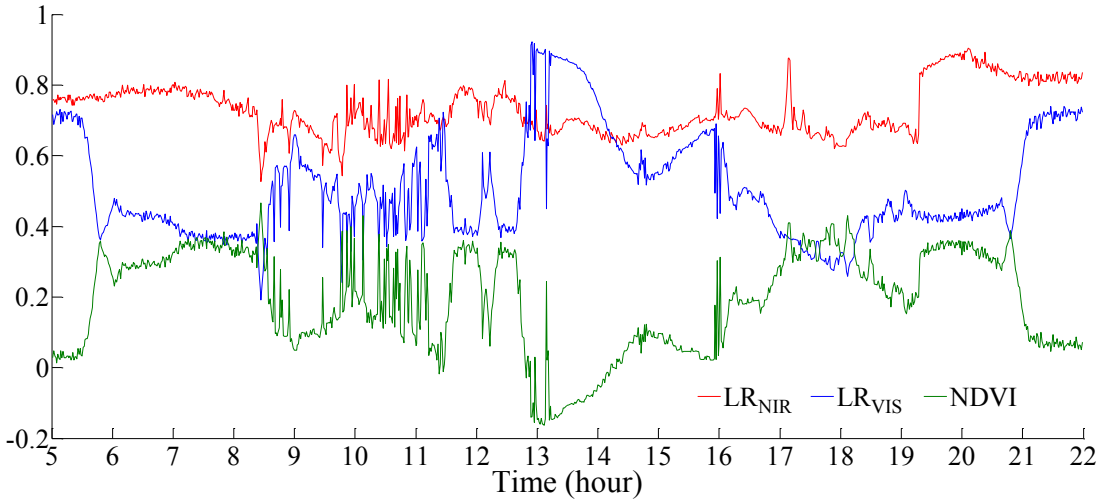

Figure 5.7: Measurements over one day of LR_{NIR}, LR_{VIS} and NDVI

Figure 5.8: Over-exposed image

As discussed in Section 5.2, the light reflectance of the green plant in the NIR spectral region is expected to be greater than that in the visible region.

By reviewing the images collected in the experiment, the reason for the unexpected variation of NDVI is image overexposure (see Figure 5.8) from the visual camera, especially in the case of strong solar irradiance. This is due to a limitation of the camera's automatic adjustment to the exposure when the solar irradiance varies over a large scale. To overcome this effect on the experimental results, the visual camera is configured with a set of fixed parameters (i.e., brightness and contrast). Figure 5.9 shows one of the daily measurements of LR_{NIR}, LR_{VIS} and NDVI from 5am to 10pm after reconfiguring the visual camera.

In contrast to the outcomes in Figure 5.7, Figure 5.9 indicates that there is a notable reduction of the light reflectance in the visible spectrum, especially around

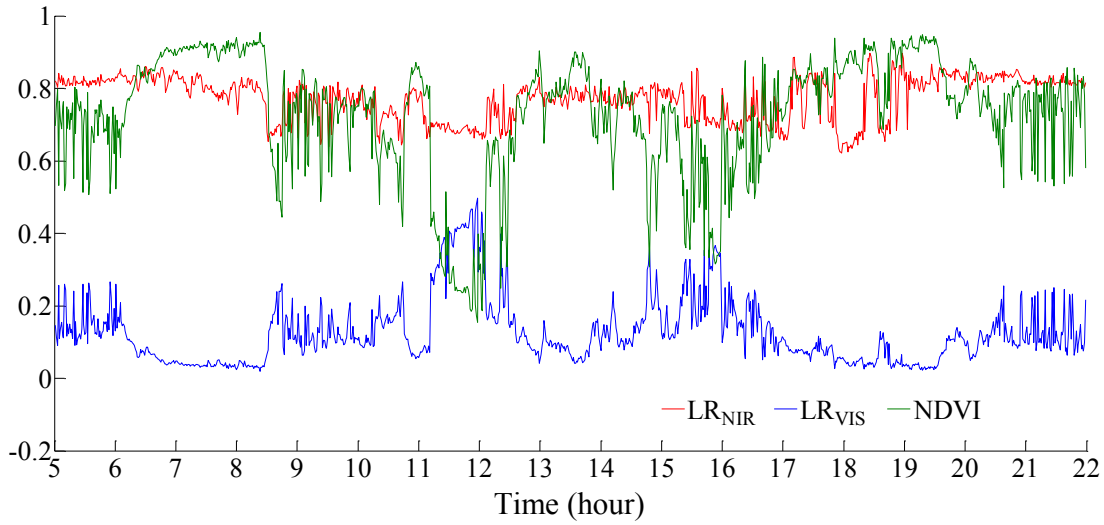

Figure 5.9: Measurements over one day of LR_{NIR}, LR_{VIS} and NDVI after camera reconfiguration

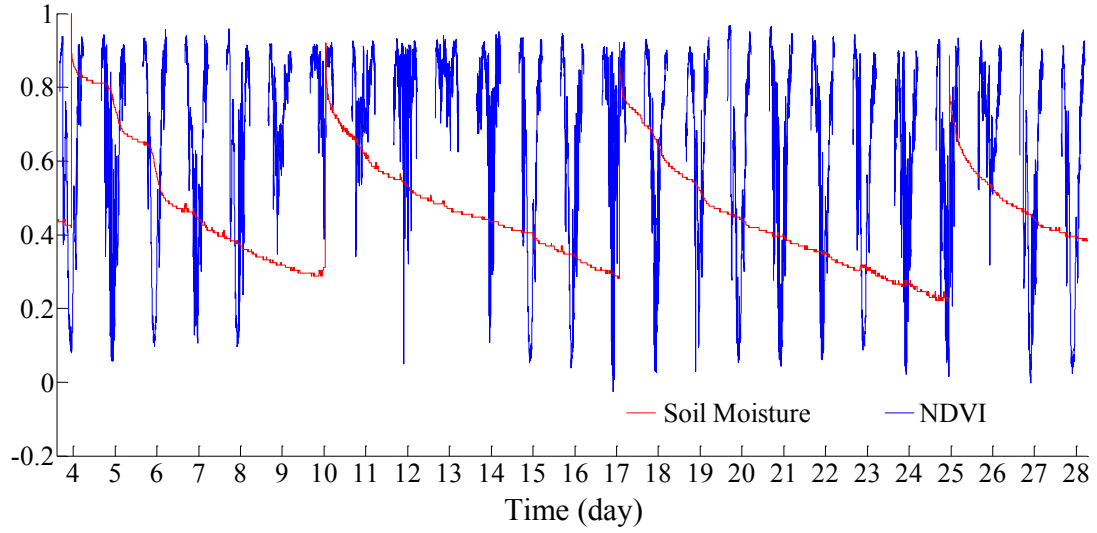

Figure 5.10: The measurements of normalized soil moisture and NDVI

mid-day. The measurements of LR_{NIR} and LR_{VIS} fluctuate at around 0.7 and 0.1, respectively, which gives an average NDVI of 0.75 by equation (5.1). Overall, most of the NDVI measurements in Figure 5.9 vary above an index of 0.5. This range is quite close to that expected of a green plant's NDVI as mentioned before. In the rest of the experiments, all the NDVI values are measured by applying the camera configuration with the fixed optical parameters.

Figure 5.10 shows the measurements of normalized soil moisture and NDVI over 24 days in summer. During the experiment, there are in total four irrigation events at

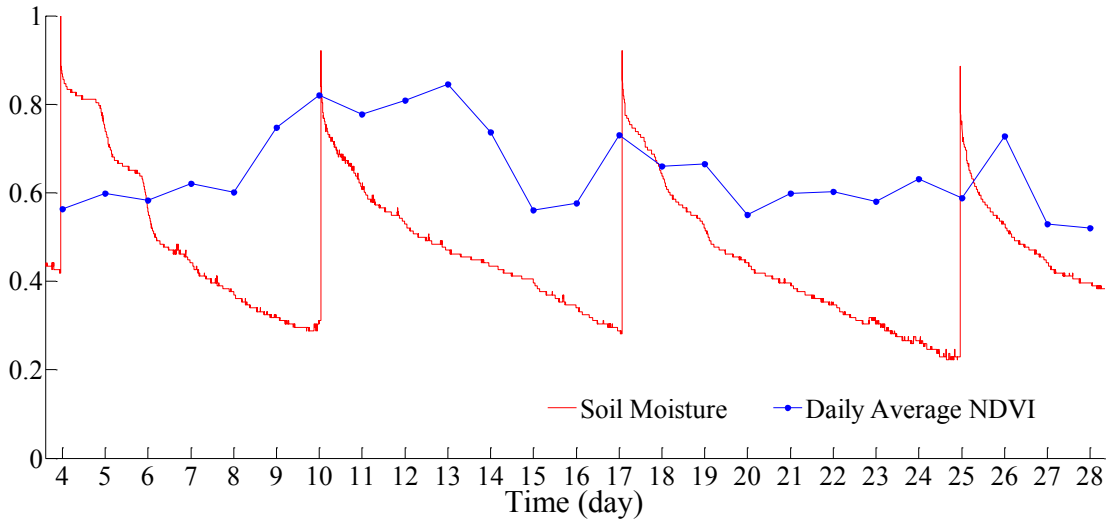

Figure 5.11: The measurements of normalized soil moisture and daily average NDVI

an interval of approximately one week. In this figure, the soil moisture exhibits a non-linear variation. Between two adjacent points of scheduled irrigation, there is a substantial reduction of the soil moisture around the first three days, and afterwards it tends to decrease linearly at a lower rate. NDVI is only measured in the daytime (from 6am to 9pm) every day, and it fluctuates between 0.1 and 0.9 in most of the days by following a pattern of its daily measurements varying from a low range (approx. 0.1-0.5) in the mid-day to a high range (approx. 0.5-0.9) in the rest of the time. In contrast, a smaller varying interval appears only in a few days (e.g., day 10 and day 13). Based on the measurements shown in Figure 5.10, it is not possible to come to a conclusion on a straightforward relationship between the soil moisture and NDVI.

Based on the NDVI measurements in Figure 5.10, the average NDVI for each day is calculated. Figure 5.11 shows the normalized soil moisture and daily average NDVI. Compared to the repeatedly varying curves of the soil moisture, the average NDVI maintains a value of approximately 0.6 and rises up to 0.8 around each irrigation point except for the first point (in day 4). Intuitively, the increase of the average NDVI in a short period may be related to the increase in soil moisture caused by the irrigation. However, they do not share the same cycle as expected. Moreover, the NDVI measurements may be affected by the projection of the canopy shadows on the experimental plant (see Figure 5.12) and the environmental variables, like temperature.

To eliminate the impact of the factors mentioned above, the second experiment is conducted in a constant environment room where an artificial constant light (from

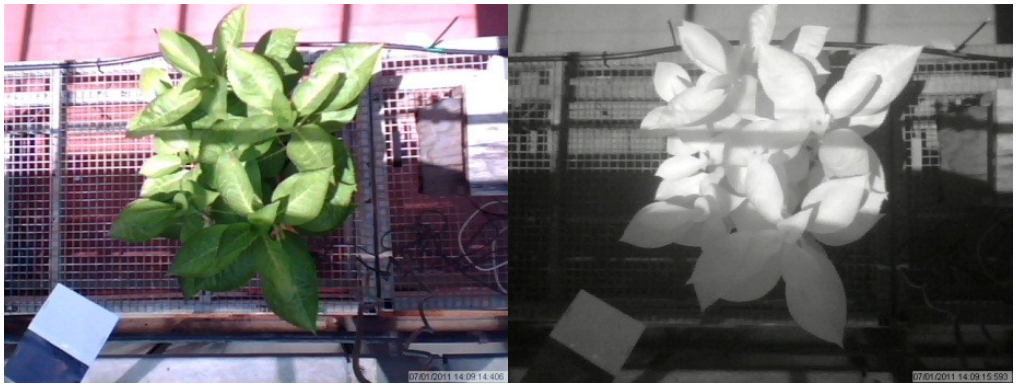

Figure 5.12: The shadow projection on the leaves

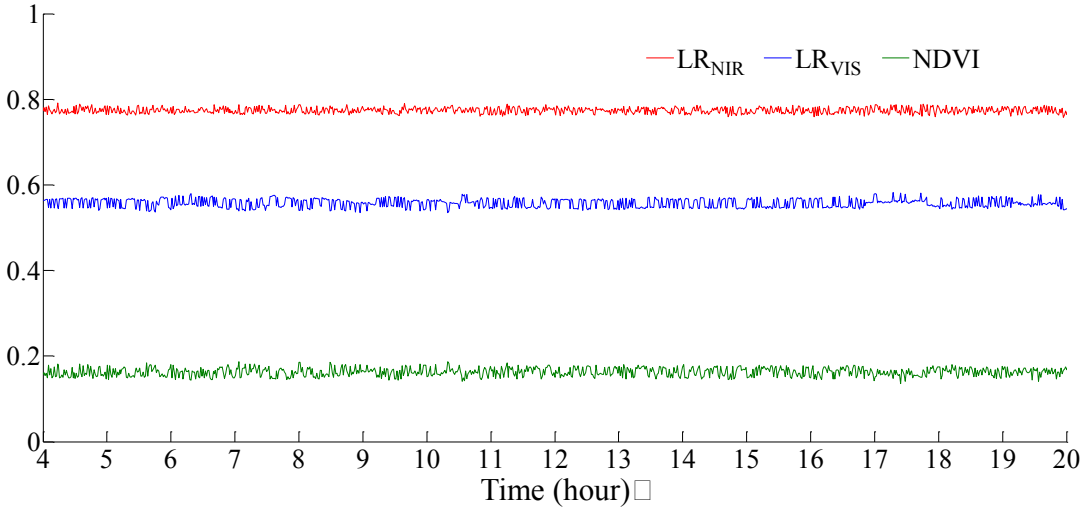

Figure 5.13: Measurements over one day of LR_{NIR}, LR_{VIS} and NDVI

4am to 8pm) is used for the plant photosynthesis and the temperature is controlled at a constant level.

In Figure 5.13, the results of LR_{NIR}, LR_{VIS} and NDVI measured in one day (4am-8pm) in the constant environment room are presented. Unlike the significant changes shown in Figure 5.10 in the glasshouse, the measurements of LR_{NIR}, LR_{VIS} and NDVI in this experiment maintain almost no changes with additive noise over a day, fluctuating around 0.78, 0.56 and 0.18, respectively. This illustrates that the light reflectance and NDVI measured in the first experiment are affected considerably by the varying solar irradiance in the daytime. Through the use of a constant light source for eliminating this impact, the NDVI is measured by applying the same approach as before.

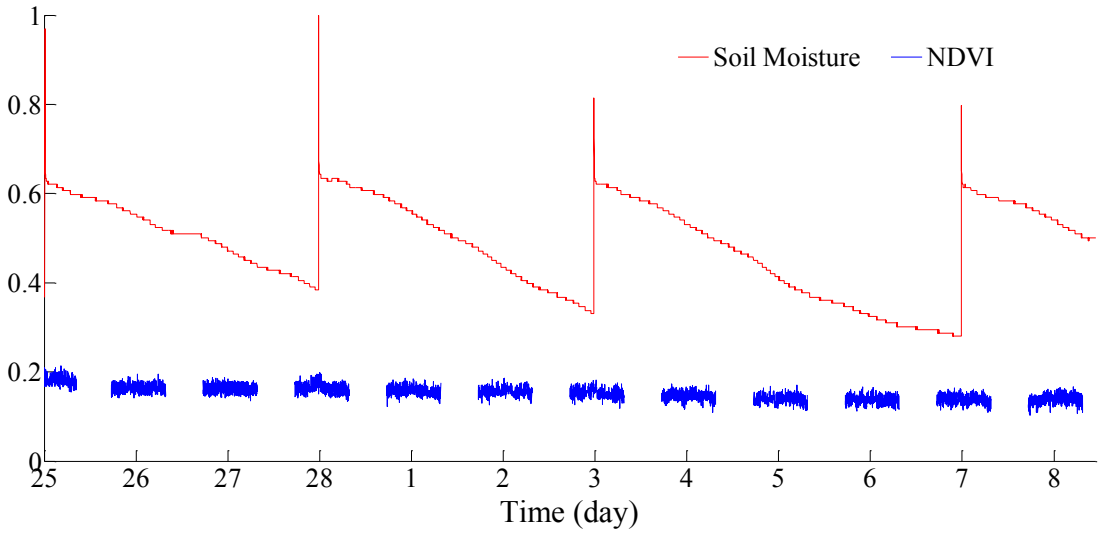

Figure 5.14: The measurements of normalized soil moisture and NDVI

Figure 5.14 presents the normalized soil moisture and NDVI measured over 11 days in the constant environment room. Since the environmental variables are much more stable than those in the first experiment, the soil moisture decreases at slightly varying rates. The NDVI, however, scarcely changes over the experimental period.

Based on the outcomes in this experiment, the observed plant has a nearly constant NDVI in the case of the various soil moisture values and constant environmental variables (light irradiance and temperature). However, referring to Section 5.2, it is more likely that there are distinct rates of the plant photosynthesis in different conditions of water supply, which would be expected to be reflected by the NDVI. This demonstrates that the low-cost cameras used in our experiments may not have enough sensitivity for the minor changes in the light reflected by the leaf surface in the photosynthesis process, or the wavelength filters inside the cameras may not be effective in preventing the light in the spectrum that is located outside the PAR and NIR regions, which interferes with the experimental results.

Another factor that could have affected the results is that it is possible that changes in NDVI may only be observed when the plant is more severely stressed than was the case in our experiments. This is a possible case to investigate in future research.

5.4 Summary

In this chapter, two experiments have been conducted in a glasshouse and constant

environment room. In both experiments, we measure the light reflectance on the surface of plant leaves in the visible and NIR spectrum in order to test whether NDVI can be measured using low-cost cameras to determine soil moisture levels. The low-cost visual and NIR cameras are used to collect the plant images, and the soil moisture is measured by using a low-cost sensor based on a WSN. According to our experimental results in both environments, it has not been concluded that the sensing technique outlined in this section can be used to sense the change of the soil moisture, since the dynamic variation of the plant photosynthesis is not reflected by our NDVI measurements. The limited sensitivity and capability of filtering the particular spectrum of our low-cost cameras may be the key reasons that affect the accuracy of the experimental results.

Chapter 6

Conclusions

There has been an increasing use of WSNs for a wide range of applications due to the ease of deploying large numbers of sensor nodes at low cost, while using regular batteries as a power supply for long-term operation without the need of frequent replacement. In addition, the use of sophisticated multi-layer protocols makes WSNs capable of operating in a self-organizing and cooperative way with high resilience to node failures. However, there are still several open issues related to the use of WSN technology. The power supply is one of the key concerns in the design of WSNs. In many applications, it is impractical to replace batteries to extend the lifetime of a sensor node, particularly in human inaccessible environments. A sensor node also has limited capabilities for on-board processing, storage and communication, which considerably increases the difficulty of designing network protocols. The research undertaken in this thesis is motivated by addressing such problems. Specifically, we focus on the design of an efficient network protocol for converge-cast communication in WSNs and the design of a power supply subsystem of a sensor node. Further, we investigate the feasibility of using low-cost image sensors for measuring soil moisture over large areas using WSNs. This chapter summarizes the conclusions of the thesis, and highlights our proposed solutions for the issues described above. At the end of this chapter, several possible directions for future research are outlined.

6.1 Summary of the Thesis

In Chapter 2, we specify the key high-level challenges and the related issues in the design of WSNs, and give a detailed survey on the representative techniques in the literature that are used to address such issues. In our survey, we first focus on high-

layer routing protocols, which are classified as data-centric, hierarchical and location-based approaches by considering the network architecture. The key routing techniques in each category are summarized individually, and a comparison is made based on several design metrics. Next, the key power management approaches for WSNs in the literature are summarized in terms of energy-aware and energy harvesting approaches on the basis of our proposed 2-level hierarchical classification method. Further, the sensor network applications for monitoring soil moisture are surveyed. We first outline the key shortcomings of traditional methodologies for this purpose, and then highlight the main practical designs and implementations using sensor network technology, which are able to overcome such problems. Finally, we give a case study of a wireless embedded device called NICTOR that is used as the WSN test bed in our thesis, and outline key functionalities and features.

Converge-cast communication is a key pattern for data collection from distributed sensors to a central station in WSNs. In Chapter 3, we focus on the study of converge-cast communication for tree-based WSNs. To overcome the issues of high complexity and latency associated with existing protocols that are hierarchical scheduling schemes, we propose an alternative converge-cast high-layer routing protocol for WSNs in a tree topology. Our protocol uses a new frame structure that is compliant with the IEEE 802.15.4 standard. The proposed beacon flooding technique in our frame structure gives an efficient solution for network synchronization within a short period. Moreover, the FIFO buffering scheme and CSMA/CA mechanism that are used in each node minimizes the packet loss during data transmission.

An experimental WSN test bed is used to evaluate the performance of our proposed converge-cast protocol based on three types of tree topologies. The results have shown that our protocol delivers comparable performance to a hierarchical scheduling protocol in terms of the successful delivery ratio and packet delay. Due to the use of a simple frame structure, our protocol has much lower complexity in its implementation and operation. Also, the proposed scheme is compliant with the IEEE 802.15.4 standard, which makes it readily applicable to standard sensor network platforms.

Extending the battery lifetime of a sensor node is another critical issue in the design of sensor networks. This is particularly challenging for unattended WSNs in outdoor applications. In Chapter 4, we address this issue by focusing on the design of the WSN power supply subsystem. In particular, we propose a systematic design

approach for low-cost solar power supplies as a reliable energy source for unattended WSN applications.

In our proposed design approach, a simple and robust battery recharge circuit is applied based on the concept of the Harvest-Store-Use system architecture [126], which significantly reduces the cost of the overall power supply subsystem. The main elements in our charge circuit include a solar panel, rechargeable batteries and the load. Our approach relies on a theoretical sunlight motion model, and specifies a 4-step design procedure for the calculation of the parameter constraints for the elements in the charge circuit. By selecting appropriate parameter values for the power supply subsystem, a node can operate in an indefinite lifetime. Most importantly, our design approach accounts for the variations of the load requirements and the sunlight conditions over time, and does not require adaptive schemes that change the duty cycle parameter during network operation, which greatly lowers the protocol complexity and improves the utilization of sensor nodes.

The performance of our proposed design approach is evaluated by using an experimental WSN test bed. Two experiments are conducted separately in autumn and summer. The first experiment presents a mismatch case between the load requirements and the power supply subsystem. During the experimental period, residual battery energy fluctuates at low levels, and it depletes after a few days. This is expected because this subsystem is not adequately dimensioned. The second experiment shows a case that a sensor node operates for an indefinite lifetime under varying sunlight conditions, when its power supply subsystem is dimensioned according to our design approach. From the experimental results, our design approach is able to reflect the effects of sunlight conditions and the load power requirements on the power supply subsystem. By following the proposed design procedure, the subsystem is capable of providing sufficient energy to the given load with an indefinite lifetime.

In Chapter 5, we focus on measuring soil moisture levels over large areas. The knowledge from field-scale moisture measurements can help to significantly reduce the amount of water that is used in agricultural irrigation. Traditional methodologies for the measurement of moisture levels use either a sensor probe in the ground or expensive imaging sensors with special filters. In contrast, we propose a scalable plant-based approach to estimate moisture levels over large areas by using image-based sensing. In particular, we utilize low-cost imaging devices to monitor the

changes of green plant photosynthesis by measuring its *Normalized Difference Vegetation Index (NDVI)* and investigate the feasibility of using such an index for estimating the moisture levels in a field. In our feasibility studies, we present an experimental methodology that can avoid the bias produced in many existing techniques using a single measurement point, and outline the experimental results under two practical deployments.

The first experiment is undertaken in an agricultural field. In this experiment, low-cost visual and near-infrared cameras are used to periodically measure the light reflectance on the surface of plant leaves in order to obtain values of NDVI, while a sensor probe is buried in the soil for the measurements of the moisture levels. Then, the relationship between the NDVI and true soil moisture measurements are investigated by using a simple correlation approach. Based on the measurements over 24 days, we analyze the variations of normalized soil moisture and NDVI based on a 1-minute and 1-day sampling interval, separately. However, a straightforward relationship between two variables cannot be concluded, since there are unexpected changes of the NDVI measurements. The reason for this may be the projection of the canopy shadows on the experimental plant and other environmental variables that impact on the results.

The second experiment is conducted in a constant environment room where air temperature and light is controlled at a constant level. The same experimental methodology and analysis approach are used as in the first experiment, but the effect of several environmental variables on the experimental results is eliminated. Based on the result in this experiment, the NDVI shows almost no change over the experimental period. This is an unexpected outcome under a variety of water supply conditions, which is most likely caused by the low-cost imaging sensors used in our experiments. Specifically, our imaging sensors may not have enough sensitivity for the minor changes of light reflectance on the leaf surface, or the spectral filters may not effectively filter the light from outside the spectrum of the *Photosynthesis Active Region* and near-infrared, thus affecting the experimental results.

6.2 Future Research

This section outlines several possible directions for future research.

The performance of many routing protocols in WSNs is currently evaluated based on analytical models or software simulations. The main drawback of using such approaches is that the evaluation result may have a bias from the real performance in practical deployments, since the environment in the real world is usually far more complicated than the available simulation models. Thus, it is important that the protocols that have been proposed in the literature are evaluated in a practical implementation. For the proposed converge-cast routing protocol for tree-based WSNs in Chapter 3, energy efficiency has not yet been addressed. For future work, a comparison in terms of energy efficiency with other protocols can be undertaken by using an experimental WSN test bed.

A solar energy harvesting approach to extending the battery lifetime of a sensor node has been presented in Chapter 4. An issue for future work is the use of a more sophisticated charge circuit. For example, a module that prevents overcharging the battery can be utilized to avoid any damage, and the solar panels can operate at their maximum power point by using a regulator chip. Another possible direction is how to adapt the choice of N in the calculation of Q_{ave} in Section 4.4.3 in order to accommodate changing solar conditions in autumn and spring, compared to the averaging periods needed for summer and winter.

In addition, an open issue is how to implement the emergency reactions that a WSN protocol performs when batteries are nearly depleted. The challenge is to finalize and transmit important data in a fast and reliable way with the extremely limited remaining energy. To facilitate this, technologies for battery capacity detection and highly efficient WSN protocols are needed.

In Chapter 5, the feasibility studies of using low-cost imaging sensors for the determination of soil moisture levels has not come to a positive conclusion. The limitations of our low-cost cameras in terms of their sensitivity and capability may be the key reasons for the inaccuracy of the NDVI estimation in our experimental results. This experiment may be replicated in the future by applying more sophisticated and professional imaging sensing devices with well-designed filters having wider range sensitivity. In addition, there is scope to improve our approach to calculating the light reflectance in our experiments, especially when calculating the incoming light intensity.

Bibliography

[1] A. Abu-Baker, H. Huang, E. Johnson, and S. Misra, "Green diffusion: data dissemination in sensor networks using solar power," in *Proceedings of the 8th IEEE Consumer Communications and Networking Conference on Wireless Consumer Communication and Networking,* 2011, pp. 803-807.

[2] K. Akkaya and M. Younis, “A survey on routing protocols for wireless sensor networks,” *Ad Hoc Networks*, vol. 3, no. 3, pp. 325-349, May. 2005.

[3] I. F. Akyildiz, W. Su, Y. Sankarasubramaniam, and E. Cayirci, "A survey on sensor networks," *IEEE Communications Magazine*, vol. 40, no. 8, pp. 102-114, Aug. 2002.

[4] I. F. Akyildiz, W. Su, Y. Sankarasubramaniam, and E. Cayirci, “Wireless sensor network: a survey,” *Computer Networks*, vol. 38, no. 4, pp. 393-422, Mar. 2002.

[5] I. F. Akyildiz, M. C. Vuran, and O. B. Akan, “A cross-layer protocol for wireless sensor networks,” in *Proceedings of the 40th Annual Conference on Information Sciences and Systems*, 2006, pp. 1102-1107.

[6] J. N. Al-Karaki and A. E. Kamal, "Routing techniques in wireless sensor networks: a survey," *IEEE Wireless Communications*, vol. 11, no. 6, pp. 6-28, Dec. 2004.

[7] C. Alippi and C. Galperti, "An adaptive system for optimal solar energy harvesting in wireless sensor network nodes," *IEEE Transactions on Circuits and Systems I: Regular Papers*, vol. 55, no. 6, pp. 1742-1750, Jul. 2008.

[8] H. Alwan and A. Agarwal, "A survey on fault tolerant routing techniques in wireless sensor networks," in *Proceedings of the 3rd International Conference on Sensor Technologies and Applications*, 2009, pp. 366-371.

[9] G. Anastasi, M. Conti, M. Di Francesco, and A. Passarella, "Energy conservation in wireless sensor networks: a survey," *Ad Hoc Networks*, vol. 7, no. 3, pp. 537-568, May. 2009.

[10] T. Arampatzis, J. Lygeros, and S. Manesis, "A survey of applications of wireless sensors and wireless sensor networks," in *Proceedings of the 13th Mediterrean Conference on Control and Automation*, 2005, pp. 719-724.

[11] Atmel, *8-bit Atmel Microcontroller with 128Kbytes In-System Programmable Flash - Atmega128/Atmega128L*. [Online]. Available: http://www.atmel.com/Images/doc2467.pdf

[12] T. E. Avery and G. L. Berlin, *Fundamentals of Remote Sensing and Airphoto Interpretation*, 5th ed., Macmillan: Prentice Hall, 1992.

[13] S. Bandyopadhyay and E. J. Coyle, “An energy efficient hierarchical clustering algorithm for wireless sensor networks”, in *Proceedings of the 22nd Annual Joint Conference on the IEEE Computer and Communications*, 2003, pp. 1713-1723.

[14] S. Basagni, I. Chlamtac, V. R. Syrotiuk, and B. A. Woodward, "A distance routing effect algorithm for mobility (DREAM)," in *Proceedings of the 4th ACM/IEEE International Conference on Mobile Computing and Networking*, 1998, pp. 76-84.

[15] A. C. M. Beljaars, P. Viterbo, M. J. Miller, and A. K. Betts, "The anomalous rainfall over the United States during July 1993: sensitivity to land surface parameterization and soil moisture anomalies," *Monthly Weather Review*, vol. 124, pp. 362-383, Mar. 1996.

[16] H. R. Bogena, J. A. Huisman, C. Oberdörster, and H. Vereecken, "Evaluation of a low-cost soil water content sensor for wireless network applications," *Journal of Hydrology*, vol. 344, no. 1-2, pp. 32-42, Sep. 2007.

[17] O. Boric-Lubeke and V. M. Lubecke, "Wireless house calls: using communications technology for health care and monitoring," *IEEE Microwave Magazine*, vol. 3, no. 3, pp. 43-48, Sep. 2002.

[18] R. P. Brent, *Algorithms for Minimization without Derivatives*, Englewood Cliffs, NJ: Prentice-Hall, 1973.

[19] M. Buettner, G. V. Yee, E. Anderson, and R. Han, "X-MAC: a short preamble MAC protocol for duty-cycled wireless sensor networks," in *Proceedings of the 4th International Conference on Embedded Networked Sensor Systems*, 2006, pp. 307-320.

[20] C. Buratti, "Performance analysis of IEEE 802.15.4 beacon-enabled mode," *IEEE Transactions on Vehicular Technology*, vol. 59, no. 4, pp. 2031-2045, May. 2010.

[21] E. H. Callaway, "Wireless sensor networks: architectures and protocols," in *Internet and Communications*, vol. 3, CRC press, 2004.

[22] E. Callaway, P. Gorday, L. Hester, J. A. Gutierrez, M. Naeve, B. Heile, and V. Bahl, "Home networking with IEEE 802.15.4: a developing standard for low-rate wireless personal area networks," *IEEE Communications Magazine*, vol. 40, no. 4, pp. 70-77, Aug. 2002.

[23] A. Cano, E. López-Baeza, J. L. Añón, C. Reig, and C. Millán-Scheiding, "Wireless sensor network for soil moisture applications," in *Proceedings of the International Conference on Sensor Technologies and Applications*, 2007, pp. 508-513.

[24] R. Cardell-Oliver, M. Kranz, K. Smettem, and K. Mayer, "A reactive soil moisture sensor network: design and field evaluation," *International Journal of Distributed Sensor Networks*, vol. 1, no. 2, pp. 149-162, 2005.

[25] A. Cerpa, J. Elson, D. Estrin, L. Girod, M. Hamilton, and J. Zhao, "Habitat monitoring: application driver for wireless communications technology," *ACM SIGCOMM Computer Communication Review*, vol. 31, no. 2, pp. 20-41, Apr. 2001.

[26] G. Chalhoub and M. Mission, “Cluster-tree based energy efficient protocol for wireless sensor networks,” in *Proceedings of the International Conference on Networking, Sensing and Control*, 2010, pp. 664-669.

[27] J. Cho and S. An, “Optimal beacon scheduling scheme for cluster-tree WPANs,” in *Proceedings of the 2nd International Conference on Sensor Technologies and Applications*, 2008, pp. 160-165.

[28] J. E. Colwell, "Bidirectional spectral reflectance of grass canopies for determination of above ground standing biomass," Ph.D. thesis, University of Michigan, USA, 1973.

[29] P. Corke, P. Valencia, P. Sikka, T. Wark, and L. Overs, “Long-duration solar-powered wireless sensor networks,” in *Proceedings of the 4th Workshop on Embedded Networked Sensors*, 2007, pp. 33-37.

[30] K. Crowley, J. Frisby, S. Murphy, M. Roantree, and D. Diamond, “Web-based real-time temperature monitoring of shellfish catches using a wireless sensor network,” *Sensors and Actuators A: Physical*, vol. 122, no.2, pp. 222-230, Aug. 2005.

[31] T. V. Dam and K. Langendoen, "An adaptive energy-efficient MAC protocol for wireless sensor networks," in *Proceedings of the 1st International Conference on Embedded Networked Sensor Systems*, 2003, pp. 171-180.

[32] M. Damas, A. M. Prados, F. Gómez, and G. Olivares, "HidroBus system: fieldbus for integrated management of extensive areas of irrigated land," *Microprocessors and Microsystems*, vol. 25, pp. 177-184, Feb. 2001.

[33] K. Dantu, M. Rahimi, H. Shah, S. Babel, A. Dhariwal, and G. S. Sukhatm, “Robomote: enabling mobility in sensor networks”, In *Proceedings of the 4th International Symposium on Information Processing in Sensor Networks*, 2005.

[34] Decagon Devices, *ECH$_2$O Soil Moisture Sensor - Operator’s Manual for Models EC-20, EC-10, and EC-5 (Version 10)*. [Online]. Available: http://www.decagon.com/education/ech2o-10-ech2o-20-manual/

[35] G. M. Dunn, K. J. Langford, and E. W. R. Barlow, "Regional and economic benefits through smarter irrigation," in *Proceedings of the Australian National Committee on Irrigation and Drainage*, 2006.

[36] D. Estrin, R. Govindan, J. Heidemann, and S. Kumar, "Next century challenges: scalable coordination in sensor networks," in *Proceedings of the 5th ACM/IEEE International Conference on Mobile Computing and Networking*, 1999, pp. 263-270.

[37] T. J. Farrar, S. E. Nicholson, and A. R. Lare, "The influence of soil type on the relationships between NDVI, rainfall, and soil moisture in semiarid Botswana. II. NDVI response to soil moisture," *Remote Sensing of Environment*, vol. 50, no.2, pp. 121-133, Nov. 1994.

[38] J. Gakkestad and L. Hanssen, "Powering wireless sensor networks nodes in Northern Europe using solar cell panel for energy harvesting," in *Proceedings of the 4th IFIP International Conference on New Technologies, Mobility and Security (NTMS)*, 2011, pp. 1-5.

[39] J. A. Gamon, C. B. Field, M. L. Goulden, K. L. Griffin, A. E. Hartley, G. Joel, J. Peñuelas, and R. Valentini, "Relationships between NDVI, canopy structure, and photosynthesis in three Californian vegetation types," *Ecological Applications*, vol. 5, no. 1, pp. 28-41, Feb. 1995.

[40] D. M. Gates, *Biophysical Ecology*, New York: Springer-Verlag, 1980.

[41] Geoscience Australia, *Astronomical Information*. [Online]. Available: http:// www.ga.gov.au/geodesy/astro/

[42] R. R. Gillies, W. P. Kustas, and K. S. Humes, "A verification of the 'triangle' method for obtaining surface soil water content and energy fluxes from remote measurements of the Normalized Difference Vegetation Index (NDVI) and surface," *International Journal of Remote Sensing*, vol. 18, no. 15, pp. 3145-3166, 1997.

[43] M. A. Green, K. Emery, Y. Hishikawa, and W. Warta, “Solar cell efficiency tables (version 36),” *Progress in Photovoltaics: Research and Applications*, vol. 18, no. 5, pp. 346-352, Aug. 2010.

[44] F. Gustafsson, F. Gunnarsson, N. Bergman, U. Forssell, J. Jansson, R. Karlsson, and P.-J. Nordlund, “Particle filters for positioning, navigation, and tracking”, *IEEE Transactions on Signal Processing*, vol. 50, no. 2, pp. 425-437, Feb. 2002.

[45] Z. J. Haas and B. Liang, “Ad hoc mobility management with uniform quorum systems,” *IEEE/ACM Transaction on Networking*, vol. 7, no. 2, pp. 228-240, Apr. 1999.

[46] D. O. Hall and K. K. Rao, *Photosynthesis*, 6th ed., Cambridge, UK: Cambridge Univerisity Press, 1999.

[47] S. M. Hedetniemi, S. T. Hedetniemi, and A. L. Liestman, “A survey of gossiping and broadcasting in communication networks”, *Networks*, vol. 18, no. 4, pp. 319-349, 1988.

[48] J. Heidemann, N. Bulusu, J. Elson, C. Intanagonwiwat, K. Lan, Y. Xu, W. Ye, D. Estrin, and R. Govindan, "Effects of detail in wireless network simulation," in *Proceedings of the SCS Multiconference on Distributed Simulation*, 2001, pp. 3-11.

[49] J. Heidemann, B. Silva, C. Intanagonwiwat, R. Govindan, D. Estrin, and D. Ganesan, “Building efficient wireless sensor networks with low-level naming,” in *Proceedings of the 18th ACM Symposium on Operating Systems Principles*, 2001, pp. 146-159.

[50] W. B. Heinzelman, *Application-Specific Protocol Architectures for Wireless Networks*, Ph.D. thesis, Massachusetts Institute of Technology, 2000.

[51] W. R. Heinzelman, A. Chandrakasan, and H. Balakrishnan, "Energy-efficient communication protocol for wireless microsensor networks," in *Proceedings of the 33rd Annual Hawaii International Conference on System Sciences*, 2000, pp. 1-10.

[52] W. Heinzelman, J. Kulik, and H. Balakrishnan, "Adaptive protocols for information dissemination in wireless sensor networks," in *Proceedings of the ACM Annual International Conference on Mobile Computing and Networking*, 1999, pp. 174-185.

[53] A. Henderson-Sellers, "Soil moisture: a critical focus for global change studies," *Global and Planetary Change*, vol. 13, no. 1-4, pp. 3-9, Jun. 1996.

[54] J. L. Hill and D. E. Culler, "Mica: a wireless platform for deeply embedded networks," *IEEE Micro*, vol. 22, no. 6, pp. 12-24, Nov/Dec. 2002.

[55] N. M. Hoang and V. N. Son, “Disjoint and braided multipath routing for wireless sensor networks”, in *Proceedings of the International Symposium on Electrical and Electronics Engineering*, 2005, pp. 1-7.

[56] T.-C. Hou and V. Li, "Transmission range control in multihop packet radio networks," *IEEE Transactions on Communications*, vol. 34, no. 1, pp. 38-44, Jan. 1986.

[57] T. A. Howell, "Irrigation scheduling research and its impact on water use," in *Proceedings of the International Conference on Evapotranspiration and Irrigation Scheduling*, 1996, pp. 21-33.

[58] J. Hsu, S. Zahedi, A. Kansal, M. Srivastava, and V. Raghunathan, "Adaptive duty cycling for energy harvesting systems," in *Proceedings of the 2006 International Symposium on Low Power Electronics and Design*, 2006, pp. 180-185.

[59] *Information Technology – Telecommunications and Information Exchange between Systems – Local and Metropolitan Area Networks – Specific Requirements – Part 11: Wireless LAN Medium Access Control (MAC) and Physical Layer (PHY) Specifications*, IEEE Standard 802.11 – 1999.

[60] *Information Technology – Telecommunications and Information Exchange between Systems – Local and Metropolitan Area Networks – Specific Requirements – Part 15.1: Wireless Medium Access Control (MAC) and*

Physical Layer (PHY) Specifications for Wireless Personal Area Networks (WPANs), IEEE Standard 802.15.1 – 2005.

[61] *Information Technology – Telecommunications and Information Exchange between Systems – Local and Metropolitan Area Networks – Specific Requirements – Part 15.4: Wireless Medium Access Control (MAC) and Physical Layer (PHY) Specifications for Low-Rate Wireless Personal Area Networks (LR-WPANs)*, IEEE Standard 802.15.4 – 2006.

[62] C. Intanagonwiwat, R. Govindan, and D. Estrin, "Directed diffusion: a scalable and robust communication paradigm for sensor networks", in *Proceedings of the ACM Annual International Conference on Mobile Computing and Networking*, 2000, pp. 56-67.

[63] X. Jiang, J. Polastre, and D. Culler, "Perpetual environmentally powered sensor networks," in *Proceedings of the 4th International Symposium on Information Processing in Sensor Networks*, 2005, pp. 463-468.

[64] C. F. Jordan, "Derivation of leaf-area index from quality of light on the forest floor," *Ecology*, vol. 50, no. 4, pp. 663-666, Jul. 1969.

[65] R. Jurdak, P. Baldi, and C. V. Lopes, "Adaptive low power listening for wireless sensor networks," *IEEE Transactions on Mobile Computing*, vol. 6, no. 8, pp. 988-1004, Aug. 2007.

[66] P. Kadiyala, *Non-uniform Grid-based Coordinated Routing in Wireless Sensor Networks*, ProQuest, 2008.

[67] A. Kansal, J. Hsu, S. Zahedi, and M. B. Srivastava, "Power management in energy harvesting sensor networks," *ACM Transactions on Embedded Computing Systems*, vol. 6, no. 4, Sep. 2007.

[68] A. Kansal, D. Potter, and M. B. Srivastava, "Performance aware tasking for environmentally powered sensor networks," in *ACM SIGMETRICS Performance Evaluation Review*, vol. 32, no. 1, pp. 223-234, Jun. 2004.

[69] A. Kansal and M. B. Srivastava, "An environmental energy harvesting framework for sensor networks," in *Proceedings of the 2003 International Symposium on Low Power Electronics and Design*, 2003, pp. 481-486.

[70] B. Karp and H. T. Kung, "GPSR: greedy perimeter stateless routing for wireless networks," in *Proceedings of the 6th International Conference on Mobile Computing and Networking*, 2000, pp. 243-254.

[71] Y. H. Kerr, P. Waldteufel, J.-P. Wigneron, J.-M. Martinuzzi, J. Font, and M. Berger, "Soil moisture retrieval from space: the Soil Moisture and Ocean Salinity (SMOS) mission," *IEEE Transactions on Geoscience and Remote Sensing*, vol. 39, no. 8, pp. 1729-1735, Aug. 2001.

[72] V. Khavrus and I. Shelevytsky, “Introduction to solar motion geometry on the basis of a simple model,” *Physics Education*, vol. 45, no. 6, pp. 641-653, Nov. 2010.

[73] L. Kilhung, “A time tree for scheduling and topology control in wireless sensor networks,” in *Proceedings of the 4th International Conference on Embedded and Multimedia Computing*, 2009, pp. 1-6.

[74] Y. Kim, R. G. Evans, and W. M. Iversen, "Remote sensing and control of an irrigation system using a distributed wireless sensor network," *IEEE Transactions on Instrumentation and Measurement*, vol. 57, no. 7, pp. 1379-1387, Jul. 2008.

[75] S. Kim, R. Fonseca, and D. Culler, “Reliable transfer on wireless sensor networks”, in *Proceedings of the 1st IEEE Communication Society Conference on Sensor and Ad-hoc Communications and Networks*, 2004, pp. 449-459.

[76] A. Koubaa, M. Alves, and E. Tovar, “A comprehensive simulation study of slotted CSMA/CA for IEEE 802.15.4 wireless sensor networks,” in *Proceedings of the IEEE International Workshop on Factory Communication Systems*, 2006, pp. 183-192.

[77] A. Koubaa, A. Cunha, and M. Alves, “A time division beacon scheduling meachnism for IEEE 802.15.4/ZigBee cluster-tree wireless sensor networks,”

in *Proceedings of the 19th Euromicro Conference on Real-Time Systems*, 2007, pp. 125-135.

[78] E. Kranakis, H. Singh, and J. Urrutia, "Compass routing on geometric networks," in *Proceedings of the 11th Canadian Conference on Computational Geometry*, 1999, pp. 51-54.

[79] B. Krishnamachari, D. Estrin, and S. Wicker, "Modelling data-centric routing in wireless sensor networks", in *Proceedings of the Annual IEEE International Conference on Computer Communications*, 2002, pp. 1-11.

[80] D. Krüger, C. Buschmann, and S. Fischer, "Solar powered sensor network design and experimentation," in *Proceedings of the 6th International Symposium on Wireless Communication Systems*, 2009, pp. 11-15.

[81] H. Kwon, D. Noh, J. Kim, J. Lee, D. Lee, and H. Shin, "Low-latency routing for energy-harvesting sensor networks," *Ubiquitous Intelligence and Computing*, vol. 4611/2007, pp. 422-433, 2007.

[82] T. P. Lambrou and C. G. Panayiotou, "A survey on routing techniques supporting mobility in sensor networks", in *Proceedings of the 5th International Conference on Mobile Ad-hoc and Sensor Networks*, 2009, pp. 78-85.

[83] P. Lee, M. Han, H.-P. Tan, and A. Valera, "An empirical study of harvesting-aware duty cycling in environmentally-powered wireless sensor networks," in *Proceedings of the 2010 IEEE International Conference on Communication Systems*, 2010, pp. 306-310.

[84] J. Li, J. Jannotti, D. S. J. De Couto, D. R. Karger, and R. Morris, "A scalable location service for geographic ad hoc routing," in *Proceedings of the 6th International Conference on Mobile Computing and Networking*, 2000, pp. 120-130.

[85] X. Liu, C. Leckie, and S. K. Saleem, "Performance evaluation of a converge-cast protocol for IEEE 802.15.4 tree-based networks," in *Processing of the 6th*

International Conference Intelligent Sensors, Sensor Networks and Information, 2010, pp. 73-78.

[86] Logitech, *Webcam C120*. [Online]. Available: http://www.logitech.com/en-au/support-downloads/downloads/webcams/devices/6065/

[87] G. Lu, B. Krishnamachari, and C. S. Raghavendra, "An adaptive energy-efficient and low-latency MAC for data gathering in wireless sensor networks," in *Proceedings of the 18th International Parallel and Distributed Processing Symposium*, 2004, p.224.

[88] A. Mainwaring, J. Polastre, R. Szewczyk, D. Culler, and J. Anderson, "Wireless sensor networks for habitat monitoring," in *Proceedings of the 1st ACM International Workshop on Wireless Sensor Networks & Application*, 2002, pp. 88-97.

[89] A. Manjeshwar and D. P. Agrawal, "TEEN: a routing protocol for enhanced efficiency in wireless sensor networks," in *Proceedings of the 15th International Parallel and Distributed Processing Symposium*, 2001, pp. 2009-2015.

[90] M. Maróti, B. Kusy, G. Simon, and Á. Lédeczi, "The flooding time synchronization protocol", in *Proceedings of the 2nd International Conference on Embedded Networked Sensor Systems*, 2004, pp. 39-49.

[91] C. Ó. Mathúna, T. O'Donnell, R. V. Martinez-Catala, J. Rohan, and B. O'Flynn, "Energy scavenging for long-term deployable wireless sensor networks," *Talanta*, vol. 75, no. 3, pp. 613-623, May. 2008.

[92] M. Mauve, J. Widmer, and H. Hartenstein, "A survey on position-based routing in mobile ad hoc networks", *IEEE Network*, vol. 15, no. 6, pp. 30-39, Nov/Dec. 2001.

[93] Maxon Australia, *Intermax*. [Online]. Available: http://www.maxon.com.au/products_intermax_overview.php

[94] J. A. Mazer, *Solar Cell: An Introduction to Crystalline Photovoltaic Technology*, Boston, U.S.: Kluwer Academic Publishers, 1997.

[95] M. S. McCready, M. D. Dukes, and G. L. Miller, "Water conservation potential of smart irrigation controllers on St. Augustinegrass," *Agricultural Water Management*, vol. 96, no. 11, pp. 1623-1632, Nov. 2009.

[96] T. H. Meng and V. Rodoplu, "Distributed network protocols for wireless communication," in *Proceedings of the IEEE International Symposium on Circuits and Systems*, 1998, pp. 600-603.

[97] M. Minami, T. Morito, H. Morikawa, and T. Aoyama, "Solar Biscuit: a battery-less wireless sensor network system for environmental monitoring applications," in *Proceedings of the 2nd International Workshop on Networked Sensing Systems*, 2005.

[98] R. Morris, J. Jannotti, F. Kaashoek, J. Li, and D. Decouto, "CarNet: a scalable ad hoc wireless network system," in *Proceedings of the 9th Workshop on ACM SIGOPS European workshop: Beyond the PC: New Challenges for the Operating System*, 2000, pp. 61-65.

[99] D. Noh, I. Yoon, and H. Shin, "Low-latency geographic routing for asynchronous energy-harvesting WSNs," *Journal of Networks*, vol. 3, no. 1, pp. 78-85, Jan. 2008.

[100] S. PalChaudhuri, A. K. Saha, and D. B. Johnson, "Adaptive clock synchronization in sensor networks," in *Proceedings of the International Symposium on Information Processing in Sensor Networks*, 2004, pp. 340-348.

[101] Panasonic, *Charge Methods for Nickel Metal Hydride Batteries*. [Online]. Available: http://www.industrial.panasonic.com/www-data/pdf/ACG4000/ACG4000PE2.pdf

[102] J. A. Paradiso and T. Starner, "Energy scavenging for mobile and wireless electronics," *IEEE Pervasive Computing*, vol. 4, no. 1, pp. 18-27, Jan.-Mar. 2005.

[103] C. Park and P. H. Chou, "AmbiMax: autonomous energy harvesting platform for multi-supply wireless sensor nodes," in *Proceedings of the 3rd IEEE Communications Society on Sensor and Ad Hoc Communications and Networks*, 2006, pp. 168-177.

[104] J. Parkka, M. Van Gils, T. Tuomisto, R. Lappalainen, and I. Korhonen, "A wireless wellness monitor for personal weight management," in *Proceedings of IEEE EMBS International Conference on Information Technology Applications in Biomedicine*, 2000, pp. 83-88.

[105] R. L. Pearson and L. D. Miller, "Remote mapping of standing crop biomass for estimation of the productivity of the shortgrass prairie," in *Proceedings of the 8th International Symposium on Remote Sensing of Environment*, 1972, pp. 1357-1381.

[106] R. Pearson, L. Miller, and C. J. Tucker, "Hand-held spectral radiometer to estimate gramineous biomass," *Applied Optics*, vol. 15, no. 2, pp. 416-418, Feb. 1976.

[107] F. J. Pierce and T. V. Elliott, "Regional and on-farm wireless sensor networks for agricultural systems in Eastern Washington," *Computers and Electronics in Agriculture,* vol. 61, no. 1, pp. 32-43, Apr. 2008.

[108] J. Polastre, J. Hill, and D. Culler, "Versatile low power media access for wireless sensor networks," in *Proceedings of the 2nd International Conference on Embedded Networked Sensor Systems*, 2004, pp. 95-107.

[109] J. Polastre, R. Szewczyk, and D. Culler, "Telos: enabling ultra-low power wireless research," in *Proceedings of the 4th International Symposium on Information Processing in Sensor Networks*, 2005, pp. 364-369.

[110] V. Raghunathan, A. Kansal, J. Hsu, J. Friedman, and M. Srivastava, "Design considerations for solar energy harvesting wireless embedded systems," in *Proceedings of the 4th International Symposium on Information Processing in Sensor Networks*, 2005, pp. 457- 462.

[111] I. Ramachandran, A. K. Das, and S. Roy, “Analysis of the contention access period of IEEE 802.15.4 MAC,” Department of Electrical Engineering University of Washington, Seattle, WA, Technical Report, UWEETR-2006-0003, Feb. 2006.

[112] K. Romer and F. Mattern, "The design space of wireless sensor networks," *IEEE Wireless Communications*, vol. 11, no. 6, pp. 54-61, Dec. 2004.

[113] P. Rong and M. Pedram, "Extending the lifetime of a network of battery-powered mobile devices by remote processing: a Markovian decision-based approach," in *Proceedings of the 40th Design Automation Conference*, 2003, pp. 906-911.

[114] S. Roundy, D. Steingart, L. Frechette, P. Wright, and J. Rabaey, “Power sources for wireless sensor networks,” *Wireless Sensor Networks, Lecture Notes in Computer Science*, vol. 2920/2004, pp. 1-17, 2004.

[115] T. Schmugge, "Applications of passive microwave observations of surface soil moisture," *Journal of Hydrology,* vol. 212-213, pp. 188-197, Dec. 1998.

[116] T. J. Schmugge, T. J. Jackson, and H. L. McKim, "Survey of methods for soil moisture determination," *Water Resource Research*, vol. 16, no. 6, pp. 961-979, Apr. 1980.

[117] E. Shih, S.-H. Cho, N. Ickes, R. Min, A. Sinha, A. Wang, and A. Chandrakasan, “Physical layer driven protocol and algorithm design for energy-efficient wireless sensor networks”, in *Proceedings of the 7th International Conference on Mobile Computing and Networking*, 2001, pp. 272-287.

[118] P. Sikka, P. Corke, and L. Overs, “Wireless sensor devices for animal tracking and control,” in *Proceedings of the 29th Annual IEEE International Conference on Local Computer Networks*, 2004, pp. 446-454.

[119] F. Simjee and P. H. Chou, "Everlast: long-life, supercapacitor-operated wireless sensor node," in *Proceedings of the 2006 International Symposium on Low Power Electronics and Design*, 2006, pp. 197-202.

[120] S. Singh, M. Woo, and C. S. Raghavendra, "Power-aware routing in mobile ad hoc networks," in *Proceedings of the 4th ACM/IEEE International Conference on Mobile Computing and Networking*, 1998, pp. 181-190.

[121] R. J. Smith, J. N. Baillie, A. C. McCarthy, S. R. Raine, and C. P. Baillie, “Review of precision irrigation technologies and their application,” National Centre for Engineering in Agriculture, University of Southern Queensland, Toowoomba, Technical Report, NCEA Publication 1003017/1, Nov. 2010.

[122] K. Sohrabi, J. Gao, V. Ailawadhi, and G. J. Pottie, "Protocols for self-organization of a wireless sensor network," *IEEE Personal Communications,* vol. 7, no. 5, pp. 16-27, Oct. 2000.

[123] P. Stanley-Marbell and D. Marculescu, "An 0.9 x 1.2", low power, energy-harvesting system with custom multi-channel communication interface," in *Proceedings of the Design, Automation & Test in Europe Conference & Exhibition*, 2007, pp. 1-6.

[124] I. Stojmenovic and X. Lin, "Loop-free hybrid single-path/flooding routing algorithms with guaranteed delivery for wireless networks," *IEEE Transactions on Parallel and Distributed Systems,* vol. 12, no. 10, pp. 1023-1032, Oct. 2001.

[125] I. Stojmenovic and B. Vukojevic, “A routing strategy and quorum based location update scheme for ad hoc wireless networks,” Computer Science, SITE, University of Ottawa, Technical Report, TR-99-09, 1999.

[126] S. Sudevalayam and P. Kulkarni, "Energy harvesting sensor nodes: survey and implications," *IEEE Communications Surveys & Tutorials*, vol. 13, no. 3, pp. 443-461, 2011.

[127] M. Takaffoli, E. Elmallah, and W. Moussa, “Scheduled access using the IEEE 802.15.4 guaranteed time slots,” in *Proceedings of the IEEE International Conference on Communications*, 2010, pp. 1-5.

[128] H. Takagi and L. Kleinrock, "Optimal transmission ranges for randomly distributed packet radio terminals," *IEEE Transactions on Communications*, vol. 32, no. 3, pp. 246-257, Mar. 1984.

[129] J. Taneja, J. Jeong, and D. Culler, "Design, modeling, and capacity planning for micro-solar power sensor networks," in *Proceedings of the 7th International Conference on Information Processing in Sensor Networks*, 2008, pp. 407-418.

[130] Technical Marketing Staff of Gates Energy Products Inc., *Rechargeable Batteries Applications Handbook*, Newton, U.S.: Butterworth-Heinemann, 1998.

[131] Texas Instruments, *CC2420: 2.4 GHz IEEE 802.15.4 / ZigBee-ready RF Transceiver*. [Online]. Available: http://www.ti.com/lit/ds/symlink/cc2420.pdf

[132] The Bureau of Meteorology Australia, *Solar Exposure for Australia*. [Online]. Available: http://www.bom.gov.au/jsp/awap/solar/index.jsp

[133] S. Tilak, N. B. Abu-Ghazaleh, and W. Heinzelman, "A taxonomy of wireless micro-sensor network models," *ACM SIGMOBILE Mobile Computing and Communications Review*, vol. 6, no. 2, pp. 28-36, Apr. 2002.

[134] M. Tubaishat and S. Madria, "Sensor networks: an overview," *IEEE Potentials*, vol. 22, no. 2, pp. 20-23, Apr.-May 2003.

[135] C. J. Tucker, "Red and photographic infrared linear combinations for monitoring vegetation," *Remote Sensing of Environment,* vol. 8, no. 2, pp. 127-150, May. 1979.

[136] C. M. Vigorito, D. Ganesan, and A. G. Barto, "Adaptive control of duty cycling in energy-harvesting wireless sensor networks," in *Proceedings of the 4th IEEE Communications Society Conference on Sensor, Mesh and Ad Hoc Communications and Networks*, 2007, pp. 21-30.

[137] K.-H. Vik, C. Griwodz, and P. Halvorsen, “Constructing low-latency overlay networks: tree vs. mesh algorithms,” in *Proceedings of the 33rd IEEE Conference on Local Computer Networks*, 2008, pp. 36-43.

[138] C. A. Vincent and B. Scrosati, *Modern Batteries: an Introduction to Electrochemical Power Sources*, 2nd ed., New York: John Wiley & Sons, 1997.

[139] T. Voigt, H. Ritter, and J. Schiller, "Utilizing solar power in wireless sensor networks," in *Proceedings of the 28th IEEE International Conference on Local Computer Networks*, 2003, pp. 416-422.

[140] N. Wang, N. Zhang, and M. Wang, "Wireless sensors in agriculture and food industry - recent development and future perspective," *Computers and Electronics in Agriculture,* vol. 50, no. 1, pp. 1-14, Jan. 2006.

[141] J. Weier and D. Herring, *Measuring Vegetation (NDVI & EVI)*. [Online]. Available: http://earthobservatory.nasa.gov/Features/MeasuringVegetation/

[142] J.-P. Wigneron, J.-C. Calvet, T. Pellarin, A. A. Van De Griend, M. Berger, and P. Ferrazzoli, "Retrieving near-surface soil moisture from microwave radiometric observations: current status and future plans," *Remote Sensing of Environment,* vol. 85, no. 4, pp. 489-506, Jun. 2003.

[143] A. Woo and D. E. Culler, "A transmission control scheme for media access in sensor networks," in *Proceedings of the 7th Annual International Conference on Mobile Computing and Networking*, 2001, pp. 221-235.

[144] P. Würfel, *Physics of Solar Cells: from Basic Principles to Advanced Concepts*, 2nd ed., Weinheim, Germany: Wiley-VCH, 2009.

[145] N. Xu, "A survey of sensor network applications," *IEEE Communications Magazine,* vol. 40, no. 8, pp. 102–114, 2002.

[146] Y. Xu, J. Heidemann, and D. Estrin, "Geography-informed energy conservation for Ad Hoc routing," in *Proceedings of the 7th International Conference on Mobile Computing and Networking*, 2001, pp. 70-84.

[147] K. Yao, R. E. Hudson, C. W. Reed, D. Chen, and F. Lorenzelli, "Blind beamforming on a randomly distributed sensor array system," *IEEE Journal on Selected Areas in Communications*, vol. 16, no. 8, pp. 1555-1567, Oct. 1998.

[148] F. Ye, H. Luo, J. Cheng, S. Lu, and L. Zhang, "A two-tier data dissemination model for large-scale wireless sensor networks," in *Proceedings of the 8th International Conference on Mobile Computing and Networking*, 2002, pp. 148-159.

[149] W. Ye, J. Heidemann, and D. Estrin, "An energy-efficient MAC protocol for wireless sensor networks," in *Proceedings of the 21st Annual Joint Conference on the IEEE Computer and Communications Societies*, 2002, pp. 1567-1576.

[150] M. Younis, M. Youssef, and K. Arisha, "Energy-aware routing in cluster-based sensor networks", in *Proceedings of the 10th IEEE/ACM International Symposium on Modeling, Analysis and Simulation of Computer and Telecommunication Systems*, 2002, pp. 129-136.

[151] Y. Yu, R. Govindan, and D. Estrin, "Geographical and energy aware routing: A recursive data dissemination protocol for wireless sensor networks," Computer Science Department UCLA, Technical Report, UCLA-CSD TR-01-0023, May, 2001.

[152] Y. Zhang and M. Fromherz, "A robust and efficient flooding-based routing for wireless sensor networks," *Journal of Interconnection Networks,* vol. 7, no. 4, pp. 549-568, Sep. 2006.

[153] ZigBee Alliance, *ZigBee Specification Overview*. [Online]. Available: http://www.zigbee.org/Specifications/Zigbee/Overview.aspx